Rainfall variability and change in South Africa (1976-2065)

Tisang Manabalala Ncube (11636283)

This dissertation is submitted in fulfillment of the requirements for the degree of Masters of Environmental Sciences

Department of Geography and Geo-Information Sciences

School of Environmental Sciences

University of Venda

Supervisor: Dr. H, Chikoore

Co-supervisor: Dr. M.M, Bopape,

South Africa Weather Service (SAWS)

2019

DECLARATION

I acknowledge that I have read and understood the University's policies and rules applicable to postgraduate research, and I certify that I have, to the best of my knowledge and belief, complied with their requirements.

I declare that this dissertation, save for the supervisory guidance received, is the product of my own work and effort. I have, to the best of my knowledge and belief, acknowledged all sources of information in line with normal academic conventions.

I further certify that the work done is original, and that the material to be submitted for examination has not been submitted, either in whole or in part, for a degree at this or any other university.

I have subjected this document to the University‘s similarity checking procedures and I consider it to be free of any form of plagiarism.

Signature …….

Date …….

ACKNOWLEDGEMENTS

First and foremost, I would like to express my sincere gratitude to my supervisors; Dr. Chikoore, H and Dr. Bopape, M.M, who provided invaluable advice, guidance, support, and encouragement throughout this degree. Thank you.

I am also very grateful to Mr. Makgoale Thabo from the South African Weather Services (SAWS), for sharing his knowledge, advice and expertise in downloading, running and analyzing climate models. I appreciate his help and patience in guiding me through the challenges. Not forgetting, Ms. Mulovhedzi Patience for the help with GrADS training.

This degree was supported with the financial assistance provided by the National Research Foundation of South Africa (NRF) in collaboration with the Applied Centre for Climate and Earth Systems Science (ACCESS). This study was also supported by a Water Research Commission (WRC) project titled “Hydrological Modelling of Climate Impacts for Development of Adaptation Strategies: The Case Study of Luvuvhu River catchment Limpopo South Africa. WRC Project No: K5/2771/1”, led by Prof. JO Odiyo.

DEDICATION

My utmost appreciation is directed to the enormous support given by my family (Mr and Mrs Manabalala), for always being a constant source of support and encouragement throughout my university education. Not forgetting Ms. Mundalamo M, for the encouragement and emotional support throughout the research.

ABSTRACT

Rainfall is undoubtedly the most significant factor for life's continuity. South Africa is prone to future climate uncertainties due to global climate change. The aim of this study is to investigate rainfall variability and change in South Africa on a present day (1976-2005), near-future (2006-2035) and far-future (2036-2065) climate. For the study, 3 RCMs (REMO2009, RCA4 and CCLM4-8-17), forming part of CORDEX-Africa project were nested within 5 different CIMP5_GCMs of low resolution. GPCC precipitation, NOAA GHCN_CAMS Land Temperature and other NCEP reanalysis products were useful in validating models in simulations of present-day climate. RCP4.5 and RCP8.5 emission scenarios from IPCC-AR5 were used for future climate projections. On the validation, each regional climate model displayed different signature on simulations, rainfall in particular because this is a variable that is affected most by sub-grid process. Simulations nested within MIROC5 simulated more precipitation than simulations forced with other GCMs, due to more large-scale moisture convergence into the nested domain. There were differences in projections of RCM nested within the same GCM, as well as with the same RCM nested within different GCMs, on the future. Models nested within MPI project wetter conditions over the eastern parts of Limpopo, while the other two projected drier conditions in the same area. REMO2009 forced on MPI uniquely projected drying of Western Cape throughout the seasons on both RCPs and futures. Simulations conducted with the RCP8.5 scenario forcing are generally found to be associated with either a larger increase in temperature, or an increase in area associated with higher temperature increases. CCLM4-8-17 forced on HadGEM2 projected below average temperatures over the northwest parts of the country under the RCP8.5 scenarios. MPI driving model projected a general reduction of evaporation values, with lowest over northeast, northwest parts and south coastal parts of South Africa, in contrary to adjacent oceans. In this study, we have sought to identify the sources of uncertainties amongst model simulations between either the RCMs or the driving GCMs.

Key-words: Rainfall, projections, variability, change, models, nesting

TABLE OF CONTENTS

LIST OF FIGURES

LIST OF TABLES

LIST OF ACRONYMS

CCLM4	***Cosmo Climate Limited-Area Modeling***
CMIP5	***Coupled Model Intercomparison Project***
CNRM_CM	***Centre National de Recherches Me´te´orologiques-Climate Model***
CORDEX	***Coordinated Regional Downscaling Experiment***
ENSO	***El Nino Southern Oscillation***
ESGF	***Earth System Grid Federation***
GCM	***Global Climate Model***
GFDL	***Geophysical Fluid Dynamics Laboratory***
GHG	***Green House Gases***
GPCC	***Global Precipitation Climatology Centre***
HadGEM2	***Hardley Centre Global Environment Model***
ITCZ	***Inter Tropical Convergence Zone***
MIROC	***Model Interdisciplinary Research On Climate***
MJO	***Madden-Julian Oscillation***
MPI_ESM _LR	***Max-Plank-Institute Earth System Model- Low Resolution***
RCA	***Rossby Centre Regional Model***
RCM	***Regional Climate Model***
RCP	***Representative Concentration Pathway***
REMO	***REgional MOdel***
TTT	***Tropical Temperate Troughs***
SAM	***Southern Annular Mode***
MJO	***Madden–Julian Oscillation***

CHAPTER 1: INTRODUCTION AND BACKGROUND

1.1 Introduction

Rainfall is undoubtedly the most significant determining factor for life's continuity. Therefore, detailed knowledge of rainfall is an important prerequisite for many applications across the world; such as, sustainable agricultural and hydrological management (Qwabe, 2014). Global attempts to understand rainfall variability and change are not new, yet rainfall still remains the most difficult climate variable to predict and understand despite its importance in human existence. The Southern African region is prone to the occurrence of droughts, floods and other extreme weather and climate events (Dedekind *et al.,* 2016; Phakula 2018) directly posing devastating impacts on agriculture, water resources, the economy and social well-being. The reliance of the economies of countries within southern Africa on weather and climate sensitive sectors makes the region more vulnerable to extreme weather and climate events, as well as the impacts of climate change (Shongwe *et al*., 2009; Engelbrecht *et al.,* 2011).

Climate change and variability are two related key terms that refer to significant deviations in the mean state of the climate persisting for an extended period, typically over decades and variations in the mean state and other statistics of the climate on all temporal and spatial scales, beyond individual weather events, respectively (Ninan and Bedamatta, 2012; IPCC, 2013; Du Plessis and Schloms, 2017). Climate change may either be induced by natural internal processes or external factors such as persistent changes to atmospheric composition or changes in land use. The impacts of climate change are projected to pose serious challenges to the national development of South Africa, considering high levels of inequality and rooted poverty (Ziervogel *et al.*, 2014). The increased rate of greenhouse gasses emission is projected to worsen the current problem of global warming (Engelbrecht *et al*., 2015), hence altering the characteristics of extreme weather and climate events globally.

In order to prepare for the impacts of climate change, it is crucial that information on possible changes is provided, and such information can be obtained from climate models. Climate models are mathematical representations of the climate system based on laws of physics which include conservation of mass, energy and momentum. They are important tools for improving our understanding and predictability of the climate behavior on seasonal, annual and decadal timescales and making projections of future climates and beyond (Flato et al., 2013). Regional Climate Models (RCMs) have a higher spatial resolution compared to Global Climate Models (GCMs) because they run over smaller domains which cover an area of interest. GCMs are run

over the whole globe, and the resolution possible with them is determined by the available computational resources. RCMs are nested within GCMs which provide time-dependent lateral boundary conditions, and this procedure is called dynamical downscaling. RCMs are widely used to provide projections of how the climate may change locally though they use the same laws of physics described in terms of mathematical equations as global models (Bellucci et al., 2008). RCMs have been widely used for local climate investigations and these models have been found to have exceptional benefits. RCMs are able to capture the average statistics of daily precipitation on scales of a few grid boxes and they are better at resolving mountainous and coastal areas for instance, where a distance of 50 km can mean a dramatic change in climate (Kjellström et al., 2010 (Edwards, 2011).

The uncertainty in climate simulations can be represented through the use of multi-models and ensembles (Knutti et al., 2014). Previous studies have shown that the use of a multi-modelling systems outperforms a single model. Multi-models are believed to provide more reliable information and higher confidence of results is common as compared to a single model (Dam et al., 2015), though all models have deficiencies. Work done by Palmer et al., (2005) on ENSO showed that a multi-model average yields better results than a single model. For several climate model generation's, a multi-model average for a variety of variables typically corresponds better with observations of present-day climate.

However, for a single variable, the multi-model combination poses huge shortcomings, for instance, it might not be significantly better than the single best model. Furthermore, using averaged multiple models usually shows characteristics that do not resemble those of any single model. Hence, some characteristics may be physically implausible and overestimated (Anav et al., 2013). In some instances, an average state may not exist when there is a bifurcation amongst the models (Knutti et al., 2014).

Modeling frameworks and International coordinated efforts have gained traction in recent decade and some of these include, Coordinated Regional Downscaling Experiment (*CORDEX)* (Giorgi et al., 2009). Through CORDEX simulations were performed over different domains, and a number of models were used to simulate climate projections over the identified domains. One of the identified domain covers the whole of Africa, and a number of studies (Mascaro *et al.,* 2015; Lennard *et al.,* 2018; Maure *et al.,* 2018) have focused on this domain. The initiative represents a major collaborative endeavor aimed at developing downscaled climate projections and producing a comprehensive evaluation of climate change consisting of experts from all over Africa

continent, evaluating the performance of multi-model ensembles of regional climate projections (Myra, 2015). The program produces dynamically downscaled high-resolution regional climate data over specified area of interest using forcing data from either GCMs or reanalysis archives. The models are driven by GCM simulations which were produced for CMIP5 and applied on the IPCC_AR5 report.

When projecting the future, climate models are forced with GHG emissions for identified emission scenarios. Garland et al., (2015) used six simulations produced by the Conformal Cubic Atmospheric Model (CCAM) nested within six different GCMs to investigate impacts of human health across the continent on projected future warming under RCP8.5 emission scenario. The study found that, Africa has already experienced increasing warming trends and it is likely that surface temperatures across Africa will increase at a rate faster than the projected global average increases in surface temperatures. Over South Africa, up to 2050 and beyond, a pattern of drier conditions to the west and south are projected and a risk of wetter conditions over the east coast are projected under low mitigation scenarios (LTAS, 2013). However, rainfall projections over the region are associated with high degree of uncertainties and need more thorough focus and research.

1.2. Weather and climate of South Africa.

South Africa experiences a variety of climatic regimes which are largely semi-arid, with significant variability on several time scales (Landman and Tennant, 2000; Tyson *et al.,* 2002). Southern Africa's geographic location, steep orography, contrasted oceanic surroundings and atmospheric dynamics are conducive for extreme weather events and high inter-annual variability (Fauchereau *et al*., 2003). Climatic regimes of South Africa are largely delimited by the teleconnections and feedbacks, physical features and seasonality, outlined below.

1.2.1 Teleconnections and feedbacks

Variability of climate, ranging from intra-seasonal to inter-decadal timescales over southern Africa are governed by global modes of variability and feedback processes. Teleconnections play an important role of influencing the climate of the region, for instance, the Southern Annular Mode (SAM) and Madden Julian Oscillation (MJO) (Myra, 2015). The El Nino Southern Oscillation (ENSO) in the equatorial Pacific Ocean is also an important control of rainfall variability associated with the occurrence of floods and droughts over the region. Furthermore, several studies have demonstrated the influence of ENSO on the climate of southern Africa (e.g. Mason et *al.,* 1994; Tyson and Preston-White, 2000; Kane, 2009). ENSO events have been linked to dry conditions

over the eastern sector of the sub-continent (Chikoore, 2015). Moreover, regional circulation patterns and atmospheric stability may also be altered as a result of various feedback mechanisms.

1.2.2 Physical features

The landscape is distinguished by an interior plateau and a sharp escarpment to a narrow coastal belt. The topography of South Africa varies from the altitude of less than 300 m along the coastal areas and over 3000 meters over the eastern escarpment (Phakula, 2018). The average height of the escarpment ranges from 1500 m above the sea level on the south east, to about 3000 m in the Drakensberg (Kruger, 2006; Bhaktawar and Van Niekerk, 2012). Hence the plateau is characterized by plains above 1200m above sea level. The region is also bounded by the Atlantic and the Indian Oceans to the west and east respectively. Ocean currents largely influence sea surface temperatures over the region. The cold Benguela current on the west flow towards the equator whilst the Agulhas current flows poleward (south) along the eastern coast (Mason *et a*l., 1999). Heat and moisture fluxes into the atmosphere above the warm Agulhas Current have a significant influence on the regional climate (Rouault et *al., 2003;* Chikoore and Jury 2010, 2018*)*. Variability in the Agulhas current region is linked to climate variability over South Africa. Enhanced cumulus convection occurs above the Agulhas and warm moist advection significantly results in rainfall along the coast. In contrast, the cold Benguela current on the west coast is mostly linked to upwelling and aridity (Jury, 2018). However, the current plays a crucial role in the development of heat low (Angola Low) and the propagation of heavy clouds (Reason and Smart (2015*).* Differences in sea temperatures between the 2 oceans largely contribute to the spatial gradients over the region. A combination of topography and the surrounding oceans (Figure 1.1) play a pivotal role in governing the weather and climate of the region.

1.2.3 Seasonality

South Africa's climate is modulated by synoptic features that range from the tropics to temperate regions and is also characterized by a strong seasonal cycles. For instance, the descending limb of the Hadley cell and Tropical Temperate Troughs (TTT) are crucial controls of weather and climate over the region (Kruger, 2004). Conditions that occur during austral summer season (December-January-February) include the permanent and semi-permanent Atlantic and the South Indian Ocean High (Figure 1.2a*)*. The SIOH plays an important role of advecting moist by south easterly winds into the eastern parts of region; Limpopo, Kwa-Zulu Natal (Jury et al., 1999). The cool and drier recurved winds flowing from the SAH converge with the south easterly trade winds at the moisture boundary resulting in heavy rains. During the winter season high pressure

systems are displaced further northwards over the interior, together with the ITCZ, resulting in weak surface heating over southern Africa. Thermal troughs weaken and disappear due to absence of heat low s over the interior (Kruger, 2004). On the other hand, the Subtropical highs merge over the interior, favoring subsidence and clear skies. Southern African subcontinent receives almost all its rainfall during DJF, except the southwest region of the Western Cape Province, which receives frontal rainfall from the passage of mid-latitude cyclones during winter season and a small margin along the south coast which receives throughout the year. Subsidence inversions usually occur over the interior of the subcontinent which creates drier conditions and less rainfall (Figure 1.2b).

1.3. Problem analysis and motivation

The earth's climate is rapidly changing, largely attributed to human activities that have led to the release of GHGs into the atmosphere. These increased GHGs emissions have led to changes on the climate variables (Garland *et al.,* 2015) as a result, global warming poses devastating threats on various climate sensitive sectors. Several studies are conducted on generating possible future projections of likely changes in atmospheric variables. South (ern) Africa, is also vulnerable to the effects of climate change due to its geographical location in the dry sub-tropics and socio-economic landscape (Engelbrecht *et al.,* 2015; Dedekind *et al.,* 2016).

A large number of climate-change studies have been performed over the continent using high-resolution numerical regional climate models (e.g. Tadross *et al.,* 2005; Engelbrecht et al., 2015). Some studies have focused on projected changes in rainfall and temperature over southern Africa (e.g. Engelbrecht *et al.,* 2015). However, notably very few studies have dealt with the variability and change of rainfall specifically in South Africa, basing on the latest RCP4.5 and RCP8.5 emission scenarios using multi models which form part of CORDEX, for which this study intends to investigate. In general, emission scenarios prescribe a GHG emissions pathways for the future, and then climate models use these emissions pathway to project the future climate. These RCP scenarios have given potential insights into how global and regional atmospheric circulations may change in response to anthropogenic forcing. This may lead to more clarity on rainfall variability of future climates (Engelbrecht *et al.,* 2009). This study intends to cover these gaps by investigating rainfall variability and change on a future climate over South Africa.

1.4. Research Aim

The aim of this study is to investigate the variability and change of rainfall in South Africa, on a historical baseline (1976-2005), to project near future (2006-2035) and far future (2036-2065) climate projections, using several GCMs driving different RCMs from the CORDEX-Africa project using both the RCP 4.5 and RCP 8.5 emission scenarios.

1.5 Research questions

- How well do models simulate the observations.
- To what extent do projected changes in rainfall seasonality and inter-annual variability differ between both emission scenarios?
- Are the RCMs or driving GCMs the main sources of uncertainty in future climate change projections?
- Are changes in evaporation as important as changes in rainfall in the future?

1.6 Specific objectives

- To validate present day model simulations (1976-2005) against observations.
- To study projected rainfall variability and change in the near future *(*far future*)* climate 2006-2035 (*2036-2065)* over South Africa with a grid spacing of 0.5° using RCP4.5 and RCP8.5 emission scenarios.
- To examine the sources of uncertainty amongst models on future projections.
- To analyze future trends in evaporation in a warming climate over South Africa.

1.7 Description of study area

The study area for this work is South Africa (Figure 1.3) which is the southern tip of the southern African subcontinent, found in the subtropics (22-35°S and 15-35°E). The study area focus will extend (15-36°S and 0-50°E) when analyzing other variables such as geopotential height, so as to have a broader view and understanding of large scale circulations. South Africa is the area of interest because of its high degree of climate variability on different time scales. Owing to its latitudinal location, the weather and climate of the country is affected by temperate and tropical latitude circulation systems and also by the high pressure systems in the subtropics which are semi-permanent. For convenience purposes, there are some parts that are labelled A-E on the study map. The given names are used in Chapter 4-6 when analyzing the spatial distribution of variables.

1.8 Research outline

The dissertation is divided into six chapters: **Chapter One**, provides the introduction, background, problem statement, aim, specific objectives and justification of the research. The description of the study area and telecommunications governing weather and climate of South Africa is also done in this section. ***Chapter Two*** presents a literature review on regional climate modeling activities and important rain-bearing systems over southern Africa. Studies that have modelled rainfall on present and future climates are also discussed. ***Chapter Three*** details the methodology of the study, including a description of data, the global and regional models used and their setup for simulations. Chapters Four and Five present and discuss the results of the present study. ***Chapter Four*** aims to validate the ability of climate model (s) to reproduce present-day climate over South Africa in relation to observations. ***Chapter Five*** discusses rainfall future projected changes due to elevated greenhouse gasses, using medium-high mitigation (RCP4.5) and low mitigation (RCP8.5) scenarios, supported by changes in surface temperature and evaporation flux. ***Chapter Six*** provides a summary of the key findings, suggestions for future avenues of research and offers concluding remarks.

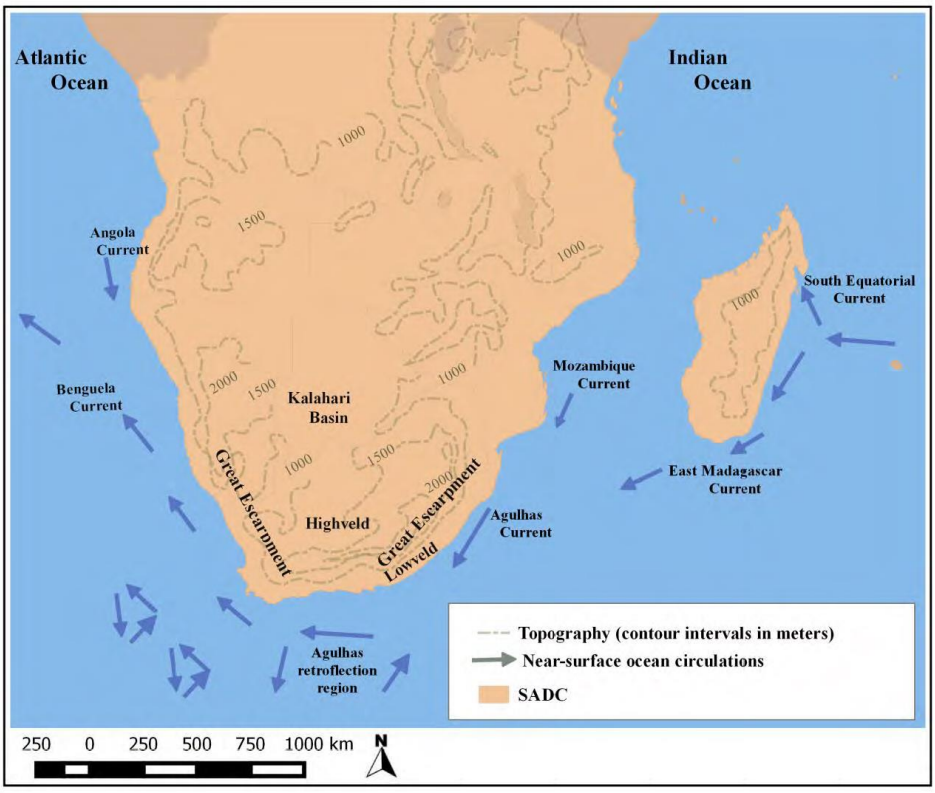

Figure 1.1. Topography and surrounding oceans influencing weather and climate over South (ern) Africa. (Source: Myra, 2015).

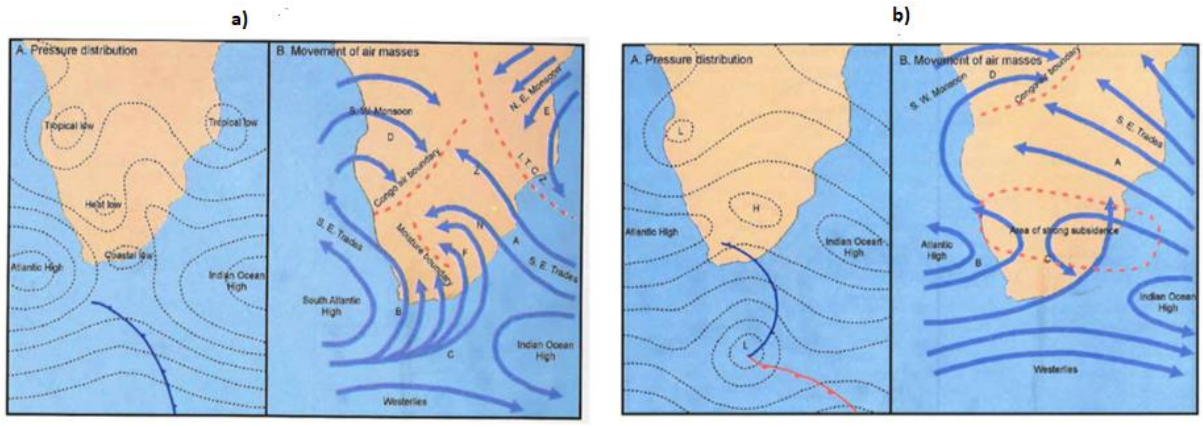

Figure 1.2. **(a)** Summer (**b)** Winter seasons' pressure distribution and air masses movement over Southern Africa. (Kruger, 2004).

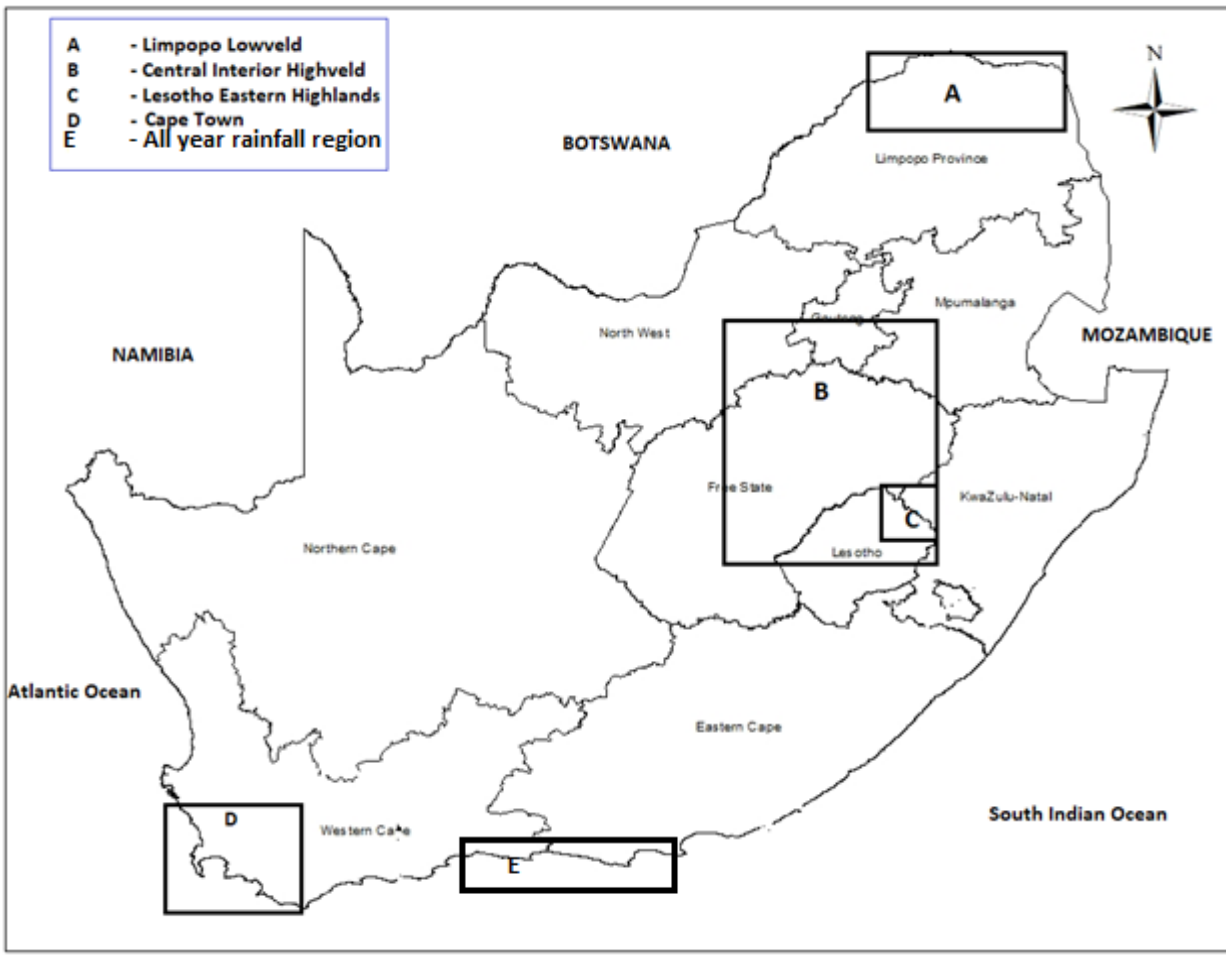

Figure 1. 3 Study area map of South Africa, including neighboring countries and oceans. Each areas has 0.5° pixels.

CHAPTER 2: LITERATURE REVIEW

2.1 Introduction

A comprehensive review of the literature of climate change on rainfall from a global perspective is presented in this chapter. This section evaluates existing knowledge and establishes possible gaps to generate research questions for the study. Another important aspect of this chapter is to identify and assess the methods and climate modeling techniques done in previous studies. This chapter is organized into thematic areas and begins with primarily understanding the variability of rainfall and the bearing systems surrounding South Africa. It also outlines how other researchers used climate models to investigate future climate variables.

2.2 Large-scale circulation patterns affecting South (ern) Africa

2.2.1 El Nino Southern Oscillation (ENSO)

The ENSO is a large-scale disturbance of the ocean-atmosphere system governing over the Equatorial Pacific Ocean. The system tends to have great influence on weather and climate over globe (Trenberth, 1996; Sheinbaum, 2003; Phakula, 2018; Wang *et al*., 2017). The large scale disturbance is known to strongly govern rainfall variability on seasonal timescale in Asia, Australia and Southern Africa (Chakraborty and Krishnamurti, 2003: Cork *et al.,* 2004). The term Southern Oscillation refers to variations in temperature of the tropical eastern Pacific Ocean surface, with the warming known as El Nino and the cooling as La Nina, and in air surface pressure in the tropical western Pacific (Phakula, 2018)**.** The variations are associated with warm phase accompanying high air surface pressure in the western Pacific, while the cold phase accompanies low air surface pressure in the western Pacific. ENSO events are usually studied in order to understand the season climate variability over months to years (Wang *et al.,* 2017). The influence generally results in anomalous wet and dry conditions during the austral summer over southern Africa (Phakula, 2018). There is a strong ENSO effect in monthly precipitation in different regions. El Niño and La Nina events are associated with drier conditions over most parts of southern Africa; for example, 1997/98 and 1999/00 cases respectively (Figure 2.1).

Their occurrence is associated with shifts in the locations of the tropical-temperate trough systems to the ocean east of Madagascar (Tadross *et al.,* 2006). The 2015/16 summer rainfall season over the region appeared to be the driest on record since the well-publicized droughts of the early 1980s and 1990s; with critical impacts on agriculture, water and food security well covered in the media. It has had particularly significant impacts (Archer et al., 2017). However, a few studies (e.g. Pomposi et al., 2018; Siderius et al., 2018) have found that not all El Niño's result in drought

conditions over southern Africa. In general, El Niño affects the circulation, causing high pressure over southern Africa and intensification of the Botswana high.

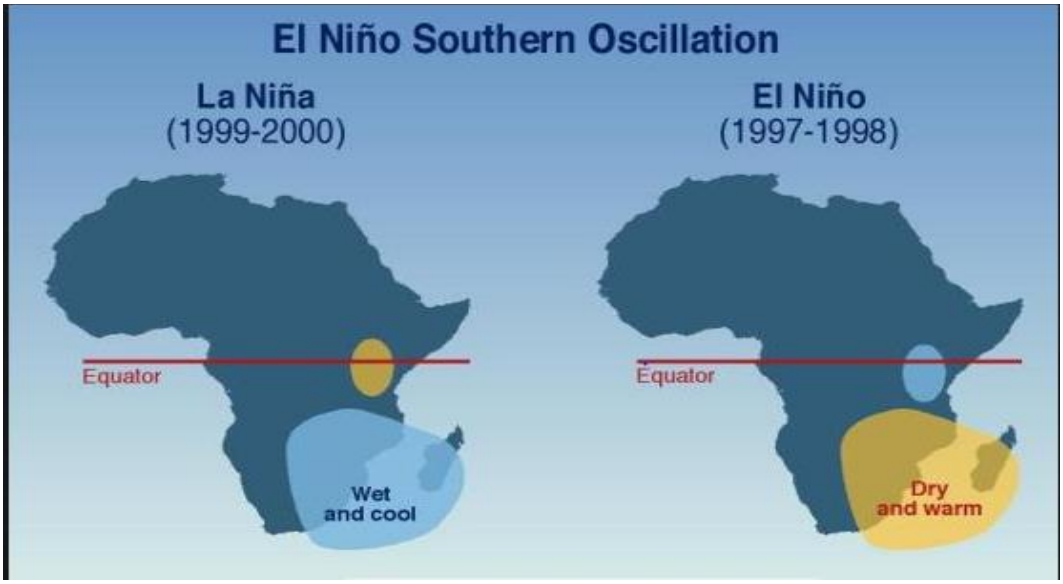

Figure 2.1 El Nino Southern Oscillation phenomenon affecting Southern Africa during austral summer (Source: http://www.grida.no/resources/7049, accessed on 02/10/2018).

2.2.2 Madden-Julian Oscillation (MJO)

The MJO is important in modulating weather and climate of southern Africa (Hart et al., 2013). It is characterized by eastward circulation of large-scale tropical deep convection clusters from Indian Ocean to the western Pacific Ocean *(*Figure 2.1*)* (Chakraborty and Krishnamurti, 2003; Zhou, 2012; Phakula, 2018). A recent study by Jones, (2018) found that the MJO is an important mode of tropical intra-seasonal variability. Its effects on weather depend on the state or phase of certain climate phenomena (e.g., ENSO), and their combined effects may lead to extreme weather events. The influential nature of the MJO has also been noted on occurrences of extreme weather events due to tropical cyclones (Zhang, 2013).

Several studies have suggested that the MJO to have influence on certain major flood events. Pohl and Camberlin (2006) alluded that, the MJO modifies the direction of the lower-layer moisture fluxes, through an influence on the Indian Ocean High (IOH) over the southern Africa region. The MJO is involved in scale interactions across a wide range of spectrum from the diurnal cycle to inter-annual variability (Moncrieff et al. 2012). Improved MJO forecasting benefits prediction of tropical cyclones extratropical weather regimes. The MJO affects precipitation in

remote areas by modifying the strength of meridional overturning circulations (He et al. 2011) and moisture transport.

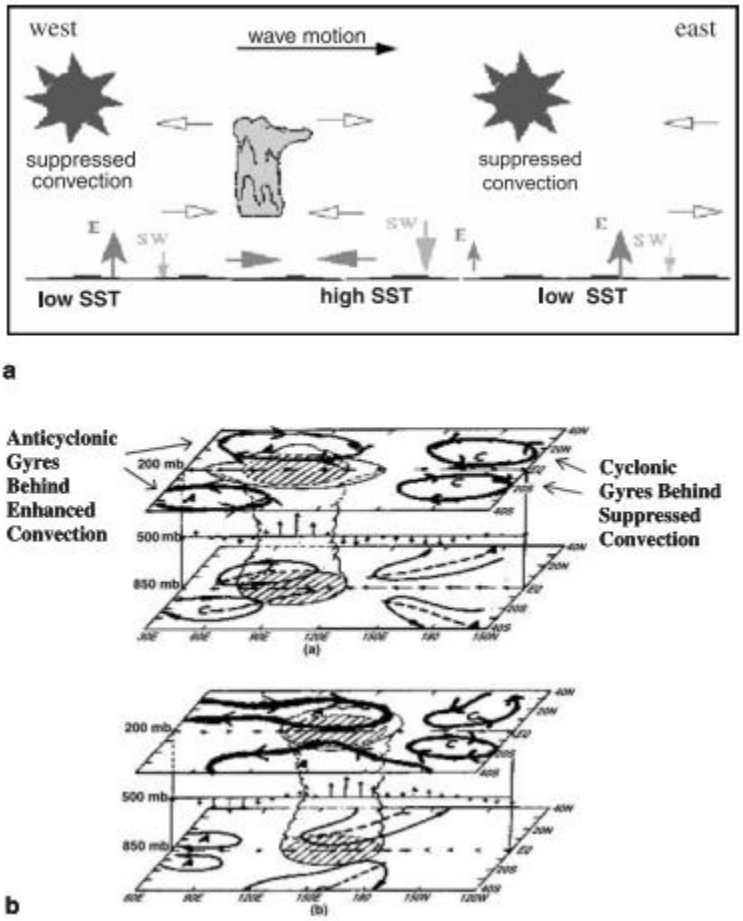

Figure 2.2 Schematic and 3D structure of MJO (Source: Chakraborty and Krishnamurti, 2003)

2.2.3 Subtropical Indian Ocean Dipole (SIOD)

Sea Surface Temperatures (SSTs) at a regional scale, vary over the Indian Ocean. They are also well known to influence the inter-annual rainfall fluctuations over South Africa (Reason, 2001). Subtropical Indian Ocean Dipole (SIOD) is the major climate mode in the Indian Ocean, controlling the SST anomalies (Behera and Yamagata, 2001). The SIOD is significant at the inter-annual scale during austral summer, and this climatic mode oscillates between two phases: positive and negative phases (Reason, 2001). The positive phase is characterized by positive SST anomalies at the south-western side of the Indian Ocean and negative SST anomalies at the south-east (Australian side), while the reverse occurs during a negative phase (Behera and Yamagata, 2001; Reason, 2001). The positive phase of the SIOD influences the positive anomalous rainfall over

many regions in southcentral Africa, while the negative phase leads to negative anomalous rainfall (Behera and Yamagata, 2001). Reason (2002), further highlighted that during the negative phase of the SIOD, decreased precipitation is observed over the south-eastern part of South Africa influenced by low-level divergence. Furthermore, decreased evaporation over the cold pole at the south-west Indian Ocean during a negative phase lead to less moisture advection towards Mozambique and south-eastern Africa (Reason, 2001). The negative moisture advection is influenced by a high-pressure anomaly, produced above the colder SIOD pole side which weakens the onshore flow to Mozambique and hinterlands.

2.3 Rain-bearing systems over South Africa

2.3.1 Tropical Temperate Troughs

Cloud bands resulting from Tropical–Extratropical (TE) interactions are common features in many regions, typically presenting as an elongated region of cloudiness rooted in the tropics and extending poleward and eastward into the mid latitudes (Hart et al., 2010; Hart et al., 2013) They link up with upper-tropospheric frontal systems rooted in the mid-latitude westerly circulation (Chikoore *et al.,* 2015). Cloud bands convergence zones are usually tilted equator wards and are linked with the Southern branches of the ITCZ. Over the South Africa, cloud bands are the major synoptic rainfall-producing weather system during the summer (Harrison 1984; Phakula, 2018). The spatial distribution of rainfall and low-level winds explain that TTT extends from Angola across Botswana into the Limpopo Valley until they dissipate in SE of South African and adjacent ocean *(Figure 2.3)* (Jury 2016). In previous studies, Mulenga, (1999) and Cretat et al., (2012) alluded that these low-pressure systems are linked to the occurrence of intense rainfall, about 60% of South Africa's summer rainfall total.

Northeast winds usually convey moist air from the Indian Ocean into the cloud band. Cloud bands always turn in a spiral from north-west to south-east towards the higher latitudes, thus they are called North-West cloud band (Mulenga 1998). Furthermore, the structure of this weather system in the Southern Hemisphere varies from simple to extremely complex and they are steered by the large-scale westerly flow (Tyson and Preston-Whyte 2000). In most studies and observation, rainfall distribution in southern Africa shows a clear correlation to cloud band occurrence (Lindesay, 1988). TTTs were responsible for 52 extreme rainfall events from 1979-1999 (MacKellar et al., 2014).

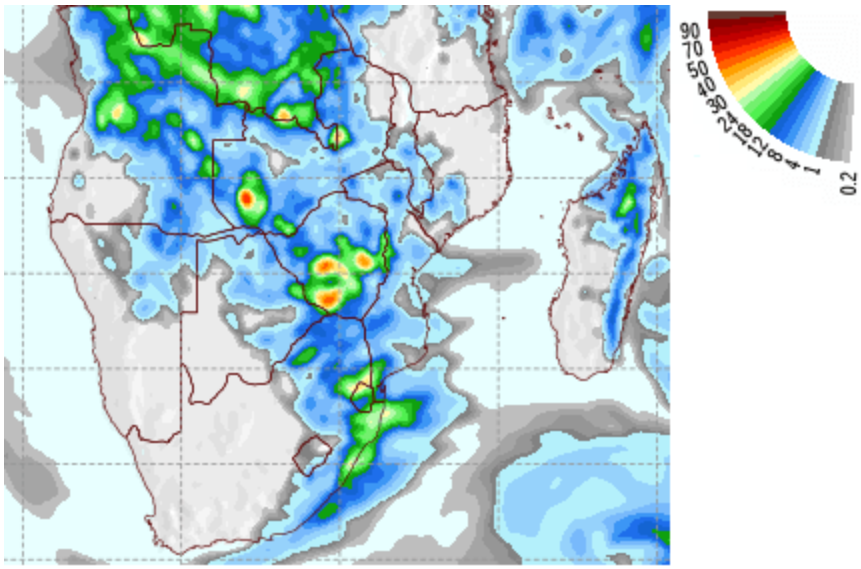

Figure 2.3. March 2014 rainfall (mm/day) from NW cloud bands over southern Africa (Source: GFS; http://wxmaps.org/pix/af.vv.html).

2.3.2 Inter-Tropical Convergence Zone (ITCZ)

ITCZ is a region of pronounced convective activity in which tropical processes occur; a low-pressure area where trade winds from both hemispheres converge, resulting in convective uplift. Closed tropical lows and troughs form within the convergence zone (Tyson and Preston-Whyte, 2000). The system is associated with maximum global heating and descending of the motion over the subtropical high-pressure belt, hence largely governed by the combination of insolation and Hadley circulation (Chikoore, 2005). The movement of the ITCZ shows a clear annual cycle over southern Africa. In summer, the troughs fluctuate southwards of the equator, and links with the Angola low and produce widespread rains over the entire Limpopo valley interior, eastern parts of South Africa. Ker et al., (1978) mentioned that it moves along rain belts, such as cloud bands, which are important in producing rainfall to most areas.

The position of the ITCZ during summer season is also important for major river basins, such as Zambezi, and Limpopo River. During the La Nina phase of ENSO, the ITCZ trough can extend towards the tropic Capricorn (Mwafulira, 1999). Southern Africa receives abundant rainfall between November and March, when the trough is south. In a normal southern African rainy season, the ITCZ influence covers central Tanzania to southern Zimbabwe and north of South Africa. They constitute a region of major latent heat release in the tropical atmosphere of southern Africa. Unlike in winter, it migrates northwards of the equator (Kruger, 2006). The oscillation of

the ITCZ during summer and winter seasons *(Figure 2.4)* is mostly influenced by pressure changes south of Africa (Ker et al., 1978; Chikoore, 2005) and a mid-tropospheric anticyclone system established over Botswana, pushing the ITCZ away.

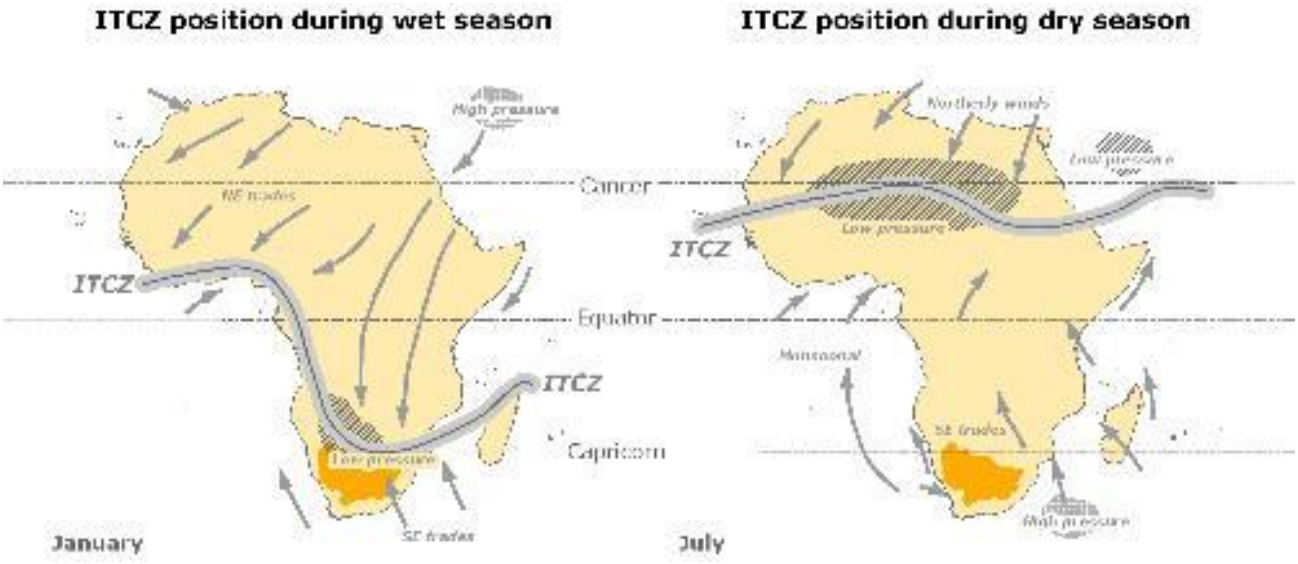

Figure 2.4. Inter-Tropical Convergence Zone variation across Africa throughout the year. (Source: Ker et al. 1978).

2.3.3 Cold fronts and Ridging Anticyclones

Cold fronts and ridging subtropical anticyclones are the most important systems in the western and Eastern Cape during the winter season (Tyson and Preston-Whyte 2000). Driven by high pressure systems, cold fronts are characterized by moving cold air from the southwest of the Atlantic Ocean to south-east through the south coast of South Africa (*Figure 2.5a).* They occur due to migration of weather systems all the time but bring rainfall during winter season (Figure 2.5a). Favorable conditions for convection are produced to the rear of the front, wherein convergence at low-level in airflow with southerly component are at its peak (Mac Hutchon 2006). Cold fronts are generally associated with distinctive cloud bands, which extends from the coast to near inland.

The migration of the high-pressure system influencing rainfall over South Africa, are dominant during June- July (Mac Hutchon 2006; MacKellar et al., 2013). The system is basically associated with subsidence over much of the interior of southern Africa. They tend to be static for a length of time on the southeast coast (*Figure 2.5b)* during winter. The nature of the high-pressure system's rotation, anticlockwise, enhances advection of warm moist *(hooking-like motion*) from

the Indian Ocean towards the coast and adjacent interior. Convection of moisture results in heavy rains in areas such as Eastern Cape and some parts of Kwa-Zulu Natal (Tyson and Presto-Whyte 2000). Preston-Whyte and Tyson (1988) found that, both ridging highs and cold fronts approximately account for 16-25% of total rainfall over the sub-region.

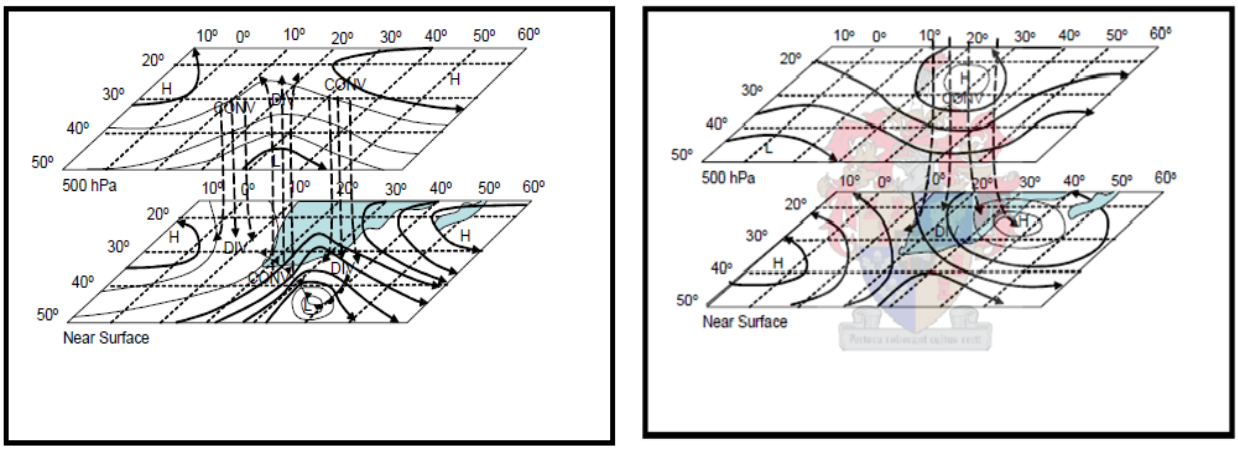

A B

Figure 2.5. Schematic representation of circulation (near-surface and 500hPa) associated with cold fronts (a) and ridging anticyclones (b) over the south coast of South Africa. (Source: Mac Hutchon 2006).

2.3.4 Tropical cyclones

Tropical cyclones are intense, cyclonically rotating low-pressure weather systems that form over the warm tropical oceans (Smith, 2006). The South West Indian Ocean (SWIO) and the Mozambique Chanel are breeding grounds for tropical cyclones, influencing rainfall over South Africa. An average of eleven tropical disturbances reaches the stage of tropical cyclone intensity over the SWIO per year (Malherbe et al., 2013). Approximately 6% of tropical cyclones make landfall over the adjacent subcontinent of southern Africa (Vitart et al., 2003). Such weather systems make landfalls as they track westwards over the region, hence, they develop over the Indian Ocean (Malherbe *et al* 2011) and account for widespread heavy rains and flooding over the eastern parts of the southern African interior, including the Limpopo River Basin (Malherbe et al., 2013).

The tropical cyclone season of 2011-12 had frequent cyclogenesis over the Mozambique Channel resulting in heavy rains and flooding over low-lying and coastal areas of South Africa (*Figure 2.6).* In the SWIO basin, the austral summer months of Jan-Feb have the highest peak for tropical cyclogenesis (Chikoore *et al.,* 2015). The occurrence tropical cyclones over the South Indian Ocean positively correlates with the La Nina phase. Recent studies have been done to investigate

the shift and frequency of cyclones affecting southern Africa due to anthropogenic forcing and climate change. For instance, Malherbe et al., (2013) used the CCAM model, forced with the bias-corrected sea surface temperatures and sea-ice of six coupled global climate models (CGCMs). A simultaneous increase in January to March rainfall over northern Mozambique and southern Tanzania and a decrease further south over semi-arid areas such as the Limpopo River Basin was projected. This also agrees with Muthige et al., (2018) who used 5 CORDEX regional climate models to project shifts towards East Africa.

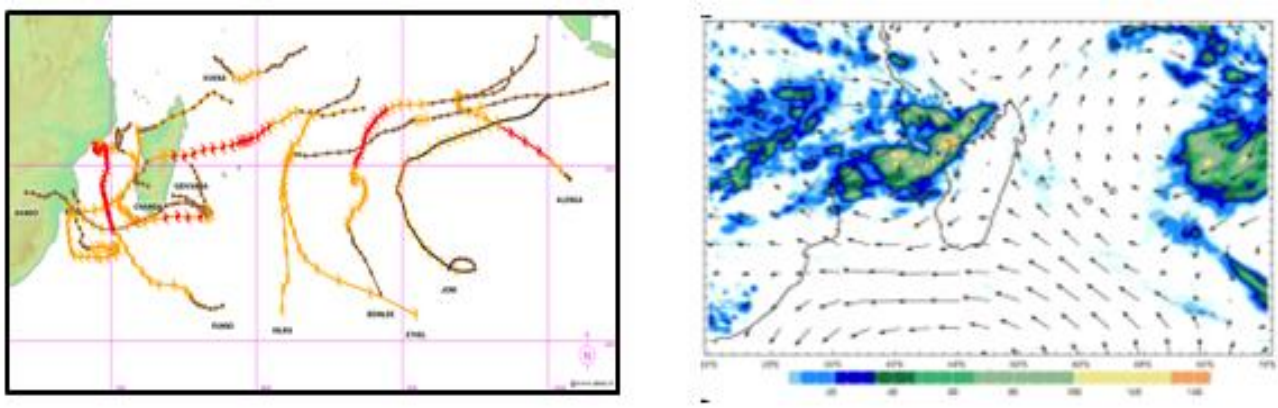

Figure 2.6. January- March 2012 storm tracks (Source: Chikoore *et al.* 2015).

2.3.5 Cut off lows

Cut-off lows are one of a major rainfall contributor in South Africa. They are deep low-pressure systems, reaching its peak in the middle troposphere, where they form at 500 hPa steering levels (Tyson and Preston-Whyte, 2000). This is when the upper air system separates from the principal westerly flow of the mid-latitudes and it is generally said to be “cut-off” from its westerly flow, forming a cut-off low (Molekwa, 2013). When the low is deep and extends towards the lower troposphere, it forms a surface low (Figure 2.7). Strong winds and widespread heavy precipitation are associated with such system (e.g. McInnes et al. 1992; Katzfey and McInnes 1996; Llasat et al. 2007; Porcu` et al. 2007). Thereafter, when the system weakens, precipitation becomes less intense and ceases. However, it needs to be noted that the definition of the cut-off low weather systems varies to some extent through literature. Here, it is defined as a low-pressure system that separates from a planetary circulation that spins off autonomously as it is no longer linked to the westerly wave (Tyson and Preston-Whyte 2000). This weather system is identifiable because it loses all its momentum and can locate over a region for a number of days or propagate slowly before dispersing. It is linked with instability in the atmosphere and prevailing convection (Potgieter, 2009). It can also bring anomalous weather patterns over a region. It is one of the main

drivers of damaging floods and consist of semi-annual variation (Molekwa, 2013). Its peak is from March to May and September to November, with their lowest frequencies between December and February (Singleton and Reason, 2007).

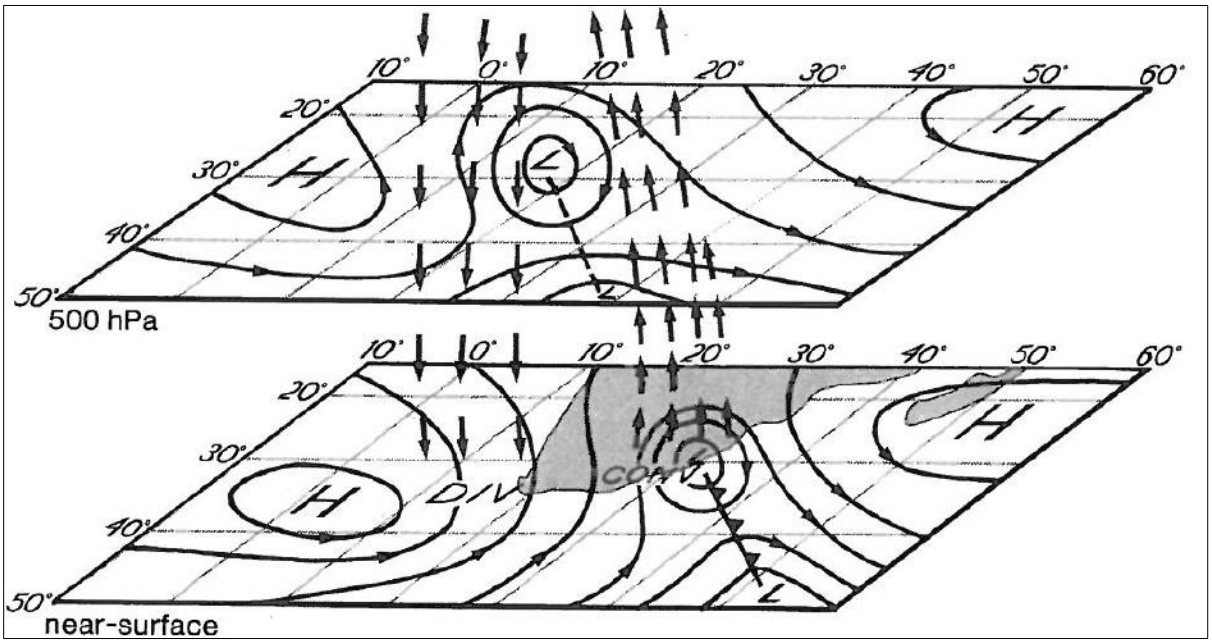

Figure 2.7. 500 hPa and the near surface circulation with the vertical flow associated with a typical Cut-off Low (Source: Preston-Whyte and Tyson, 1988).

2.4 Rainfall characteristics and their effects over South (ern) Africa.

2.4.1 Wet and dry spells

The intensity and frequency of rainfall distribution has an effect on wet and dry spells over southern Africa. Largely the temporal distribution and the nature of these spells have a huge impact for decision making on water resources, agriculture and rural communities (Cook et al., 2004). Phakula, (2018) found that the timing and amount of rainfall determines the quality of rainy season. For instance, the intense rains in northeast South Africa during February/March 2000 over northern South Africa and surrounding areas (Rouault et al., 2002; Kijazi and Reason, 2011). Due to major parts of southern Africa being characterized by poor infrastructure and low socio-economic development, the extreme weather event resulted in devastation to both people and bridges, roads and other properties (Dyson and van Heerden, 2001). *Wet and dry* spells occur when at least 3-4 consecutive days of having area-average rainfall totals which are *above and below 1* respectively (Usman and Reason, 2004). Extreme wet conditions are associated with wet spell frequency and flooding while extremely dry conditions are associated with droughts. Dry spells can be a measure of rainfall characteristics even during wet periods. Recent studies have

argued that, due to the changing climate, the definition of wet and dry spells will be subject to further debate. This is because rainfall intensity is projected to increase and frequency *(no. of days*) to decrease, hence further shifting on normal summer rainfall months.

2.4.2 Onset and cessation

The onset and cessation of rainy seasons are regarded as the most critical rainfall characteristics for agricultural activities, such that they play a major role in decision making *(planting and variety of choices*)and strategizing for adaptation measures (Majisola, 2010). Usually the onset of the summer rainy season over South Africa region occurs in October and towards early November, although there are some variations on dates noted. Recent climate change studies have projected a shift in onset to later, hence this may result in poor seasonal distribution and community planning at large (Archer et al., 2017). Late onset and early cessation over southern Africa are normally governed by El Niño episodes for instance 1991/92, 2014/15 2015/16 which lead to devastating droughts, famines and loss of agricultural yields (Tadross, 205; Archer et al., 2017; Monyela, 2017).

2.4.3 Droughts

Southern Africa is susceptible to droughts due to its high inter-annual rainfall variability. Drought is one natural hazard with a complex nature in both temporal and spatial scales and is often difficult to monitor (Manatsa et al., 2010). For instance, severe drought events of 1991/92, 2002/03, 2003/04, 2014/15, 2015/16 resulted in devastating effects over northeast and surrounding areas in South Africa. Most severe droughts that occur over South Africa are largely influenced by either by the El Nino episode or regional anomalies (Reason et al., 2005). Droughts have been classified into four different categories: agricultural, meteorological, socio-economic and hydrological droughts and they are described as follows:

2.4.3.1 Meteorological drought

Meteorological drought is defined as on the basis of the degree of dryness, in comparison to a normal or average amount and the duration of the dry period. It occurs from a month to seasons and is distinguished by negative anomalous rainfall, which is influenced by large scale atmospheric modes (e.g. ENSO and SIOD), and acts as a precursor to other different kinds of droughts (Phakula, 2018; Monyela, 2017).

2.4.3.2 Hydrological drought

A hydrological drought refers to a persistently low discharge and volume of water in streams and other storages. It is characterized by rainfall shortages over a long period of time (12-24 seasons

to years) and it is manifested on surface water supply (Rouault and Richard, 2003; Monyela, 2017). It is a natural phenomenon, but may be influenced by human activities such as excessive extraction. Also changes in land use may affect the magnitude of hydrological drought (Phakula, 2018).

2.4.3.3 Agricultural drought

An agricultural drought can be defined as a situation whereby there is no sufficient soil moisture to support crop production (Tadross, 2005; Manatsa et al., 2010; Monyela, 2017). The time scale for an agricultural drought to occur in weeks to months, for instance drought can happen if 2 weeks rainfall is low. (Rouault and Richard, 2003). A good definition of agricultural drought should account for the susceptibility of crops during different stages of crop development. Deficit topsoil moisture at planting may hinder germination, leading to low plant yield per hectare (Phakula, 2018).

2.5 Regional climate models and their most recent application over southern Africa

2.5.1 Advantages of RCMs

Recent climate change studies use a combination of GCMs and RCMs with the latter used to obtain simulations of very high resolution on local scales. A number of RCMs developed across the globe have been applied over Africa (e.g. Engelbrecht et al., 2011; Hewitson et al., 2012; Kalognomou et al., 2013). Over smaller areas applications beyond the non-hydrostatic limit are feasible (Dedekind et al., 2016), however these are mostly practical in the shorter timescales and used to make weather simulations. In that regard the models are then termed numerical weather prediction models, and the generic term to describe dynamically downscaled models is limited area models. Higher resolution of RCMs provide avenues to improve climate simulations along areas with complex topography and along coastal regions (Nikulin et al., 2012). It allows RCMs to capture aspects of regional and local climate often missed in coarse resolution GCM simulations. The traditional method of dynamical downscaling to produce climate simulations is forcing RCMs with GCMs at their lateral boundaries, and this methodology is associated with a number of problems for future projections. Another procedure that is used in dynamical downscaling is the use of variable resolutions that provide high resolution over an area of interest, and the resolution is lowered as one moves away from the area of interest (e.g. Engelbrecht et al., 2015). Variable resolution global models such as CCAM may be advantageous because they avoid the traditional lateral boundary value problems (Dedekind et al., 2016).

2.5.2 Recent application of RCMs in southern Africa

Climate models have proven to be useful tools to detail climate simulations and a large community of researchers worldwide are using these (Rummukainen, 2010). GCMs and their complements, RCMs, are sophisticated numerical tools used to explore the climate system and understand a variety of processes (Myra, 2015; Shalaby et al., 2017). These models solve complex mathematical equations using numerical methods, and are often run on super computers (Trenberth, 1992; Myra, 2015). The main equations that are solved by these models represent conservation of energy, mass and momentum (Figure 2.8) of the atmosphere (Giorgi and Mearns, 1991; Fesser et al., 2011). RCMs are forced along lateral boundaries by either GCM or reanalysis, and this method has several strengths and shortcomings (Rummukainen, 2010).

In the Southern Hemisphere, climate communities have lagged behind in regional climate modelling activities when compared to other users in different regions of the world. In particular Africa, research focused on climate modelling has been minimum due to a number of factors. These include lack of computational facilities, lack of human resources, capital and inadequate climate data (Myra, 2015). Dynamical downscaling technique *efforts* over southern Africa started in the late 20th century. The initial activities were the nesting of CSIRO-DARLAM in a global climate model over the domain of southern Africa. This study showed that a limited area model could capture patterns of observed rainfall notwithstanding some biases and improve the climatology simulation of the global climate model (Joubert *et al.,* 1999).

The ability of RCMs to simulate important atmospheric features and large-scale modes of variability influencing the southern African climate has gained traction by numerous studies. For instance, Engelbrecht et al., (2009; 2011; 2015) explored with a variable resolution global model Conformal-Cubic Atmospheric Model CCAM and illustrated the capability of the CCAM as a downscaling tool at the climate-change time scale. The procedure involved applying CCAM in stretched-grid mode over southern and tropical Africa to obtain simulations of approximately 60 km resolution *(*Figure 2.9). The resolution decreased to about 400 km in the far-field. All simulations were performed on the Centre for High Performance Computing (CHPC) cluster in South Africa. The model captured the west-east gradient in rainfall distribution over South Africa well, and the relatively dry conditions that occur in a zonal band stretching from Botswana to the Limpopo River basin of South Africa and Zimbabwe (Engelbrecht *et al.,* 2015).

Early studies of the CORDEX-Africa project have focused on the models ability to simulate the spatial and temporal variability of rainfall over southern Africa. The findings (e.g. Kalognomou et al., 2013) have proved that the RCMs are important in providing useful information and add value to their driving boundary condition data. Several CORDEX studies alluded the importance of ensemble mean which generally outperformed individual RCMs. For instance, Nikulin et al. (2012) showed the individual RCMs which exhibited wet or dry biases over ensemble. The biases that occurred in these studies were linked to the model configuration and simulation of moisture transport over the region (Myra, 2015). Although, the individual model captured important aspects of El Nino and La Nina that influence rainfall over the region.

Recent results produced for the South African Weather Service (SAWS) (2017) climate change atlas, using a 9 member-ensemble mean of RCA4 RCM, showed simulated values that were more realistic in the west, although rainfall was lower than observed in the Cape Town region. Also, the models were able to capture changes over large landscape, thus the Great Highlands of Lesotho which also influences rainfall in South Africa. Shongwe *et al.* (2014) found the CORDEX models performing well in rainfall simulation of monthly austral summer seasons. The study noted some biases occurring in some models. The RCMs were able to simulate the spatial migration of the seasonal rainfall and Interannual variability. Other studies have examined the ability of the ensemble to capture patterns in the frequency and intensity of precipitation extremes (for example, Kjellström *et al.;* 2013 Pinto *et al.,* 2013). There is high confidence that the maturing of CORDEX initiatives will improve and strengthen the quality of individual model simulations and future projections.

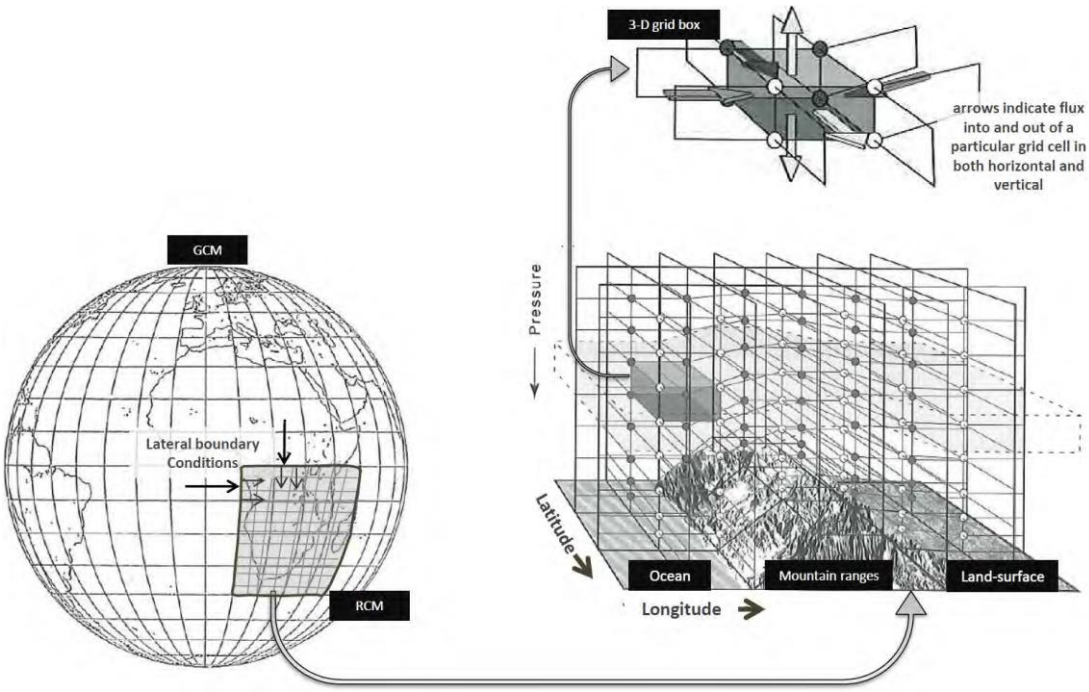

Figure 2.8 GCM output driving a RCM to simulate local conditions (ocean, mountain ranges and land surface) in 3-D at high resolution in greater detail (Source: Myra, 2015).

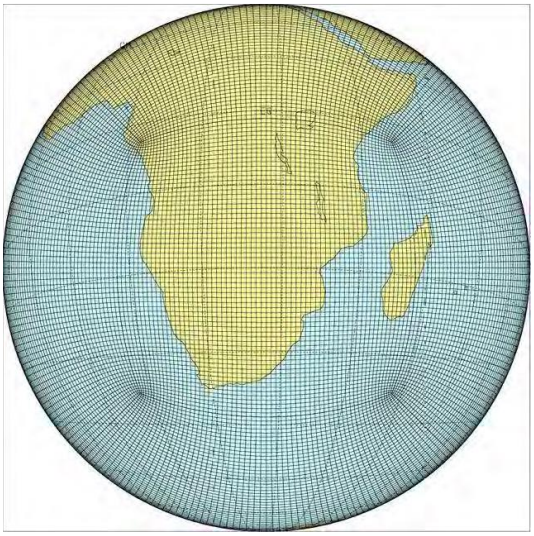

Figure 2.9. C64 stretched conformal-cubic grid over Southern Africa and tropical Africa. The resolution is about 60 km over the area of interest and decreases to about 400 km in the far-field (Source: Engelbrecht et al 2011).

2.6 Emission scenarios

Emission scenarios are different pathways that can be followed resulting in different concentrations of GHGs depending on the commitments (or lack) by different governments to reduce emissions into the atmosphere. The scenarios are based on an extensive assessment of driving forces (IPCC, 2013). Population growth coupled with the use of resources play a major role in driving the rate of carbon dioxide, Methane and Nitrous oxide emissions into the atmosphere. The Special Report on Emissions Scenarios (SRES) scenarios were used in AR4 (IPCC, 2007) and they are as follows;

- A1FI – high end of range - where a rapid rate of temperature change is driven by a continued dependence on fossil fuels and rapid economic growth throughout the next century.
- A2 – upper mid-range - for a very heterogeneous world where economic development is regionally-oriented and economic growth and technological change are relatively slow.
- B2 – lower mid-range – where the emphasis is on local solutions to economic, social, and environmental sustainability with less rapid and more diverse technological change.
- B1 – low end of range – where the focus is on global solutions to economic, social and environmental sustainability. Clean, efficient technology is introduced but no specific climate initiatives are taken.

Representative Concentration Pathways (RCPs) are an important development in climate research and provide a foundation for emissions mitigation and impact analysis (Hijioka et al., 2008; Jubb et al., 2013). They facilitate the exchange of information among physical, biological and social scientists. Development of the RCPs also brings together a diverse range of research communities that will help create fully integrated Earth-system models that include representation of the global economy and society, impacts and vulnerabilities. Wayne (2013) alluded that RCPs are meant to provide information on all components of radiative forcing that are used as inputs in climate modelling and atmospheric chemistry modelling and they should cover a period of up to 2100. The major difference between RCPs and SRES is that, the latter was based on socio-economic futures while RCP focused on radiative forcing projection and makes assumptions about future population, GDP, energy use (Wayne, 2014).

There are four RCPs named according to radiative forcing target level for 2100. The radiative forcing estimates are based on the forcing of greenhouse gases and other forcing agents (Van Vuuren et al, 2011; Chaturvedi, et al., 2012). These are RCP 2.6, RCP 4.5, RCP 6 and RCP 8.5

(Figure 2.10). The development of RCP 8.5 using the MESSAGE model and the International Institute for Applied Systems Analysis (IIASA) simplified future climate projections. It is characterized by assumptions of uncontrolled/ low mitigation emission of greenhouse gas over time (Riahi *et al.,* 2007). It aggregates assumptions of slow income growth coupled high population and uncertain rates of technological change and energy intensity improvements resulting of excessive emission of GHG.

The RCP6 was developed by the AIM modeling team at the National Institute for Environmental Studies (NIES) in Japan (Fujino *et al*., 2006). It is a stabilization scenario in which total radiative forcing is stabilized shortly after 2100, without overshoot, by the application of a range of technologies and strategies for reducing greenhouse gas emissions (Hijioka *et al.,* 2008). The RCP 4.5 is a stabilization scenario in which total radiative forcing is stabilized shortly after 2100, without overshooting the long-run radiative forcing target level (Clarke *et al.,* 2007). The emission scenario was developed by the GCAM modelling team at the Pacific Northwest National Laboratory's Joint Global Change Research Institute (JGCRI) in the United States (Thompson *et al*., 2011).

The RCP2.6 was developed by the IMAGE modeling team of the PBL Netherlands Environmental Assessment Agency. The emission pathway is representative of scenarios in the literature that lead to very low greenhouse gas concentration levels. Wise et al, (2009) described the scenario as peak-and-decline. This is because, its radiative forcing level first reaches a value of around 3.1 W/m2by mid-century, and returns to 2.6 W/m2 by 2100. In order to reach such radiative forcing levels, greenhouse gas emissions are reduced substantially, over time (Van Vuuren et al., 2007a).

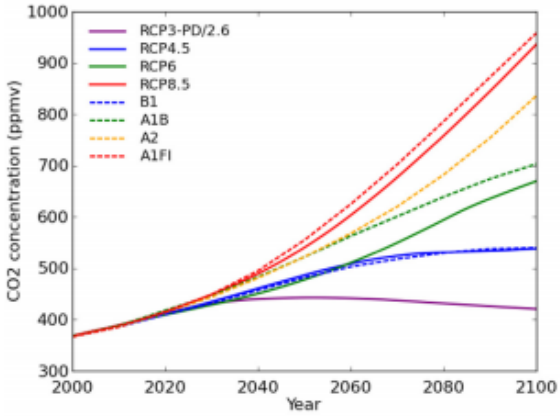

SRES	RCP	Approximate CO_2 equivalent concentrations by 2100 (ppm)
A1FI		1550
	8.5	>1370
A1B		850
	6	850
B2		800
	4.5	650
B1		600
	2.6	490

Figure 2.10. Projections of radiative forcing under different emission scenarios_SRES and RCPs (Source: Van Vuuren et al., 2011).

Table 2. 1 Description of Different RCP Scenarios for the Fifth Assessment Report (AR5) (Source: Chaturvedi, et al., 2012).

RCP	Description
RCP2.6	Radiative forcing level first reaches a value of around 3.1 W/m^2 returning to 2.6 W/m^2 by 2100. Under this scenario greenhouse gas emissions and emissions of air pollutants are reduced substantially over time.
RCP4.5	Stabilization scenario where total radiative forcing is stabilized before 2100 by employing a range of technologies and strategies for reducing greenhouse gas emissions.
RCP6.0	Stabilization scenario where total radiative forcing is stabilized after 2100 without overshoot by employing a range of technologies and strategies for reducing greenhouse gas emissions.
RCP8.5	Characterized by increasing greenhouse gas emissions over time representative of scenarios in the literature leading to high greenhouse gas concentration levels.

2.7 Summary

This chapter presented a review on previous studies relevant to the investigation of rainfall variability and projected future changes using climate models. Rain-bearing systems affecting South (*ern)* Africa, together with large scale circulation patterns that drive the systems were reviewed. The chapter summed up by reviewing models and different methodologies used by previous scholars to assess rainfall on a changing climate at given emission scenarios over Southern Africa. From the review it can be said that:

- Subtropical highs drives moisture fluxes onto the South African region via trade winds.
- The development and usage of climate models has enhanced the exploration and understanding variety of processes of climate systems.
- CORDEX RCMs can provide useful information to their driving boundary condition data.
- Single best model combination are significantly better for a single variable (e.g. precipitation) than mean ensemble model for future projection.

- Emission scenarios prescribe GHG emissions pathway for the future, hence climate models use these emissions pathway to project the future climate.
- Rainfall projections over the region is dominated by high degree of uncertainties and more focus and thorough research needs to be done.

CHAPTER 3: METHODOLOGY

3.1 Introduction

This chapter provides a full description of datasets, different models and methods of analysis used in this study. Analyzing data is important for obtaining maximum information for interpretation of climate dynamics (Mulenga 1998). The datasets employed in this study were acquired from global and regional climate centers and archives. A framework showing model forcing was then provided, GHG concentration pathways scenarios used in the study are outlined. Observations, reanalysis and model simulations span from 1976-2005 and model projections from 2006-2065.

3.2 Datasets and time periods

Precipitation is the principal variable of focus in this study. Future projections are analyzed for two 30-year periods, extending from near future (2006-2035) and far future (2036-2065), using a suitable model selected from the validation and verification process against present-day (1976-2005) climate. Models simulated long-term annual and seasonal *(averages and total accumulations)*, to generate future projected changes. Seasonal projections were considered; December-January- February (DJF), March-April-May (MAM), June-July-August (JJA) and September-October-November (SON). Annual and seasonal rainfall projections are expressed in percentages.

3.3 Observational and Reanalysis Datasets

3.3.1 Global Precipitation Climatology Centre *(GPCC)*.

GPCC precipitation data is measured by conventional (rain) gauge networks only over the global land-surface *(Figure 3.1)* (Schneider *et al.,* 2011; Schneider *et al*., 2018). It plays a crucial role in the International research community with provision for monthly precipitation analyses, based on in-situ observed data (Barrett *et al.,* 1994; Schneider *et al.,* 2011; Becker *et al.,* 2012). The GPCC's mandate is to accurately and effectively serve the user requirements with gridded precipitation availability (Rudolf *et al.,* 2011). In comparison with satellite observations, rain-gauge-based data are not subject to larger biases (Schneider *et al.,* 2011), hence adjustments, validations and verifications are very minimal. However, the usage of gauge- observed gridded data may have systematic measurement errors and incomplete observations (Rudolf *et al.,* 2011). Gauge-observed gridded precipitation is available from 1901 – present, at different spatial resolutions, these are, 2.5° x 2.5°, 1.0° x 1.0°, 0.5° x 0.5° and 0.25° x 0.25° (Rudolf et al., 2011;

Schneider *et al.,* 2011). In this study, GPCC is analyzed from 1976-2005 (present day) at a spatial resolution of 0.5° x 0.5° based on station data and also used to evaluate the simulations of models.

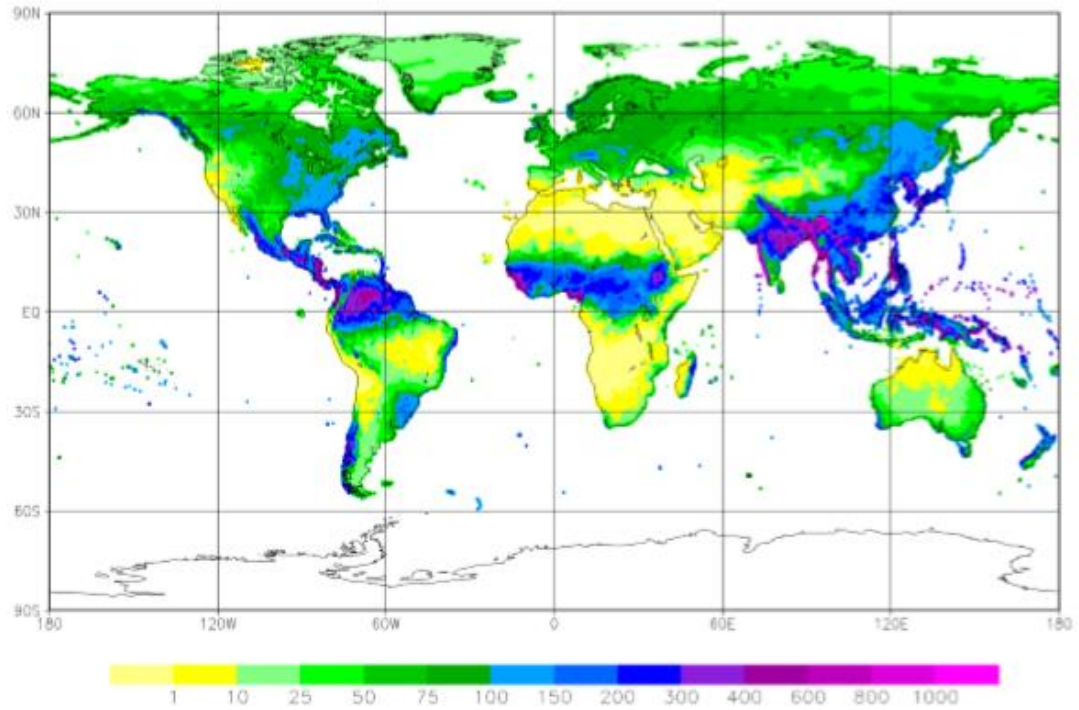

Figure 3.1 A example of climatological mean precipitation over the global-surface for July based on GPCC's 0.5°x 0.5° resolutions on the period 1950-2000 (Source: Schneider et al.,2018).

3.3.2 NOAA GHCN_CAMS Land Temperature Analysis

It is a station observation-based global land monthly mean surface air temperature dataset at latitude-longitude of 0.5°x 0.5° resolution, available from 1948 to present. It was developed recently at the Climate Prediction Center, National Centers for Environmental Prediction (CPC, NCEP). The data set tends to be different from some already existing surface air temperature data sets, such that it combines Global Historical Climatology Network version 2 and the Climate Anomaly Monitoring System (GHCN + CAMS) station observed datasets (Fan and Van der Dool 2007). For quality control purposes, the data is regularly updated in near real-time using interpolation methods. This dataset can capture most common temporal-spatial features in the observed climatology and anomaly fields over both regional and global domain (Fan and Van der Dool, 2008). This monthly mean surface air temperature data set is applied to verify the performance of model's simulation for future projections.

3.3.3 Geopotential height

Geopotential is defined as the work that must be done against the earth's gravitational field to raise a mass of 1 kg from sea level to that point (Knapp and YIN, 1996). At a particular point in the atmosphere geopotential height depends only on the height of that point and not on the path through which the unit mass is taken in reaching that point. It is used as the vertical coordinate in most atmospheric applications in which energy plays an important role. Geopotential height is used as a function of pressure, because it makes calculations more convenient (Driver, 2014). A plot of geopotential height for a single pressure level shows the troughs and ridges, highs and lows, which are typically seen on upper air charts. Thickness between difference pressure levels such as, 850 hPa and 1000 hPa heights are proportional to mean virtual temperature in that layer. Contours may also be used to calculate the geostrophic winds. The relation, in SI units, between the geopotential height Z and the geometric height z. In this study, mean geopotential height is analyzed for model validation and future prediction, at 500hPa over southern Africa.

3.3.4 Specific humidity

Specific humidity is the ratio of water vapor mass (m_v) to the air parcel's total mass (m_a) and is referred to humidity ratio (Smith et al., 1999). The SI units of measurement are grams of water vapor per kilogram of air. Given that weight is not significantly influenced by temperature or atmospheric pressure, specific humidity is much more useful as a measure of humidity. Specific humidity is an extremely useful quantity in meteorology, for example, the rate of evaporation of water from any surface is directly proportional to the specific humidity difference between the surface and the adjoining air. Furthermore, the specific humidity does not vary as the temperature or pressure of a body of air changes, as long as moisture is not added to or taken away from it (Smith et al., 1999). In this study specific humidity is also used to validate models on the present climate and future projections at near-surface (850hPa).

3.3.5 Evaporation flux

Evaporation is a process wherein liquid transforms to a gaseous state at an unrestricted surface and below the boiling point through the transfer of heat energy (Monteith, 1981). It also requires that the humidity of the atmosphere is less than the evaporating surface. Evaporation occurs owing to surface temperature, diffusion, convection or wind action. The process of convection usually occurs when water is warmer than the surrounding air. The rate per unit area ah which water vapor leaves the wet surface depends upon the properties of the overlying air and the supply of heat to the evaporating surface (Akerman, 1975). The equation is outlined as follows:

$$Ef = C\ (ew - ea) \qquad \text{(Equation 3.1)}$$

: Where *Ef* = evaporation flux (mm/day)

C = a constant

ew = the saturation vapor pressure at the water temperature in mm of mercury

ea = the actual vapor pressure in the air in mm of mercury.

In this study, evaporation flux is analyzed to determine the significant changes in a future changing climate.

3.4 CMIP5 _*GCMs* description

CMIP5 ensembles includes both Coupled Atmospheric General Circulation Models (AOGCM) and Earth System Models (ESMs) called here for brevity simply Global Climate Models (GCMs). The data is available through the ESGF website; https://esgf-node.llnl.gov/search/esgf-llnl/. A GCM is a comprehensive climate model that combines the atmosphere and ocean general circulation models, together with land and ice components (Solomon *et al*., 2007; Watanabe *et al*., 2010; Collins *et al*., 2011; Giorgetta *et al*., 2013). The global models provide a unique way of modeling the global climate. GCMs have become more useful and important tool in recent decades in addressing the issue of climate change (Watanabe *et al.,* 2010). However, these global models contain errors in various fields such as precipitation, land and sea surface temperatures. The widely used solution to such errors is to increase the resolution quality, thus from a global to a regional level (downscaling) to an extent of analyzing small-scale variables (Shaffrey *et al.,* 20 09; Watanabe *et al.,* 2010). In this study, the 5 selected GCMs of different low resolutions included; HadGEM2-ES, MIROC5, GFDL-ESM2M, MPI-ESM-LR and CNRM-CM5 (*Table 3.1*) are further described below;

Table 3. 1 Summary of GCMs, Institutes and their resolutions as used in the study.

MODEL NAME (GCMs)	INSTITUTE/ COUNTRY	RESOLUTION	LITERATURE
MIROC5	CCCMa (Canada)	1.4°X1.4°	Watanabe et al., (2011)
CNRM-CM5	CNRM-CERFACS(France)	1.4°X1.4°	Voldoire et al., (2013)
MPI-ESM-LR	MPI-M(Germany)	1.9°X1.9°	Ilyina et al., (2013)
GFDL-ESM2M	GFDL (USA)	2.0°x 2.5°	Dunne et al., 2012
HadGEM2-ES	Hadley Centre (UK)	1.8°x 1.2°	Collins et al., 2011

3.4.1 Hadley Centre Global Environment Model 2- Earth Systems *(HadGEM2-ES)*

The usefulness of climate projections depends on the accuracy and comprehensiveness of climate system. The HadGEM2 was designed for simulating and understanding the centennial scale evolution of climate (Collins *et al.,* 2011). Within the HadGEM2 family, Earth Systems *(ES)* refer to a set of models that describe the physical, biological chemical, processes within the atmosphere and the oceans and terrestrial, *Figure 3.2* (Cox *et al.,* 2000; Collins *et al.,* 2011; Martin *et al*., 2011). The particular ES model used in this study is of terrestrial and oceanic ecosystems. The system's configuration of the *ES* was the first to be run without the need of flux correction in the Met Office Hadley Centre, unlike the HadGEM1 that used artificial corrections (Cox *et al.,* 2000; Jones *et al*., 2006; Martin *et al.,* 2011). In climate models, ES allows the calculation of the impact of climate change on atmospheric composition with consistency and allows the incorporation of biogeochemical, feedbacks of climate external forces (Collins *et al.,* 2011). The HadGEM2-ES used in this study is of 1.875° x 1.25° resolution in longitude and latitude.

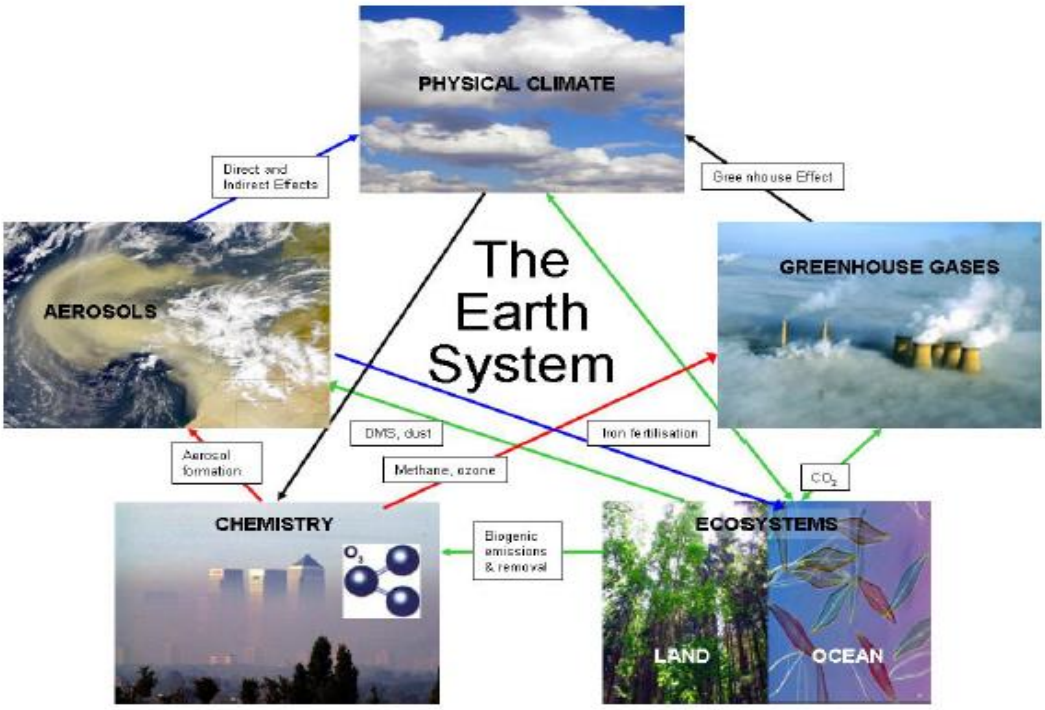

Figure 3.2 HadGEM2-ES interconnected feedbacks (Source: Collins *et al.,* 2011)

3.4.2 Model for Interdisciplinary Research on Climate Version Five *(MIROC5)*.

The Model for Interdisciplinary Research on Climate (MIROC), was developed jointly at the Center for Climate System Research (CCSR), University of Tokyo; National Institute for Environmental Studies (NIES); and Japan Agency for Marine-Earth Science and Technology (Watanabe *et al*., 2010). A new version of MIROC5 was developed based on MIROC3, but with improved atmospheric, ocean, sea-ice, land ESM components. Several previous studies, identified the MIROC5 of having improved features such as precipitation, equatorial cover, subsurface fields, and El Nino simulation and corresponded with satellite measurements that the previous MIROC3.2 model (Watanabe *et al.,* 2010; Yamazaki et al., 2009; Hurt *et al.*, 2009).

3.4.3 Geophysical Fluid Dynamics Laboratory (*GFDL-ESM2M)*

GFDL scientists played an important role in the development of two new global coupled carbon–climate Earth System Models (ESM), ESM2M and ESM2G from the previous CM2.1; to enhance our understanding the Earth's biogeochemical cycle and human's interaction with the atmospheric systems (Delworth *et al.*, 2005; Dunne *et al.,* 2013). ESM's components include physical features such as; aerosols, cloud physics and precipitation. NOAA GFDL-ESM, pressure based vertical coordinates are used along the development path of GFDLs Modular Ocean Model Version 4.1. In the study, the model used the atmospheric grid resolution of 2.0225° x 2.5° latitude and

longitude respectively. The fully coupled free running climate model ESM2M has some slight differences with ESM2G such that, ESM2M has a stronger biological carbon pump than ESM2G and reduced nutrient and oxygen biases in the southern and tropical oceans (Dunne *et al*., 2012, 2013). For this study, GFDL climate model amplified the understanding of climate variability and change at different timescales for effective future climate prediction.

3.4.4 Max-Planck-Institute Earth System Model-Low Resolution (MPI-ESM-LR)

MPI-ESM is a new version of the global Earth system model developed at the Max-Planck Institute for Meteorology in Hamburg, Germany. It is based on different Earth Systems Models (ESM) components of ECHAM6, MPIOM, JSBACH and HAMOCC for atmosphere, ocean, terrestrial and ocean's biogeochemistry respectively (Ilyina et al., 2013; Jungclaus et al., 2013; Stevens, 2013), OASIS3 being the coupler program that aggregates, exchanges fluxes and interpolates variables (Giorgetta et al., 2013). Previous researchers (e.g. Giorgetta *et al.,* 2012; Giorgetta *et al.,* 2013 and Hagemann *et al.,* 2013) used ESM with a Low Resolution (LR) on ocean and terrestrial components. MPI-ESM in the Low Resolution (LR) configuration with the atmosphere in spectral truncation of T63 and 47 vertical levels at a relatively low resolution of 1.9° x 1.9° is used in this study.

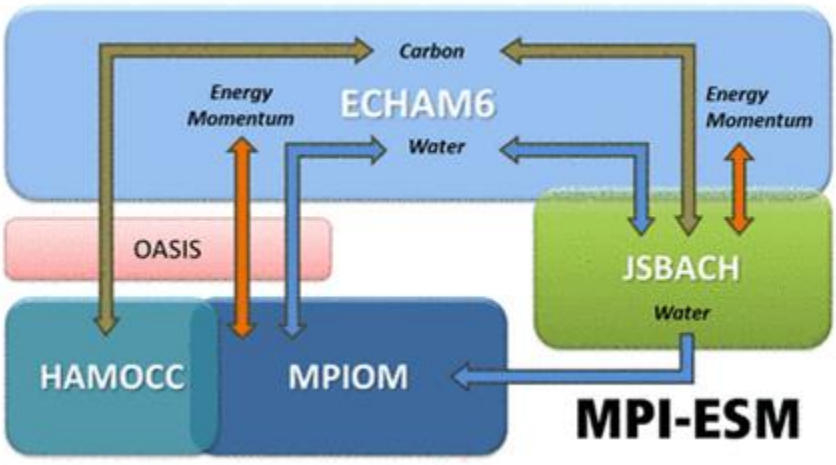

Figure 3.3 Schematic view of MPI-ESM and its components in the colored boxes (Source: Giorgetta et al., 2013).

3.4.5 Centre National de Recherches Me´te´orologiques-Climate Model Version 5 (*CNRM-CM5)*

CNRM-CM is a fundamental tool of enhancing our understanding of the climate system, performance of seasonal forecasts and future simulations on a changing future climate (Salas y Melia., 2002).Prior to the IPCC 5th Assessment report, the CM5 was developed after CM3, jointly by the *Centre National de Recherches Me´te´orologiques— Groupe d'e´tudes de l'Atmosphe`re Me´te´orologique and Centre Europe´en de Recherche et de Formation Avance´e (*CNRM- GAME and CERFACS*)* to provide an improved and updated climate model (Lucarini and Ragone., 2011; Voldoire et al., 2013). The CM5 gained popularity amongst other CNRM-CM models because it had variety component models within it. These component models include; *ARPEGE, SURFEX, NEMO, GELATO* and *TRIP*, representing the atmosphere, land-surface, ocean, sea-ice and river routing respectively (Voldoire et al., 2013). When compared with other CNRM-CMs, the CM5 has an improved horizontal resolution, new radiative scheme, improved ozone and aerosols treatment in the atmosphere (Salas y Melia., 2012). With regard to the surface climate, done by previous work done by Salas y Melia., (2012) Lucurini and Ragone., (2011), Voldoire et al., (2013), the CM5 model showed a considerately decrease hence improvement in root mean square error and mean biases. Therefore, in relation to this study, the CNRM-CM5 well suits the investigation of rainfall variability and change, due to the benefits it has over other CNMR-CM models.

3.5 CORDEX-Africa RCMs description

The use of RCMs to present appropriate spatial and temporal resolutions, reduces the uncertainty of future climatic projections because of its finer resolution than output from GCMs (Shalby et al., 2017). The spatial resolution of GCM is relatively coarse especially if applied to simulate climate change projections at a provincial scale such as South Africa. For this study, to address the limitations of spatial scale, RCMs dynamically downscale the global resolution onto a regional scale to present future climate information of South Africa. The downscaling obtained was assigned and forced across its lateral boundaries by 5 different GCMs, figure 3.4. The 3 RCMs (REMO2009, RCA4, and CCLM4-8-17) output simulations were conducted as part of the Coordinated Regional Downscaling Experiment (CORDEX)-Africa framework. The spatial grid resolutions of the CORDEX-Africa RCMs were set to longitude 0.44° and latitude 0.44°(approximately 50 km by 50 km latitude and longitude) (Luhunga *et al*., 2016).

Table 3. 2 Summary of the three Regional Climate Models used in the study.

RCM NAME	INSTITUTION	REFERENCES
REMO2009 (v1)	Helmholtz-Zentrum Geesthacht, Climate Service Center, Max Planck Institute for Meteorology (MPI-CSC)	Jacob *et al.* (2012
RCA4 (v1)	Swedish Meteorological and Hydrological Institute, Rossby Centre (SMHI)	Samuelsson *et al.* (2011)
CCLM4-8-17 (v1)	Climate Limited-area Modelling Community (CLM-Community, CLMcom)	Panitz *et al.* (2014)

3.5.1 Regional MOdel 2009 (*REMO 2009)*

The regional climate model REMO was developed at the Max Planck Institute for Meteorology in Hamburg and is based on parts of the German Weather Service EM-DM model (Rockner *et al., 2003*). It is a limited-area three-dimensional model atmospheric circulation model. The most recent hydrostatic version of *REMO2009* was developed over Europe using ECHAM4 physical parameters (Jacob *et al.*, 2012). In this study REMO2009 formed part of the CORDEX framework and dynamically downscaled the HadGEM2-ES, GFDL-ESM2M, MPI-ESM-LR and MIROC5 to a finer resolution to project rainfall in South Africa.

3.5.2 Rossby Centre regional model version 4 (*RCA4)*

The Rossby Centre of the Swedish Meteorological and Hydrological Institute (SMHI) has been developed and applying climate models since 1997 (Jones et al., 2011; Kiellstrom et al., 2016). RCA4 is the latest version and the predecessor of RCA3 model and it has been run over different CORDEX domains. It is a coupled model based on numerical weather predictions (NWP) model called *High Resolution Limited Area Model (HIRLAM)*. The primitive equation hydrostatic model uses a terrain following hybrid vertical coordinate (Giorgi and Gao, 2018). The model provides a scientific foundation for climate change modelling. In the study, RCA4 downscaled CNRM-CM5, MPI-ESM-LR, GFDL-ESM2M, HadGEM2-ES and MIROC5 and forced across lateral boundaries.

3.5.3 COSMO-Climate Limited-Area Modeling *(CCLM4)*

Developed initially by the German Weather Service and then by the European Consortium COSMO, the non-hydrostatic aimed at forecasting weather systems at high resolution (Rockel and Geyer, 2008). It provides flexible tool for different applications at favorable resolutions. The RCM COSMO CLM was later developed by the CLM-Community, in collaboration with CMCC. Bohm et al., (*2006*) alluded that, the model can be used with a spatial resolution between 1 and 50 km, regardless formulation of the dynamical equations in LM making it eligible for use at horizontal grid resolution lesser than 20 km. With respect to other regional models, the CCLM version 4 tends to continuously develop and validate meteorological versions allowing great improvement in the codes adopted in the climate studies. In this study, CCLM4 model downscaled 2 GCMs; HadGEM2-ES and MPI-ESM-LR.

3.6 GHG concentration pathways

Global atmospheric concentrations of greenhouse gases have significantly increased since the pre-industrial era, which is the main reason for global warming (Yang *et al*., 2012). The Representative Concentration Pathways (RCPs) form a set of greenhouse gas concentration and emissions pathways designed to support research on impacts and potential policy responses to climate change. RCPs are a number of four greenhouses gas concentrations paths adopted in the 5th Intergovernmental Panel on Climate Change Assessment Report 5 (IPCC-AR5) and precisely used in research and climate modelling (Moss et al., 2010; Van Vuuren et al., 2011a). RCPs describe four possible climate projections and they can be considered possible depending on how much greenhouse gases will be emitted in future. The four climate futures are RCP 2.6, RCP 4.5, RCP 6, and RCP 8.5. These RCPs consist of a possible range of scenarios for radiative forcing projections towards the year 2100. RCPs predict possible future changes in the earth's climate. Four important reasons for RCPs development include (Van Vuuren et al. 2011): covering a wider range of greenhouse gas (GHG) concentrations, a need for a wider set of parameters, scenarios covering mitigation and adaptation issues and the use of more recent insight into trends in scenario drivers. In this study, RCPs for a low mitigation resulting in high baseline greenhouse gas concentrations (RCP 8.5) and for to low mitigation (RCP 4.5) climate change are used to determine the likely future climate of South Africa.

RCP 8.5 was developed using the MESSAGE model and the IIASA Integrated Assessment Framework by the International Institute for Applied Systems Analysis (IIASA). This RCP is characterized by increasing greenhouse gas emissions over time, representative of scenarios in the literature that lead to high greenhouse gas concentration levels (Riahi *et al,* 2007). RCP 4.5

was developed by the GCAM modelling team at the Pacific Northwest National Laboratory's Joint Global Change Research Institute (JGCRI) in the United States. It is a stabilization scenario in which total radiative forcing is stabilized shortly after 2100, without overshooting the long-run radiative forcing target level (Clarke *et al*., 2007; Wise *et al.,* 2009).

Scenarios describe plausible trajectories of different aspects of the future that are constructed to investigate the potential consequences of anthropogenic climate change (Van Vuuren *et al* 2011). Scenarios represent many of the major driving forces - including processes, impacts (physical, ecological, and socioeconomic), and potential responses that are important for informing climate change policy. Scenarios for AR5 can also specify a *process* (IPCC, 2013).

3. 7 Analysis Methods

3.7.1 Pearson correlation coefficient

The Pearson correlation coefficient is a degree of association between two variables (Asuero et al., 2006; Hall 2015), alluded that, when conducting a statistical test between two variables, it is advisable to conduct a Pearson correlation coefficient value to determine just how strong the relationship is between the given variables. Generally, the coefficient value ranges between 0 and 1.00, hence if a value lies on the negative range, it means weak correlation and vice versa. In this study, correlation coefficient is used as a useful tool in model's validation for annual rainfall.

3.7.2 Standard Deviation (SD)

SD is a measure that is used to quantify the amount of dispersion of a set of data values (Wachs, 2009). A low standard deviation indicates that the data points tend to be close to the mean of the set. Hence, a higher standard deviation indicates that the points are spread out over wide range of values. It is also the square root of the variance. In this study, models are statistically validated on annual basis. The formula for standard deviation is:

$$s = \sqrt{\frac{\sum_{i=1}^{N}(x_i - \overline{x})^2}{N-1}}. \qquad \text{(Equation 3.2)}$$

Where: (x_1, x_2,) are the observed values of the sample items, $\overline{x}$, is the mean value of these observations, and *N* is the number of observations in the sample.

3.7.3 Root Mean Square Error (RMSE)

The RMSE has been used as a standard statistical metric measure model performance in several studies such as air quality, meteorology and climate research studies (Chai and Draxler, 2014). It measures average deviation from the true value, hence it cannot be calculated unless the true value is known (Chimbala, 2014). Usually it is expressed as a percentage error, multiplied by 100%. RMSE acts a standard metric for model errors.

$$RMSE = \sqrt{\frac{\sum_{i=1}^{n}(P_i - O_i)^2}{n}} \qquad \textit{(Equation 3.3)}$$

Where: P_i = projected values

:O_i = observed values

3.7.4 Case study Approach

Case study involve an in-depth place/event-based research that focuses on a particular exposure unit. Through events of past events, it allows the exploration and understanding of complex issues (Zainal, 2007). It can be considered a robust research method particularly when a holistic, in-depth investigation is required. It has become a prominent tool in climate research (Crowe *et al*., 2011). In some case studies, an in-depth longitudinal examination of a single case or event is used. Harrison et al., (2017) alluded that, examination provides a systematic way of observing the events, collecting data, analyzing information, and reporting the results over a long period of time. For this study, the approach was used to investigate the performance of models on simulating geopotential height at 500 hPa for (1991/92) and 1999/00 extreme weather events, thus, (dry spells) and wet spells over South Africa.

3.7.5 Trends analysis

A trend is a significant change over time exhibited by a random variable, detectable by statistical parametric and non-parametric procedures (Longobardi and Villani, 2010). Trend analyses, on different spatial and temporal scales, has been of great concern during the past century because of the attention given to global climate change from the scientific community. In this study time series are aggregated for inter-annual variability to assess the changes in rainfall 1976-2005 for baseline comprising of GPCC observations and model outputs and future trends which will include the best model from the validation phase. The trend analysis is constituted within a time series which is calculated as follows;

- Trend (Tt) - long term movements in the mean
- Cycles (Ct) - other cyclical fluctuations
- Residuals (Et) - other random or systematic fluctuations

The technique applies these elements to create separate models and the trend analysis is given by Xt = Tt + It + Ct + Et or multiplicatively Xt = Tt x It x Ct x Et.

3.7.6 Anomalies analysis

Anomalies are deviations from what is standard or normal (Hansen et al., 2012). They allow more accurate descriptions over larger areas than actual fields and also provide a frame of reference that allows easier analysis. Standardized inconsistencies may likewise be dictated by dividing anomalies with the long-term standard deviation. Values can be either positive or negative. The positive values indicate an above normal distribution while negative values indicate below normal. In this study, anomalies are used to analyses future changes of rainfall, temperature (annual and seasonal mean).

3.7.7 Composite analysis

Composite analysis is used in climatological studies to show common occurrences and characteristics for selected years or seasons investigated. The technique is similar to correlation analysis, as it shows better trends as compared to trends shown by individual cases (Chikoore, 2005). It is a technique used for studying structures of synoptic disturbances by displaying common features for a group of cases, which are not easily identified by individual cases as it depicts relationships within meteorological variables (Keshavamurty and Rao, 1992). In the current study, composite rainfall patterns associated with extreme weather events (dry and wet spells) over South Africa are analyzed from 1976-2005.

3.8 Grid Analysis Display System (GrADS)

Grid Analysis and Display System (GrADS) was developed by the Centre for Ocean-Land Atmosphere Studies (COLA). GrADS is a visualization tool or software that allows for displaying and manipulating earth science data. It can be used on binary, GRIB, NetCDF and HDF-SDS formats. All observed and reanalysis fields plots in this study are visualized using GrADS. The visualization tool was also used to map, model simulations as well as future projections. Several studies (e.g. Zhao and Dirmeyer, 2004; AWS, 2017), used GrADS for plotting spatial maps, therefore this study also used the system.

3.9 Summary

This study endeavors to answer the key research questions and use the outlined methodology to provide the final results and outcomes. It considers the specific objectives outlined in the study and the improvements done by other researchers in this field and other related hydro-meteorological fields that can contribute in understanding the variability and change of rainfall over the region. Daily precipitation, daily surface temperature, geopotential height at 500hPa model's data were extracted from https://esgf-node.llnl.gov/search/esgf-llnl/**.** 5 GCMs that provide lateral boundaries for 3 RCMs are described, as well as the RCMs, including their resolutions. Correlation co-efficiency, standard deviation and root mean square error are used for model validation calculated on Microsoft Excel. Grid Analysis Display System GrADS was used to visualize spatial, interpretation spatial maps for present-day and future projections.

CHAPTER 4: MODEL VALIDATION

4.1 Introduction

Climate models have proven their skill in reproducing past observations which provides confidence that at least part of the climate system is well described (Bellprat et al., 2013). It is important to first verify present-day model simulations against observations before any future climate projections can be done. This is because, one can argue that if model (s) performs well in reflecting observed climate in its present-day simulations, then the model may also perform well in future climate projections. In this study three Regional Climate Models (RCMs) with a horizontal grid spacing of about 0.4° forced with 5 different CMIP5 GCMs forming part of the CORDEX-Africa framework are analyzed. One RCM, RCA4 was forced with all five GCMs, while REMO2009 was nested within four of the GCMs. CCLM4-8-17 was nested within three of the GCMs. The models are individually evaluated by comparing present day climate with observations and reanalysis fields. The validation process focuses on the ability of models to reproduce the spatial and temporal variation of climate variables such as rainfall against observations in South Africa. A multi model comparison is performed in this chapter to investigate whether the model(s) are reliable and produce confident results that are consistent with observational and reanalysis data. This study also compares simulations forced with the same GCMs, versus simulations made with the same RCM but forced with different GCMs to investigate the biggest source of uncertainty in the simulations.

4.2 Inter-annual rainfall variability

An important measure of model performance (both GCMs and RCMs) is found in whether the model possesses the ability to capture the inter-annual variability in rainfall. The present- day runs are also forced with observed SSTs. South Africa is characterized by significant rainfall variability on inter-annual and longer timescales (Reason et al., 2005). In relation to the time series, Figure 4.1, GPCC observations showed a decreasing values (1976-1981), similar to MPI_CCLM4-8-17 and HadGEM2_RCA4, unlike all downscaling produced by REMO2009 which showed an increase. This result suggests that the increase in rainfall during the mentioned period in REMO2009 simulations is informed by the RCM itself because other RCMs forced with the same GCMs capture the decrease in rainfall. MPI_CCLM4-8-17, MPI_RCA4, HadGEM2_RCA4 and CNRM_CCLM4-8-17 well captured ‘dips’ which represent drought seasons corresponded to GPCC, which indicates differences in performance by different GCMs. The seasons that were captured by the listed models include 1982/83, 1983/84, 1984/85, 1991/92 and 2001/02. Reason et al., (2005) alluded that droughts were attributed to the maturing phase of El Niño, hence the

region tended to be dominated by substantial high pressure and offshore shifts of the local circulations which were associated with strong subsidence over the interior.

Dry spells may also be due to mid- latitude circulation dominantly on the south-west of South Africa, intensifying the advection of cool moisture and dry air from the Atlantic Ocean. The weakening of anticyclone on the South Atlantic and insufficient inflow of moist tropical air from the Seychelles-Chagos Thermocline Ridge could have also influenced the dryness conditions, (Dilmahamod, 2014). An example of 1991/92 dry season (Figure 4.2), all the downscaling's of REMO2009, RCA4 and CCLM4-8-17 that were nested within HadGEM2 captured ridges similar to the reanalysis. MPI, GFDL, MIROC5 on REMO2009 and RCA4 completely failed to capture "dips" during the well-known dry seasons mentioned above. Instead, the models exceptionally opposed the GPCC observations and showed peaks (wet and troughs spreading over the interior at mid-levels).

Geopotential heights give an indication of processes taking place in the large scale. An RCM that performs well is expected to reproduce the large scale systems as provided by the GCMs. As a result, geopotential height RCM simulations forced by the same GCM are expected to be almost similar, while the high resolution of the RCMs helps with the simulations of smaller scale processes. This is in line with the thinking that "garbage in garbage out", meaning if the input from the GCM is not useful, the RCM cannot be expected to perform well because it relies on the GCM solutions which are fed to it on its lateral boundaries. As expected (e.g. Figure 4.2) there are large similarities in simulations made with different RCMs but forced with the same GCMs. MPI is the best example of this situation, where the GCM clearly didn't reflect the large scale circulation with skill, and downscaling reproduced the results.

From 1994/95 to 1999/00 seasons on Figure 4.1, simulations made with RCA4 and REMO2009 nested within HadGEM2 were consistent with the GPCC, which showed a steady increasing trend, though rainfall totals varied. The higher rainfall amounts might be linked to the La Nina phase of ENSO, for instance, the summer season of 1999/00 where above average rainfall was experienced and resulted in widespread flooding over the Limpopo basin and adjacent areas (Chikoore et al., 2015). Simulations made with REMO2009, RCA4, and CCLM4-8-17 nested within HadGEM2; as well as the two nested within CNRM outperformed the rest of the models by showing extensive troughs at mid-levels corresponding to the reanalysis field (Figure 4.3). The season was characterized by enhanced southwestward advection of moist tropical air from the northern Mozambique Channel region (propagation of tropical cyclone Eline), linking with an

anomalous trough extending NW–SE across Limpopo basin, favouring the development of cloud-bands (Reason et al., 2005; Malherbe et al., 2011).

4.3 Annual rainfall accumulation

All the models are able to capture a west-east annual rainfall gradient (Figure 4.4). The details of the simulated rainfall pattern are however different across the different GCMs. Unlike with the geopotential height simulations, the rainfall simulated pattern seem to be more informed by the individual RCMs. For example all RCA downscaling looks patchy, with some being wetter than others. The simulation nested within MIROC shows the largest wet region over the eastern parts of the country. Simulations nested within MIROC show the largest rainfall extent over the eastern half of the country. This is in contrast to HadGEM2 whose dry western area almost matches the observations in all the regional simulations. However two of the simulations nested within HadGEM2 underestimate the rainfall over the Western Cape. Most of the models displayed a zonal belt of dry conditions (less than 500 mm/year) over Botswana and Namibia, extending over the Limpopo River Basin of both South Africa and Zimbabwe. This is maybe linked to the dominance of strong mid-level westerlies and semi aridity nature may also be induced by the descending limb on the Hadley Cell, (Figure 4.5). Tyson and Preston Whyte (2000) alluded that, the general mean circulation over southern Africa is anticyclone, and hence the mean annual visibility of the Botswana High over the interior could exacerbate the nature of the region.

Pronounced maximum rainfall over the interior Highveld of South Africa and the north-eastern highlands of Lesotho (windward side) is evident and overestimated by most models. A similar study by SAWS (2017), using RCA4 with different driving GCMs, found models overestimating rainfall over complex topography. Simulations made with the CCLM4-8-17 produced the least amount of rainfall and therefore is not associated with large rainfall overestimations. MIROC which is associated with the largest overestimations was not used to force CCLM4-8-17. One shortcoming of the *GPCC* data is that rainfall patterns may be misrepresented in areas with low density of weather stations data (Dedekind *et al*., 2016) for instance, over the Great Escarpment and north-eastern Highlands of Lesotho, which plays a crucial role in topographic rainfall in South Africa. Oceanic currents play a crucial role in moisture flux convergence along the east coast of South Africa (Banacos and Schultz, 2005). High concentrated total values (above 2000 mm/year) along the south and eastern coast of South Africa are evident in a number of REMO2009 simulations. Ridging high pressure systems contribute most to the mean annual rainfall (46%) along the coastal parts of South Africa (Engelbrecht et al., 2015). In general, when comparing with the other models, CCLM4-8-17 *and* RCA4 regional models succeed in reproducing the most

important averaged annual rainfall totals in both spatial distribution and magnitude of values, in relation to the *GPCC* observations, although very slight overestimations are noted in some few areas. The REMO RCM simulations general preformed poor, as far as the statistics are concerned, and they also display weak annual correlation, highest RMSE and deviation (*Table 4.1).*

Table 4.1 Standard deviation (STDEV) and Root Mean Square Error (RMSE) calculations for 12 model combinations against rainfall observation for annual timescale, from 1976-2005).

ANNUAL (1976-2005)		
MODEL	STDEV	RMSE
GPCC_Observation	67,96606	--------
CNRM_CCLM4-8-17	73,87039	120,387
CNRM_RCA4	71,52965	171,874
GFDL_REMO2009	86,76649	367,5623
GFDL_RCA4	77,04283	160,4559
HadGEM_CCLM4-8-17	61,60785	117,1778
HadGEM_RCA4	69,49575	85,80907
HadGEM_REMO2009	85,40017	324,6708
MIROC5_RCA4	81,78479	224,0831
MIROC5_REMO2009	69,11415	385,7997
MPI_CCLM4-8-17	45,72206	120,277
MPI_RCA4	79,14301	120,552
MPI_REMO2009	78,06431	294,9295

4.4 Annual rainfall cycle

All the models managed to capture the general annual cycle over South Africa, with winter months generally having low rainfall accumulations, with more precipitation during austral summer (Figure 4.6). GPCC denoted a smooth rise and reached its peak during the early-mid-summer. Such findings agree with Nikulin et al., (2012) in alluding the role of SIO and lower easterly winds in the lower tropospheric of advection warm moist towards the coastal interior. In contrast, REMP2009 forced with GFDL and MPI, and RCA4 nested within CNRM, exhibited late summer peaks during March and April. MIROC5- RCA4; MPI-CCLM4-8-17 and CNRM-CCLM4-8-17 showed some fluctuation during mid-late summer. May through July was characterized with a steady cessation for all the models except for GFDL on REMO2009 which showed a steady rise.

4.5 Mean annual temperatures

All the models succeed in simulating general mean annual temperatures in relation to the observed, over the region (Figure 4.7). Warmer conditions in the northern, northeastern and east-

coastal parts of the country are simulated by all models. Low values, thus cooler conditions over the eastern parts of the Lesotho highlands were captured in all the models. Some simulations were characterized by lower values in areas that are generally hot and dry almost throughout the year, for example Northern Cape and North West. For instance, RCA4 models nested with in all its GCMs Slightly lower differences in model (s) simulations comparing with observations, are noted as far as annual analysis are concerned. It may be noted that models generally perform better when simulation temperature compared to rainfall. The spread in temperature simulations is always smaller and therefore the uncertainty associated with temperature is smaller than that associated with precipitation. Warmer conditions observed almost over the entire country, significantly link with high observed actual evaporation-transpiration values (Figure 4.8). However, all the models simulated low values of evaporation in relation to the observations. The REMO 2009 simulations nested within the various GCMs correspond slightly better with observations over the interior compared to the rest of the models. Comparing Figure 4.7 and figure 4.8, the regions that are the cooler eastern half has somewhat higher evaporation values than the warmer western half of South Africa. Perhaps, soil moisture is too low in the models compared to the observed.

4.6 Seasonal mean rainfall

South Africa is one of the unique countries in the southern African region to receive rainfall throughout all seasons (Shongwe et al., 2009; Qwabe, 2014; Dedekind et al., 2016). All the model simulations adequately captured the east-west and north-south rainfall annual gradient as discussed earlier. In this section the rainfall as simulated for different seasons is discussed, and compared to the GPCC observation.

4.6.1 December-January-February (DJF) mean rainfall

South Africa receives the bulk of its rainfall during December-January-February (DJF) months. The combination of Temperature Tropical Troughs (TTTs) constitutes to almost 70% of rainfall in South Africa (Dedekind et al., 2016). The simulated rainfall distribution is very diverse across the different models (Figure 4.9). Some of the observed features of the DJF rainfall such as a dry corridor extending from eastern Botswana towards the Low-veld of Limpopo valley of South Africa were exceptionally well captured by the CCLM4-8-17 model nested within CNRM, HadGEM2-ES and MPI. This explains that the area is too dry. A huge inconsistency of other models' simulations was noted, such that an extremely wet belt, above 8 mm/day average over the east and south coastal parts through the Highveld of South Africa by REMO2009 nested within GFDL, MPI, and MIROC5 than the actual observations. Such inconsistency in simulations might be attributed to

differences in model physics. An area of high rainfall over the eastern escarpment and north east highlands of Lesotho is well captured by all the models and GPCC observations. The regional simulations nested within CNRM model for instance CCLM4-8-17 underestimated rainfall over most of the eastern parts of the country. The simulations nested within MIROC appear to be wettest, however, these agree best with the observations on this season.

4.6.2 March-April-May (MAM) mean rainfall

The rainfall pattern during the autumn season is somewhat similar to the summer however with reduced rainfall totals (Figure 4.10). The observed plot shows these reduced totals in rainfall, with some rainfall showing over the Western Cape where it is not observed on the DJF map. All the simulations where REMO was used to downscale the four GCMs simulate rainfall across the southern coast, including the Western Cape. This feature was also found in the DJF plots which suggests that the REMO model overestimates rainfall over the Western Cape. Most eastern parts of the country such as Kwa-Zulu Natal coasts showed significantly low average rainfall (at-most 4 mm/day.), while in the western part, below 3mm average are observed. Rainfall usually decrease in the east compared to the DJF season, during this transition season as shown by Kruger and Nxumalo (2017). However, almost all the model simulations overestimated rainfall over most of the eastern half of the country. Simulations nested within CNRM produce the least amount of rainfall as was the case for the DJF season. The position of the maximum rainfall in both simulations does not match the observations, with the simulated regions producing more rainfall than observed. Simulations nested with MIROC produce a lot of rainfall overestimation, with REMO2009 producing the most rainfall and somewhat showing high STDEV and RMSE *(Table 4.2b)*. RCA4 nested within MIROC produces the most rainfall compared to other RCA4 simulations. Of all the RCMs, REMO2009 produces the most rainfall compared and this result was also observed for the DJF season. CCLM4-8-17 is associated with the least amount of simulated rainfall and appears to correspond better with observations.

4.6.3 June-July-August (JJA) mean rainfall

Winter (JJA) season is strongly governed by the strengthening of lower and mid-levels subtropical high-pressure belts over the southern Africa region. Concurrently, other dominant summer systems such as the ITCZ weaken and shift northwards of the equator (Dedekind *et al.,* 2016). The circulation change is characterized by suppressed rainfall as a result of sinking air over the region, resulting in no rainfall over most of the interior. Rainfall along the southern coast and adjacent interior results mostly from cold fronts and ridging anticyclones during this season. CCLM4-5-17 simulations are found here to be associated with the least amount of rainfall. All the

simulations do overestimate the rainfall over the eastern parts of the country, and only the simulation nested within MPI captures the rainfall over the Western Cape. REMO2009 is once again associated with the most rainfall and all the simulations capture the rainfall along the Western Cape and south coast. This result is not indicative of the model being able to capture the interannual variability over the Western Cape because this rainfall is also simulated during summer and autumn. RCA4 also overestimates rainfall over the eastern parts of the country and three of the simulations capture some of the rainfall over the Western Cape, though characterized by mean lowest STDEV and RMSE (*Table 4.2c)*.

4.6.4 September-October-November (SON) mean rainfall

Spring season is characterized by the revival of warm temperatures over the land and adjacent ocean and suppression of influential high pressure systems generate rainfall over the coastal areas (Shongwe et al., 2014). As shown on Figure 4.12, observations show a positive response to the warming SIO, such that average values of 5 mm/day are visible over coastal KwaZulu Natal and progress towards Mpumalanga and decreasing values on the south coast and Cape Town. Simulations nested within CNRM again produce the least amount of rainfall compared to simulations made with other models. All the models do capture the rainfall over the eastern parts of the country with different distributions and totals. Some rainfall is still observed over the Western Cape as some remaining mid latitude system continue to form and result in some rainfall in this region. REMO 2009 continues to simulate the most rainfall especially over the south coast and the Indian oceans and also having highest STDEV and RMSE than the rest of the models (*Table 4.2d)*. Three of the five simulation with RCA4 capture the rainfall over the Western Cape during spring.

Table 4.2 Standard deviation (STDEV) and Root Mean Square Error (RMSE) calculations for 12 model combinations against rainfall observation for ***a)*** DJF, ***b)*** MAM, ***c)*** JJA and ***d)*** SON seasons from 1976-2005).

DECEMBER- JANUARY- FEBRUARY (DJF)

MODEL	STDEV	RMSE
GPCC_Observation	14,824	---------
CNRM_CCLM4-8-17	14,96973	27,435
CNRM_RCA4	13,68078	22,718
GFDL_REMO2009	14,05084	27,461
GFDL_RCA4	12,61515	19,529
HadGEM_CCLM4-8-17	10,20818	24,422
HadGEM_RCA4	13,09241	21,617
HadGEM_REMO2009	13,98121	25,291
MIROC5_RCA4	17,90743	37,78
MIROC5_REMO2009	11,76866	39,051
MPI_CCLM4-8-17	13,01342	17,569
MPI_RCA4	9,942175	16,785
MPI_REMO2009	8,494521	22,362

a)

JUNE-JULY-AUGUST (JJA)

MODEL	STDEV	RMSE
GPCC_Observation	5,180034	---------
CNRM_CCLM4-8-17	7,436475	10,362
CNRM_RCA4	7,413827	17,465
GFDL_REMO2009	10,88114	47,221
GFDL_RCA4	9,173563	18,96
HadGEM_CCLM4-8-17	7,753739	10,998
HadGEM_RCA4	7,887109	12,564
HadGEM_REMO2009	13,013	36,915
MIROC5_RCA4	5,890231	9,29
MIROC5_REMO2009	8,652274	32,068
MPI_CCLM4-8-17	6,82418	10,989
MPI_RCA4	6,692744	9,267
MPI_REMO2009	8,574105	32,524

c)

MARCH- APRIL- MAY (MAM)

MODEL	STDEV	RMSE
GPCC_Observation	13,22821	---------
CNRM_CCLM4-8-17	13,09375	20,031
CNRM_RCA4	7,413827	19,921
GFDL_REMO2009	15,80999	40,567
GFDL_RCA4	15,42996	26,745
HadGEM_CCLM4-8-17	11,04595	17,841
HadGEM_RCA4	11,60665	19,127
HadGEM_REMO2009	11,23814	39,27
MIROC5_RCA4	11,91824	26,839
MIROC5_REMO2009	11,52475	42,512
MPI_CCLM4-8-17	14,93099	21,532
MPI_RCA4	12,74399	21,041
MPI_REMO2009	12,67562	34,33

b)

SEPTEMBER-OCTOBER-NOVEMBER (SON)

MODEL	STDEV	RMSE
GPCC_Observation	12,3967	---------
CNRM_CCLM4-8-17	8,919075	18,246
CNRM_RCA4	8,653302	14,828
GFDL_REMO2009	8,841218	27,094
GFDL_RCA4	7,368635	14,4176
HadGEM_CCLM4-8-17	11,45752	16,697
HadGEM_RCA4	11,07736	15,188
HadGEM_REMO2009	10,51006	29,1376
MIROC5_RCA4	11,00317	20,1361
MIROC5_REMO2009	9,201287	29,84319
MPI_CCLM4-8-17	8,441526	17,8471
MPI_RCA4	10,86727	20,251
MPI_REMO2009	14,39442	27,8125

d)

4.7. Mean seasonal temperatures

4.7.1 December-January-February (DJF) mean temperatures

High temperatures are observed over most areas in DJF, for example, a belt of hot conditions exceeding an average of 30°C is noted over the northwest parts of South Africa through the southern parts of Botswana and Namibia (Figure 4.13). This may be attributed to existence of the Kalahari Desert, which experiences a gradual increase in near–surface temperatures yearly (Engelbrecht et al., 2015). Heat waves and prolonged periods of subsidence may typically occur over such areas, as was also shown by Engelbrecht *et al*., (2015). The models underestimated these observed temperatures, especially the very hot tongue that appears on the border of South Africa, Botswana and Namibia. The temperature pattern that reflects the topography of the region is however well captured by all models which is indicative of their high resolution. Two simulations nested within HadGEM2 (i.e. REMO2009 and CCLM4-9-17) have indications of the tongue mentioned at the border of the three countries. Simulations nested within CNRM which were associated with the least amount of precipitation also underestimate the observed temperature. It is also not obvious from the plots that REMO2009 which was associated with the most simulated rainfall has lower temperatures. Over most parts of the interior, especially the Highveld, cooler temperatures, lower than observed temperatures were generated by all the models. This may be linked to the excessive rainfall, cloud cover and more latent heat, thereby reducing temperatures.

4.7.2 March-April-May (MAM) mean temperatures

Some simulations showed high values characterized by darker spots (above 29°C) than observed over the northern parts of the country. The variability of temperatures with change of seasons was minimal over these areas (Figure 4.14). In general, there is no standard definition of heat waves, though, Dosio (2017), defined as an extended period of excessively hot weather on consecutive days on which temperatures are well above normal. Conclusively, all the models performed well in capturing the cooling of temperatures over the interior Highveld and Low-veld.

4.7.3 June-July-August (JJA) mean temperatures

In general, during winter (JJA) season, observed temperatures are lower over of almost the entire country than the rest of the models. Subtropical high-pressure systems intensify towards and over the land, so as the Botswana high is activated (MacHutchon, 2006). All the models simulated relatively lower temperature fields over most of the Highveld, in particular Lesotho highlands. The models generally overestimated the JJA temperatures. This was also observed for the DJF

season where models underestimated the high summer temperatures (Figure 4.15). This explains that JJA winter temperatures were not well represented by most of the models over the low-veld, hence there is little agreement between observations and model simulations. As the seasons progress to SON (Figure 4.16), all the models managed to well capture a transition of temperatures from JJA throughout the region in relation to the observations. Over the western parts of the country warmer temperatures were simulated to rejuvenate at a faster rate than the surrounding areas.

4. 8 Summary

In this chapter, annual rainfall accumulations, mean annual temperatures and seasonal average simulations were plotted and analyzed in relation to observations and reanalysis fields. Different cases (1991/92 and 1999/00 DJF seasons) of extreme events, were used to assess the capability of model (s) to reasonable match the present-day. Rainfall as the primary data understudy, was also studied at inter-annual timescale to determine its variability with respect to models and GPCC. Therefore, it is important to note that fundamental findings of this chapter are:

- Each regional climate models displayed different signature on simulations, rainfall in particular because this is a variable that is affected most by sub-grid process.
- REMO2009 consistently simulated the largest amount of rainfall during all the seasons and also produced rainfall over the Western Cape throughout the year.
- RCA4 was characterized by scattering extreme rainfall (dark blue) noticeable over the north-eastern highlands of Lesotho and on the Highveld.
- CCLM4-8-17 was associated with least amount of simulated rainfall.
- Simulations nested within CNRM produced the least amount of rainfall across all seasons.
- The Interannual variability of both rainfall and temperature is underestimated in all the models, with lower than observed DJF, and higher than observed temperatures in JJA captured by all models.
- Simulations nested within MIROC generally result in more precipitation than simulations forced with other GCMs.
- HadGEM2 large scale patterns generally resembles the observations
- A combination of HadGEM2_RCA4 models is used for future projection, because it corresponded better with observations, (having highest correlation, lowest RMSE and deviation) than the rest of the models, shown on Figure 4.4. The model became part of

the few managed to well capture famous seasonal climate events (*noted from different literature*) corresponding to observations.

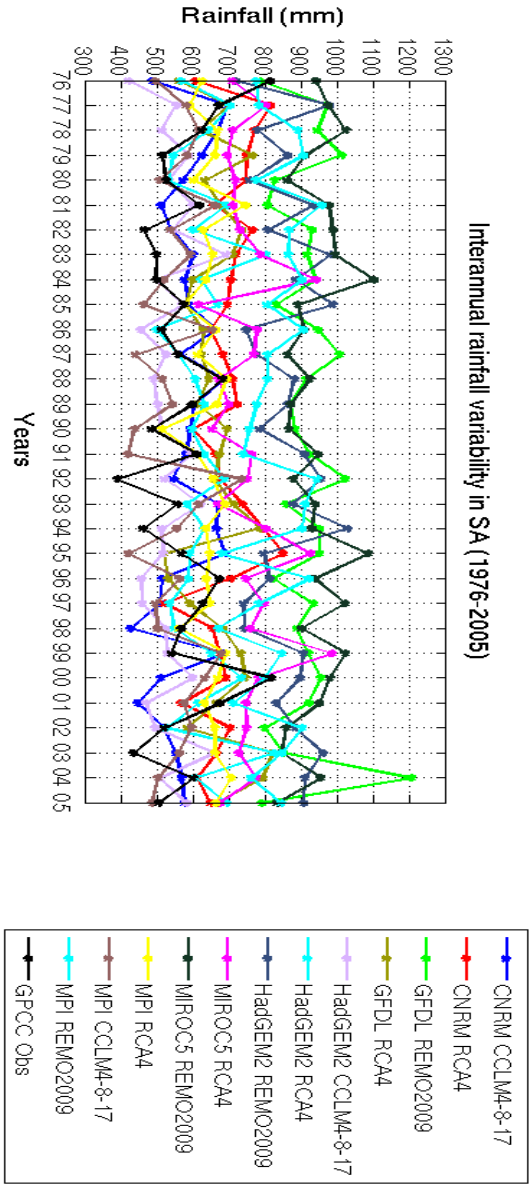

Figure 4. 1 Inter-annual rainfall variability, comparing Global Precipitation Climatology Centre (GPCC) precipitation to 12 models (GCMs forcing on RCMs), for the period 1976-2005 over South Africa.

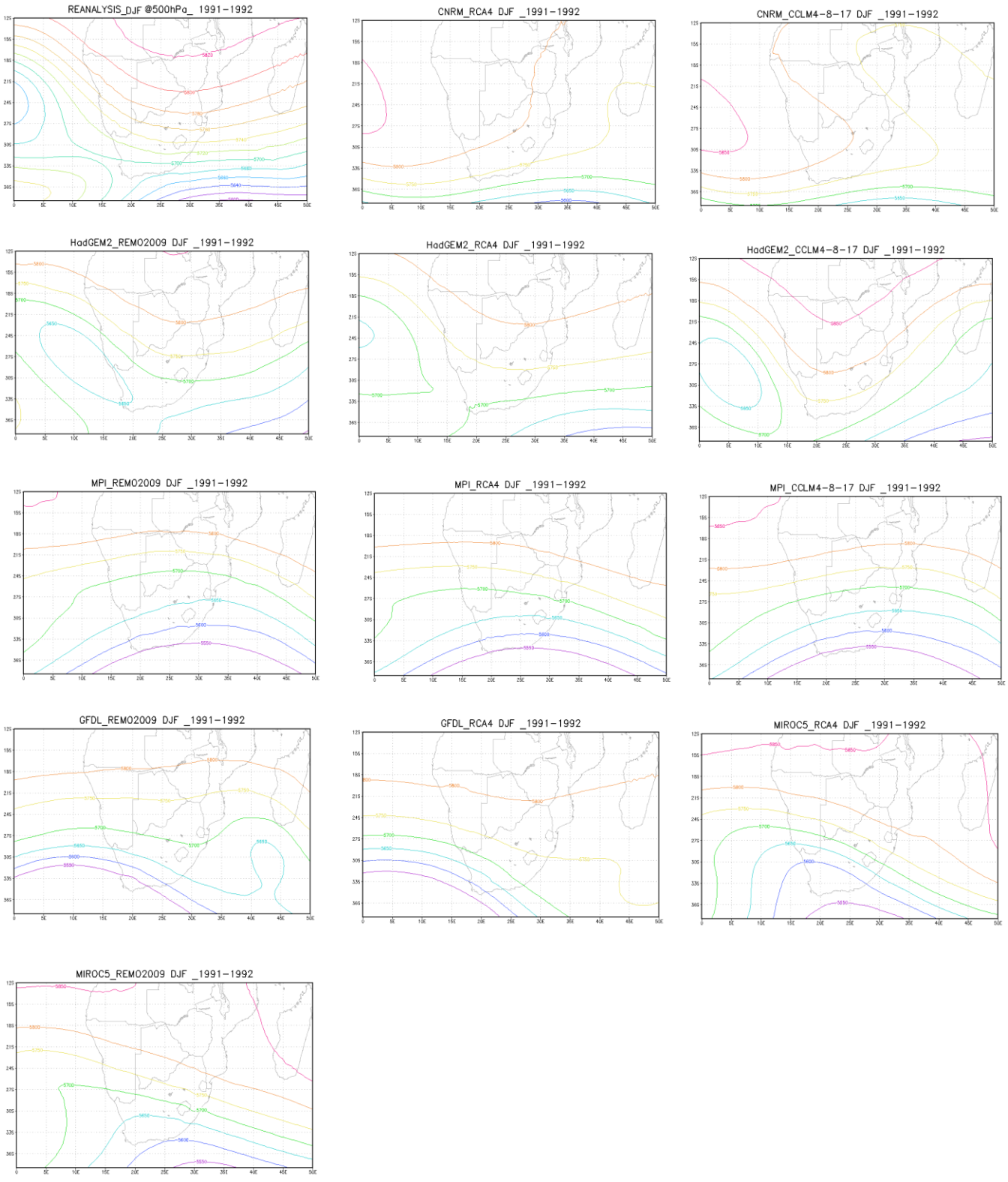

Figure 4. 2 Case study for 1991/92 DJF season, comparing Geopotential height @500hPa Reanalysis (top-left) to 12 models (GCMs forcing on RCMs).

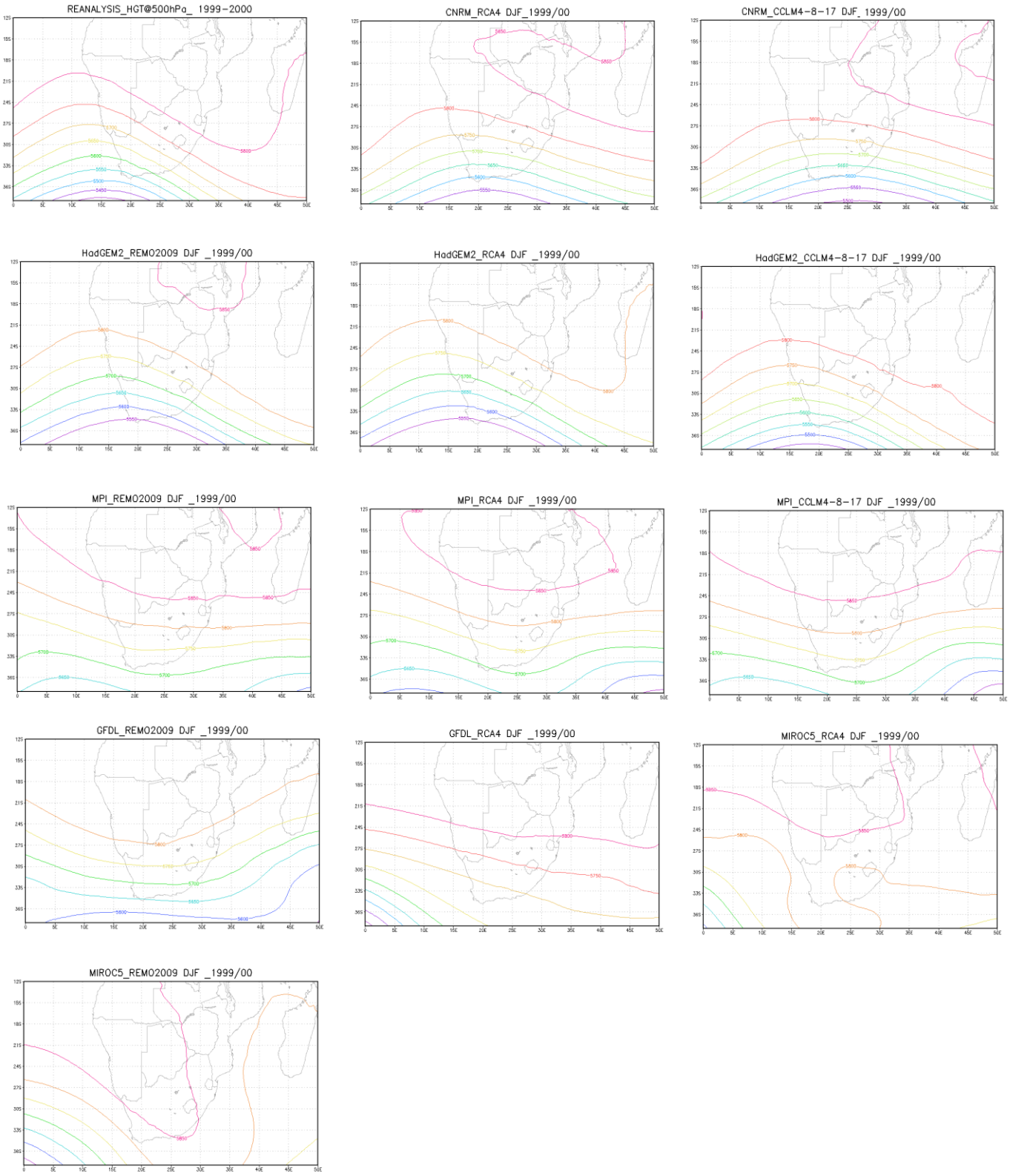

Figure 4. 3 Case study for 1999/00 DJF season, comparing Geopotential height @500hPa Reanalysis (top-left) to 12 models (GCMs forcing on RCMs).

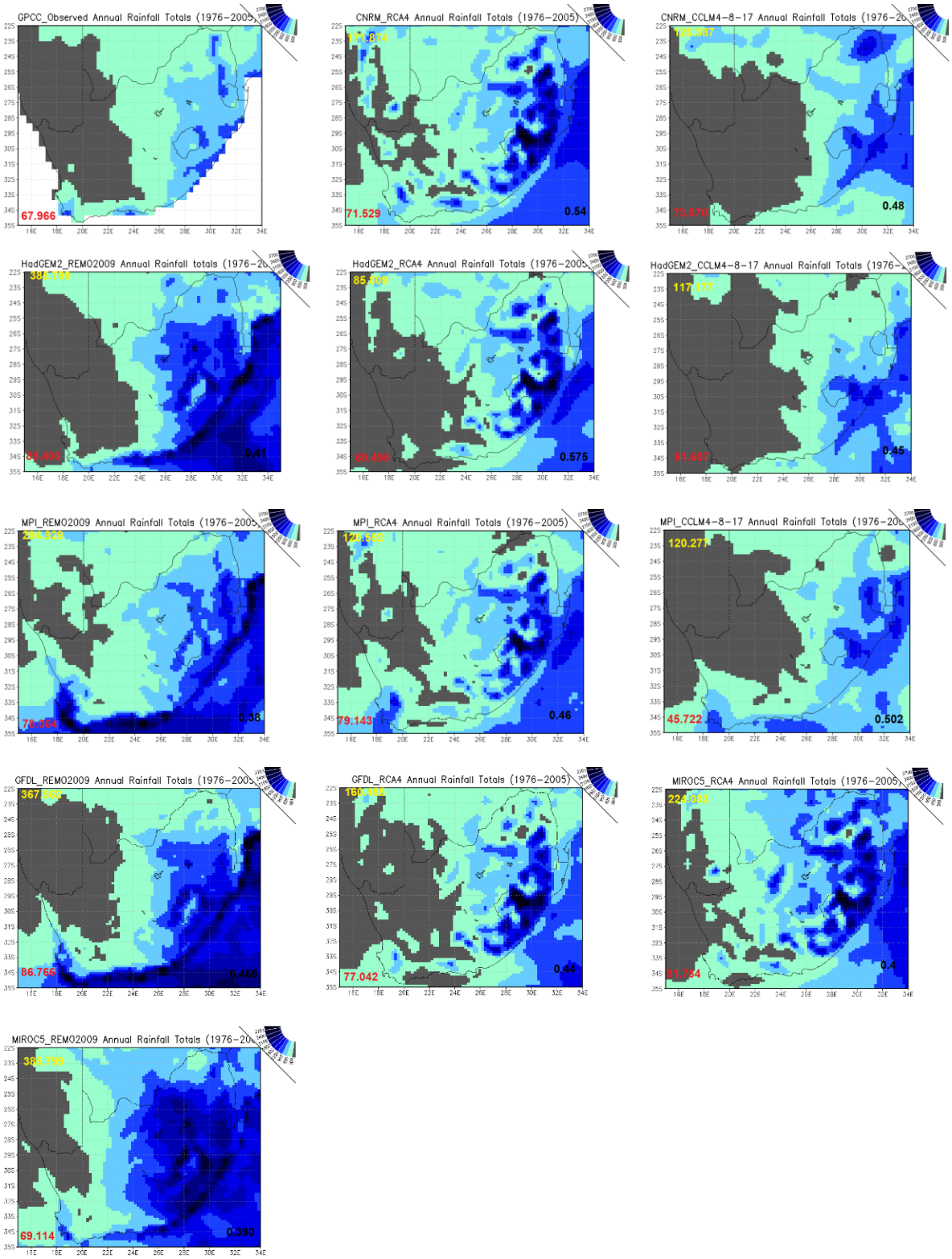

Figure 4. 4 Observed Annual total rainfall (mm/month), from Global Precipitation Climatology Centre (GPCC), compared to 12 model (GCMs forcing on RCMs) simulations, for the period 1976-2005. Values for RMSE (top left), STDEV (bottom left), and spatial r2 (bottom right).

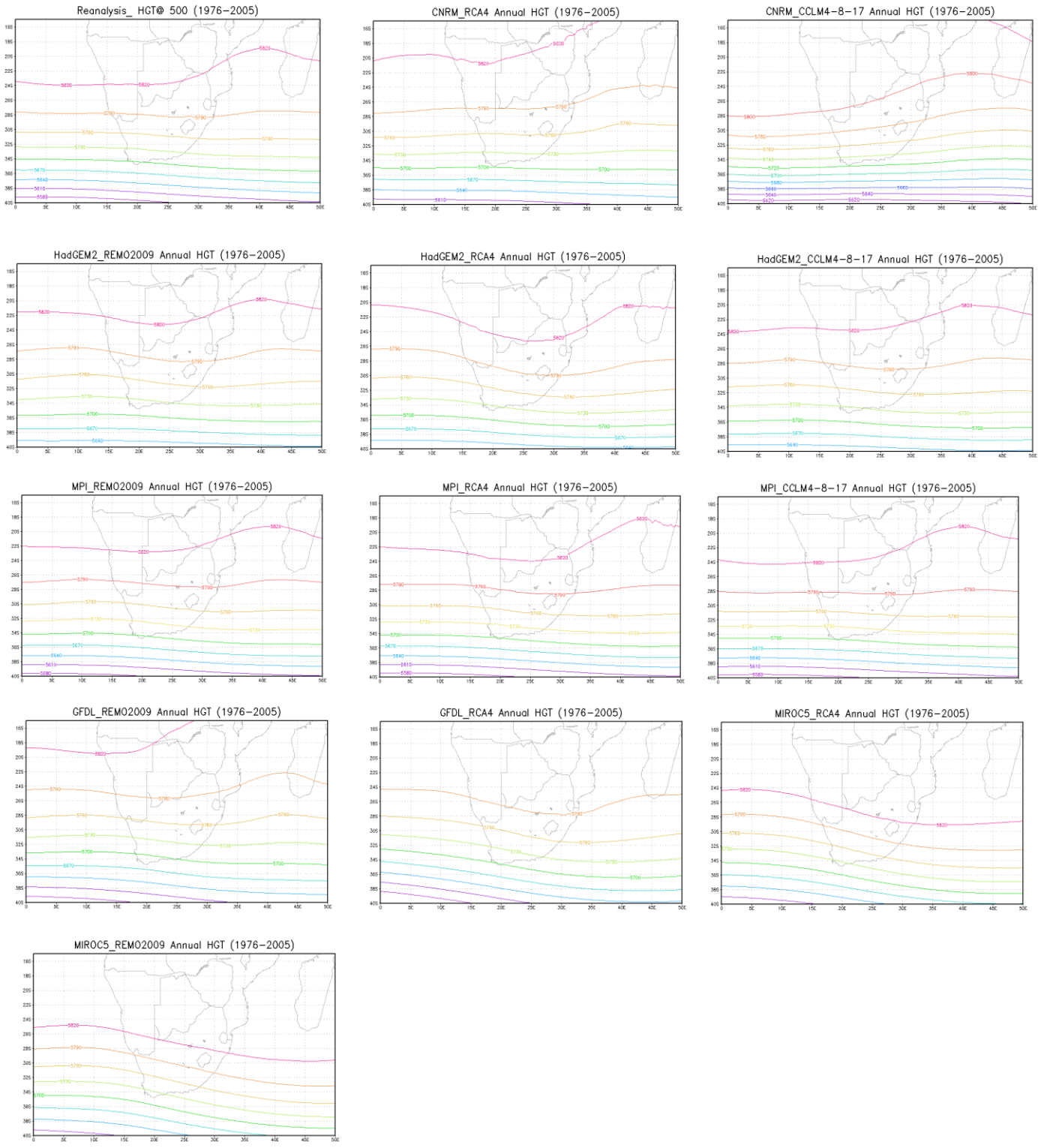

Figure 4. 5 Annual Geopotential height @500hPa Reanalysis (top-left and 12 models (GCMs forcing on RCMs), for the period 1976-2005.

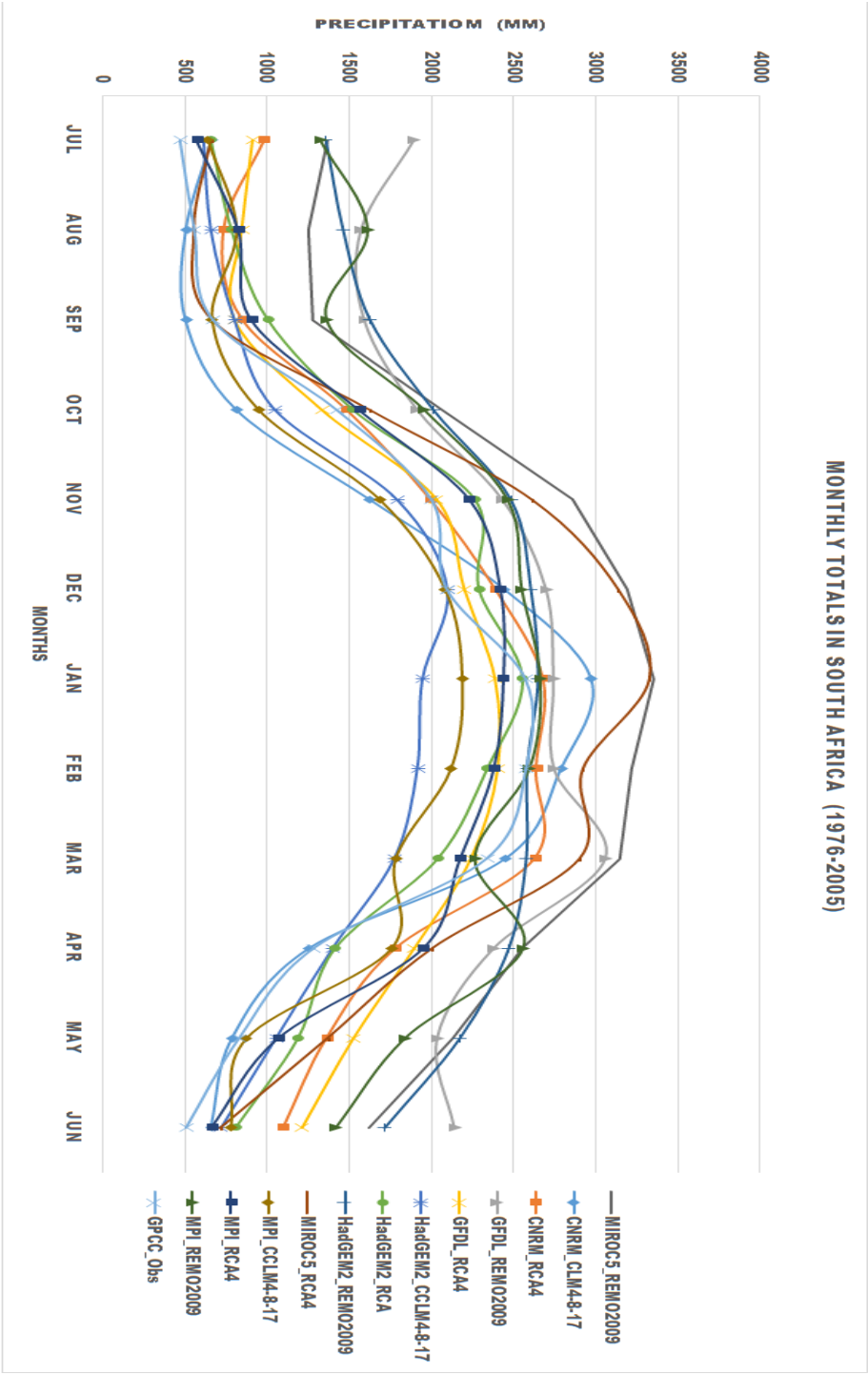

Figure 4. 6 Annual cycle comparing Global Precipitation Climatology Centre (GPCC) precipitation to 12 models (GCMs forcing on RCMs), for the period 1976-2005 over South Africa.

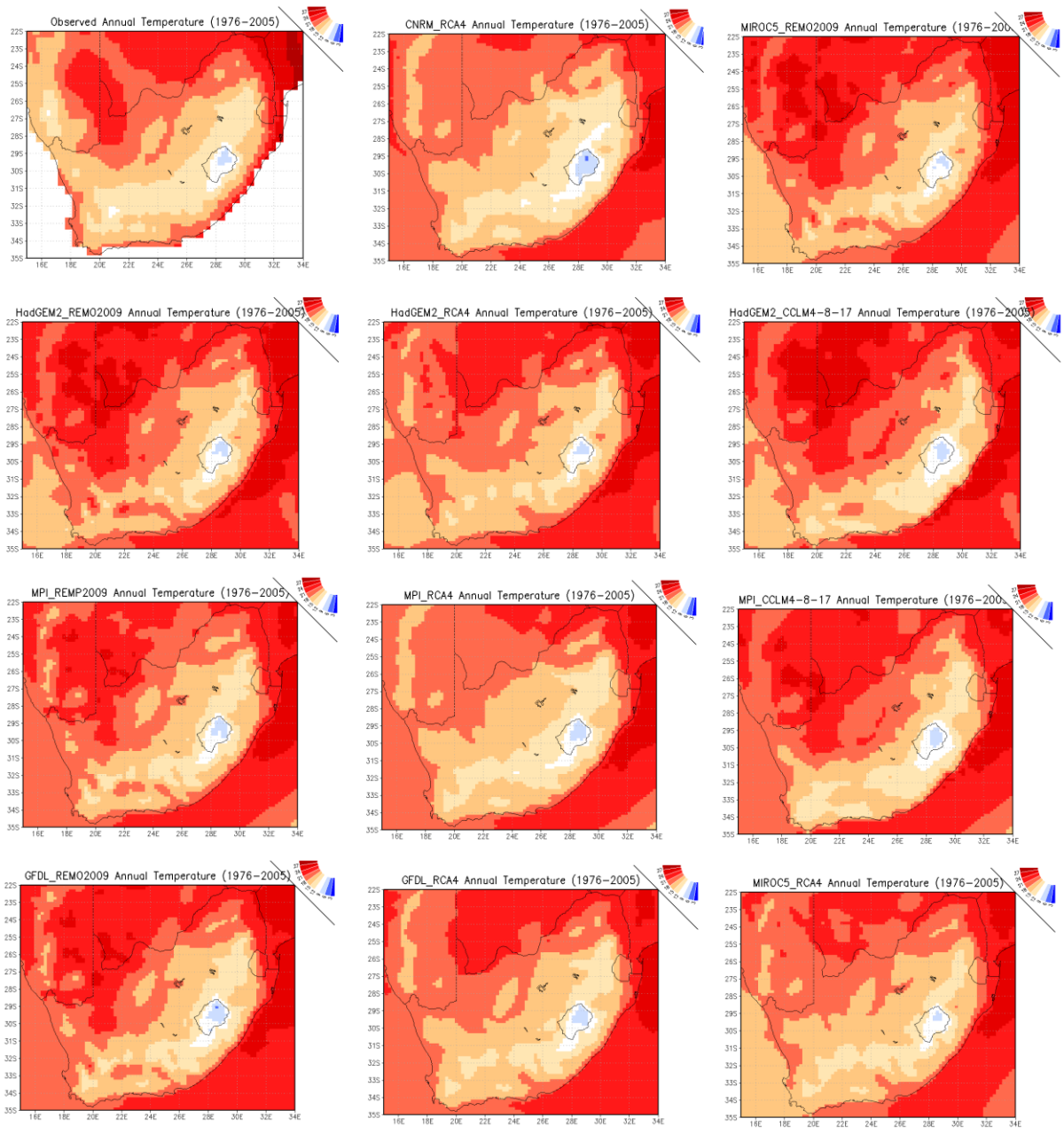

Figure 4. 7 Average of observed annual mean temperatures (°C), from the NOAA GHCN_CAMS Land Temperature Analysis (top-left), compared to 11 models (GCMs forcing RCMs) simulations from 1976-2005.

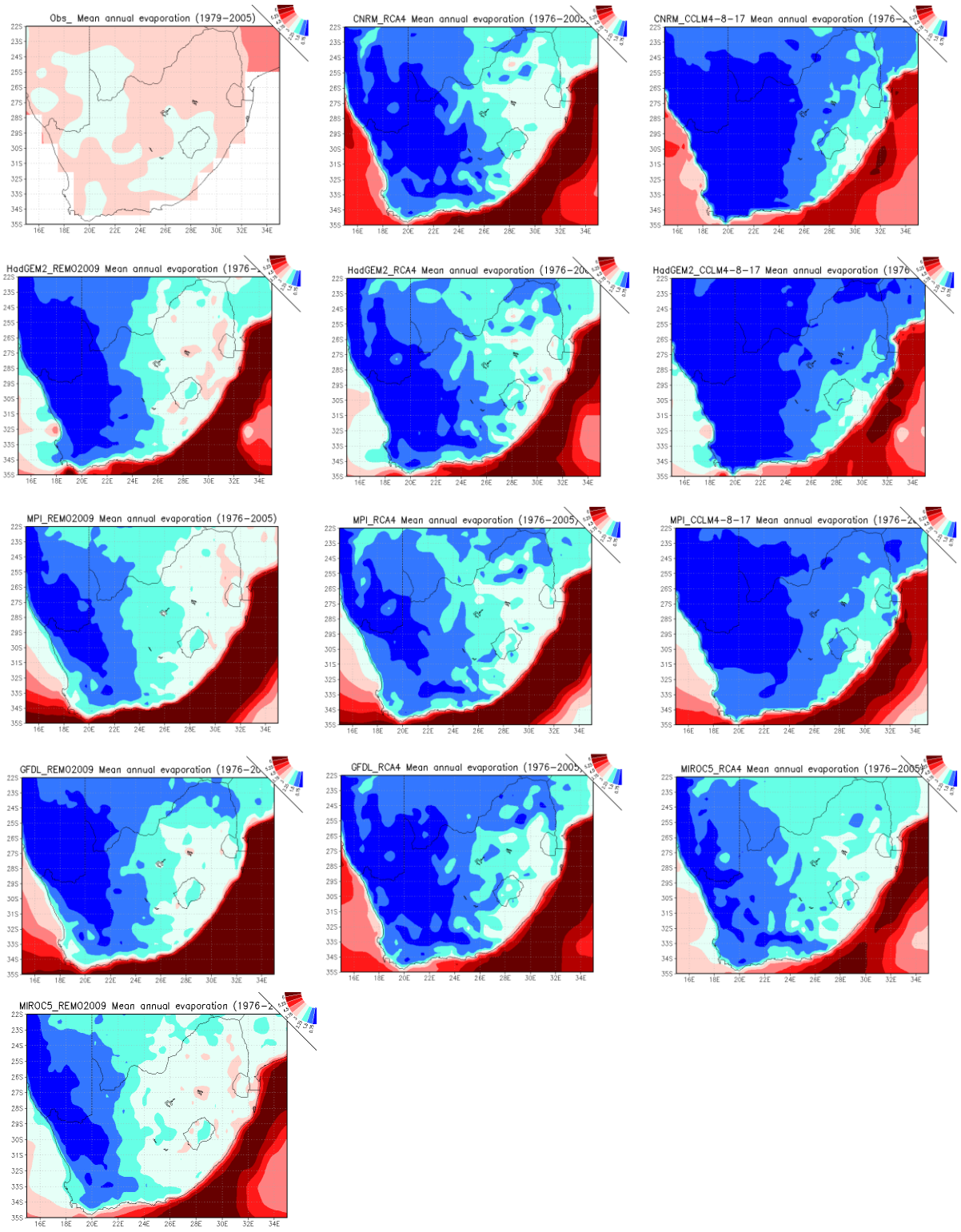

Figure 4. 8 Annual mean evaporation (mm/day), reanalysis (top left) compared to compared to 12 model (GCMs forcing RCMs) simulations from 1976-2005.

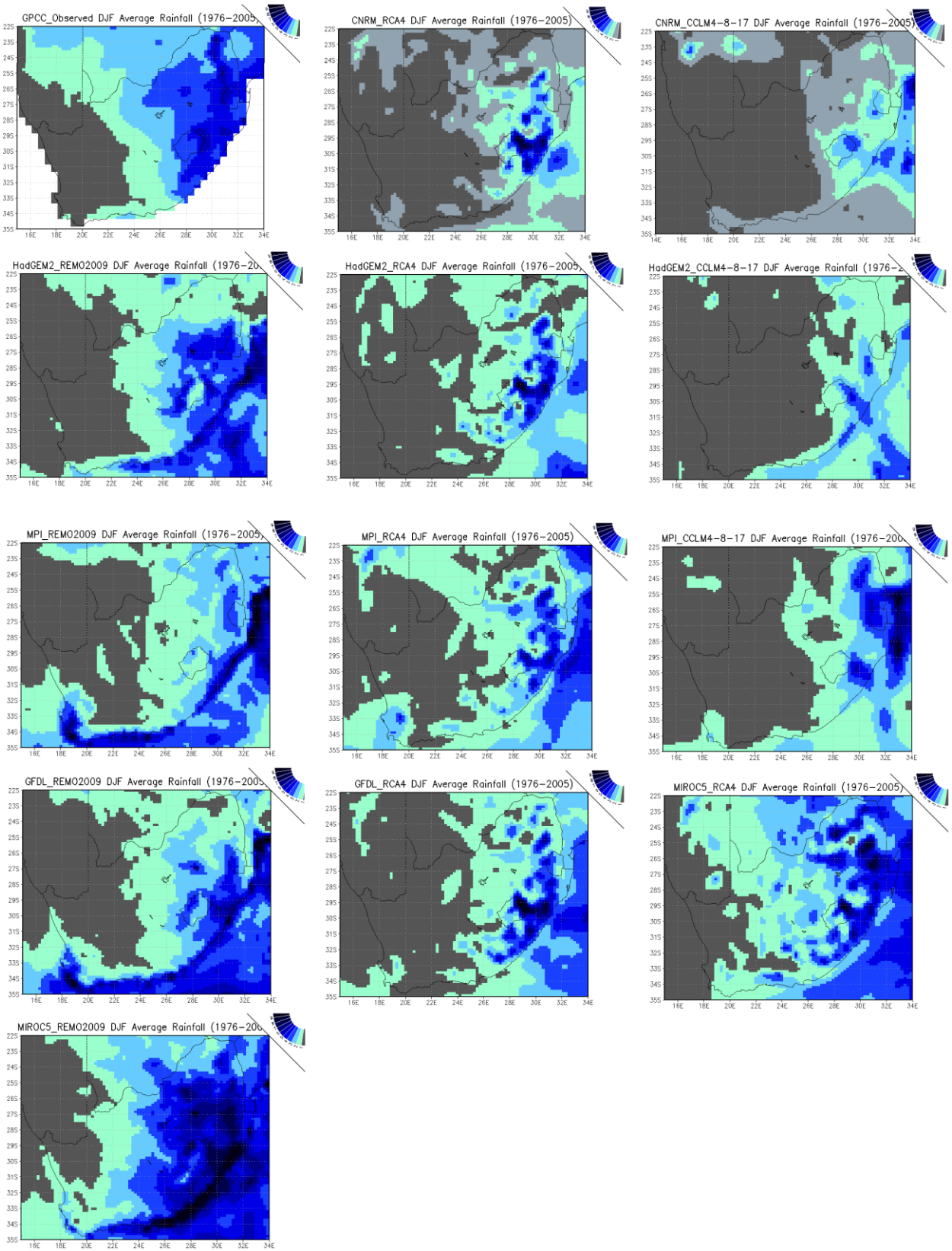

Figure 4. 9 Average of observed seasonal rainfall (mm/day) for DJF season GPCC (top left), compared to 12 model (GCMs forcing RCMs) simulations from 1976-2005.

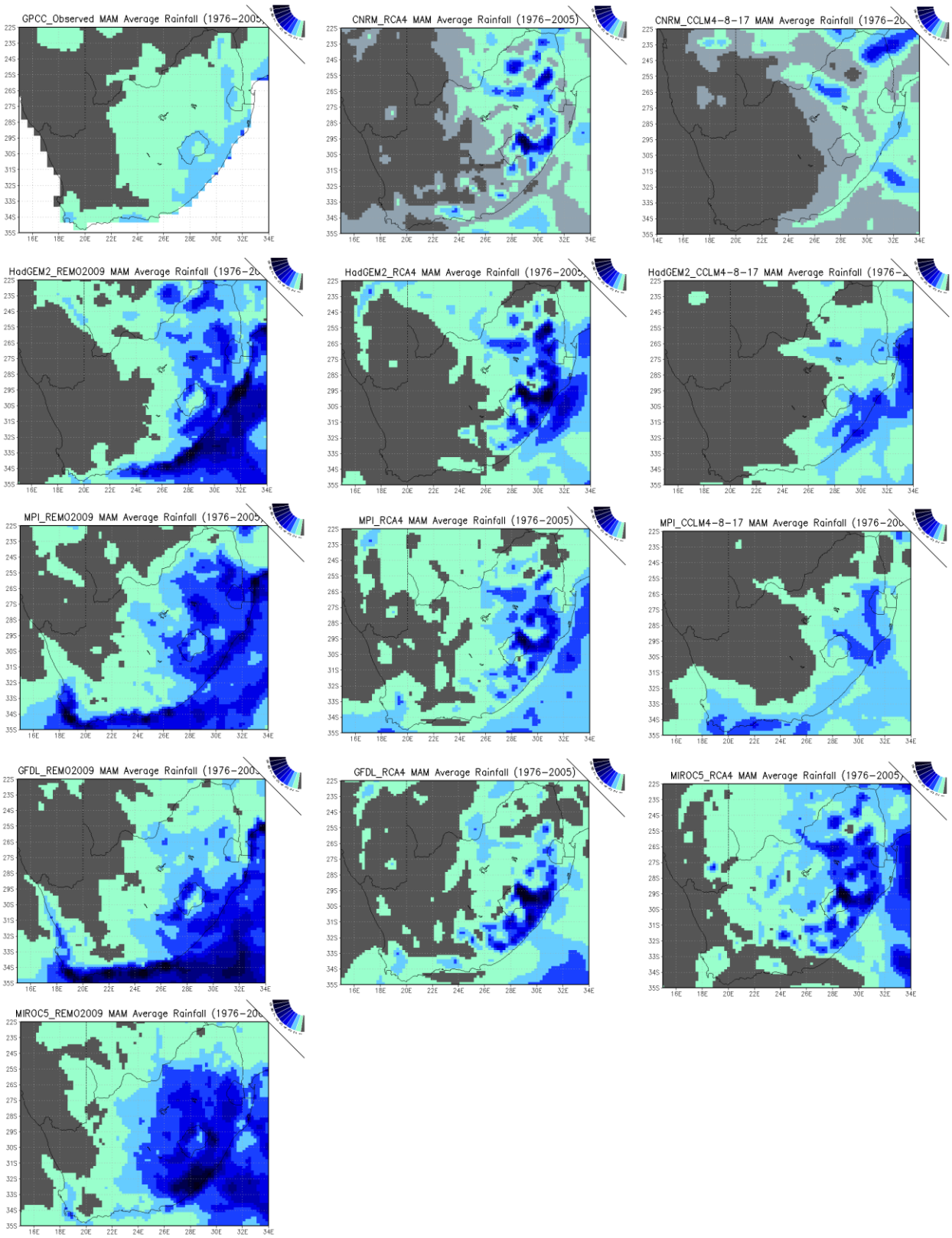

Figure 4. 10 Average of observed seasonal rainfall (mm/day) for MAM season from GPCC (top left), compared to 12 model (GCMs forcing RCMs) simulations from 1976-2005.

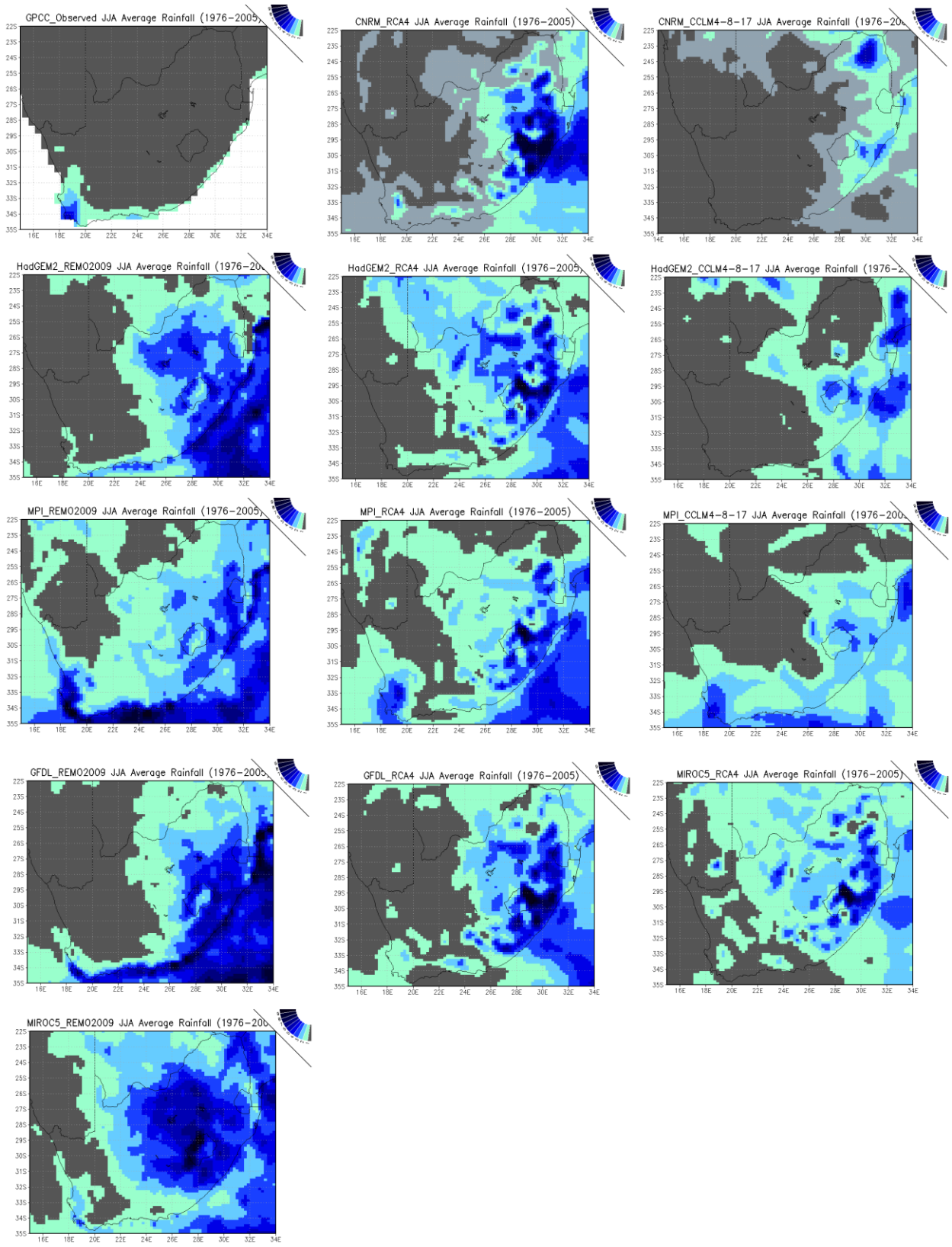

Figure 4. 11 Average of observed seasonal rainfall (mm/day) for JJA season from GPCC (top left), compared to 12 model (GCMs forcing RCMs) simulations from 1976-2005.

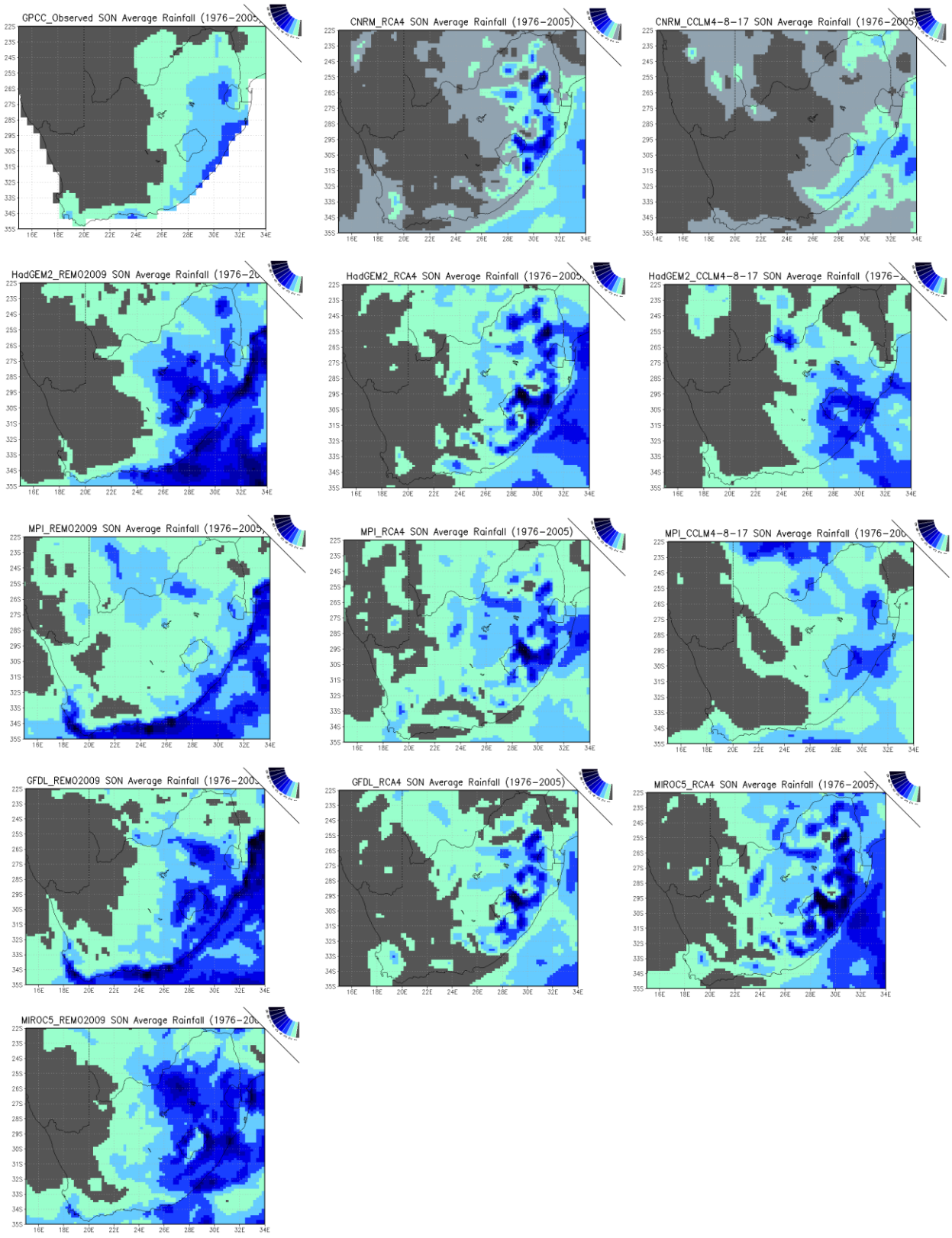

Figure 4. 12 Average of observed seasonal rainfall (mm/day) for SON season, from GPCC (top left), compared to 12 model (GCMs forcing RCMs) simulations from 1976-2005.

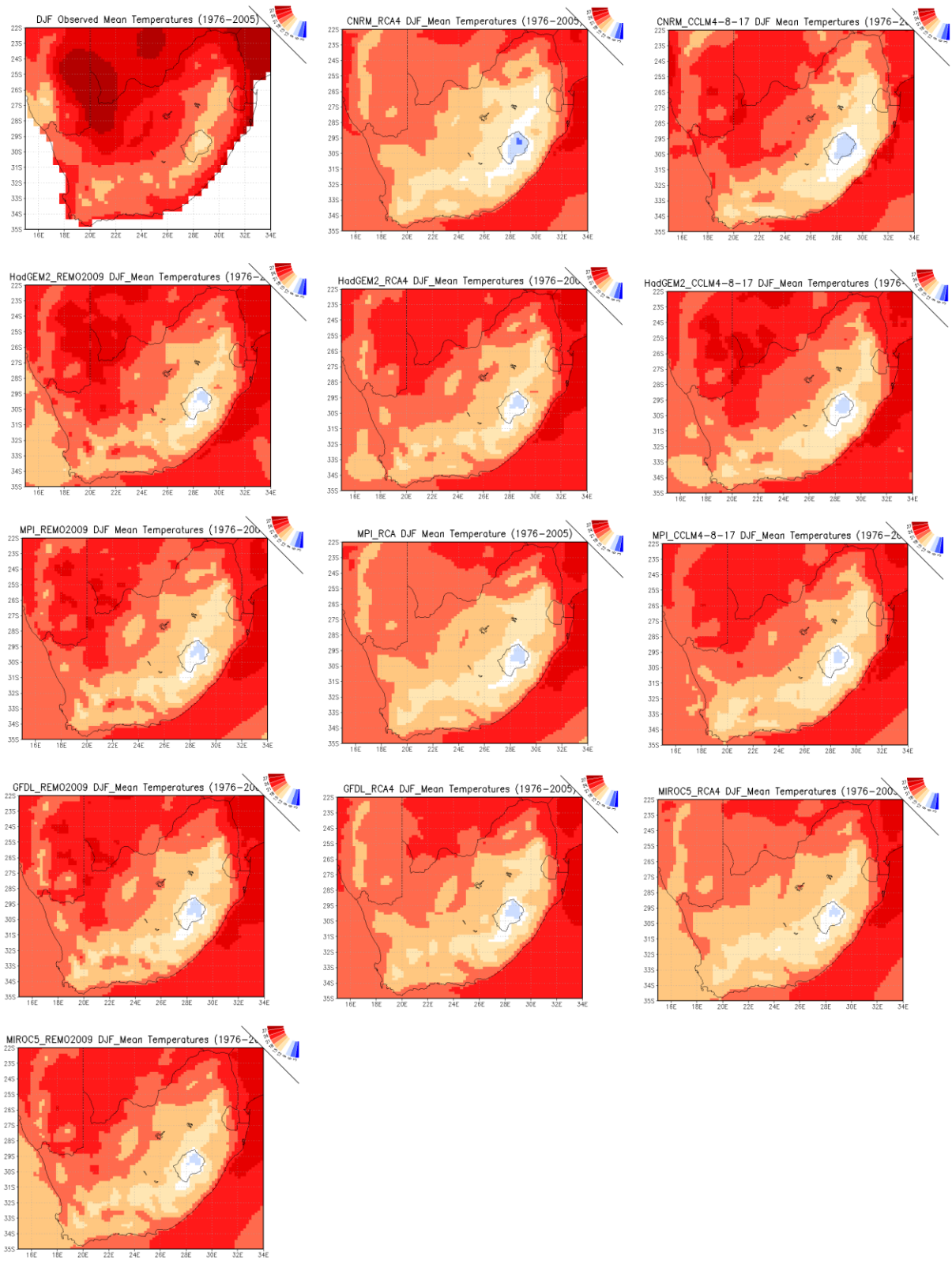

Figure 4. 13 Average of observed seasonal DJF, mean temperatures (°C), from the NOAA GHCN_CAMS Land Temperature Analysis (top-left), compared to 12 models (GCMs forcing RCMs) simulations from 1976-2005.

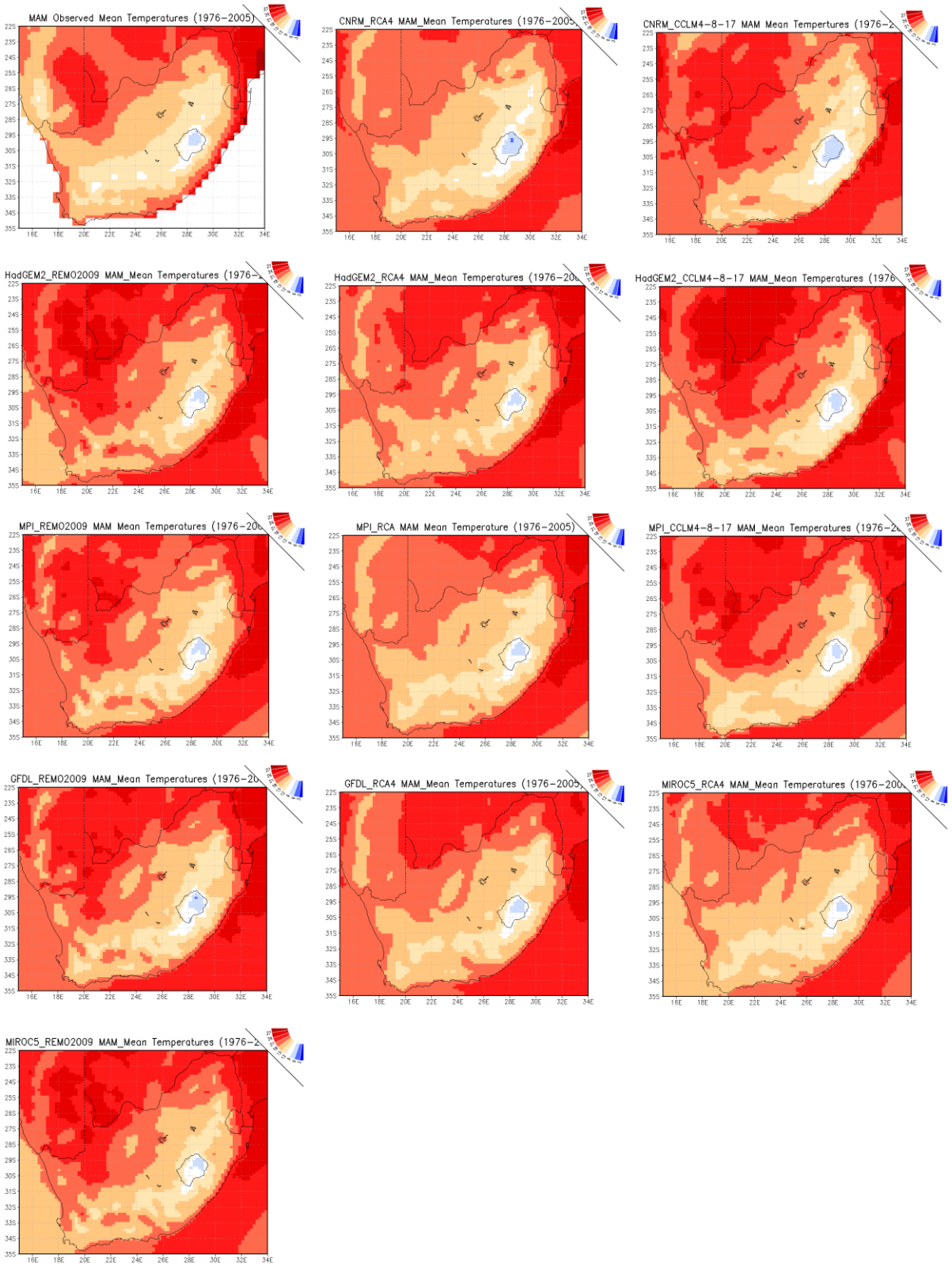

Figure 4. 14 Average of observed seasonal MAM, mean temperatures (°C), from the NOAA GHCN_CAMS Land Temperature Analysis (top-left), compared to 12 models (GCMs forcing RCMs) simulations from 1976-2005.

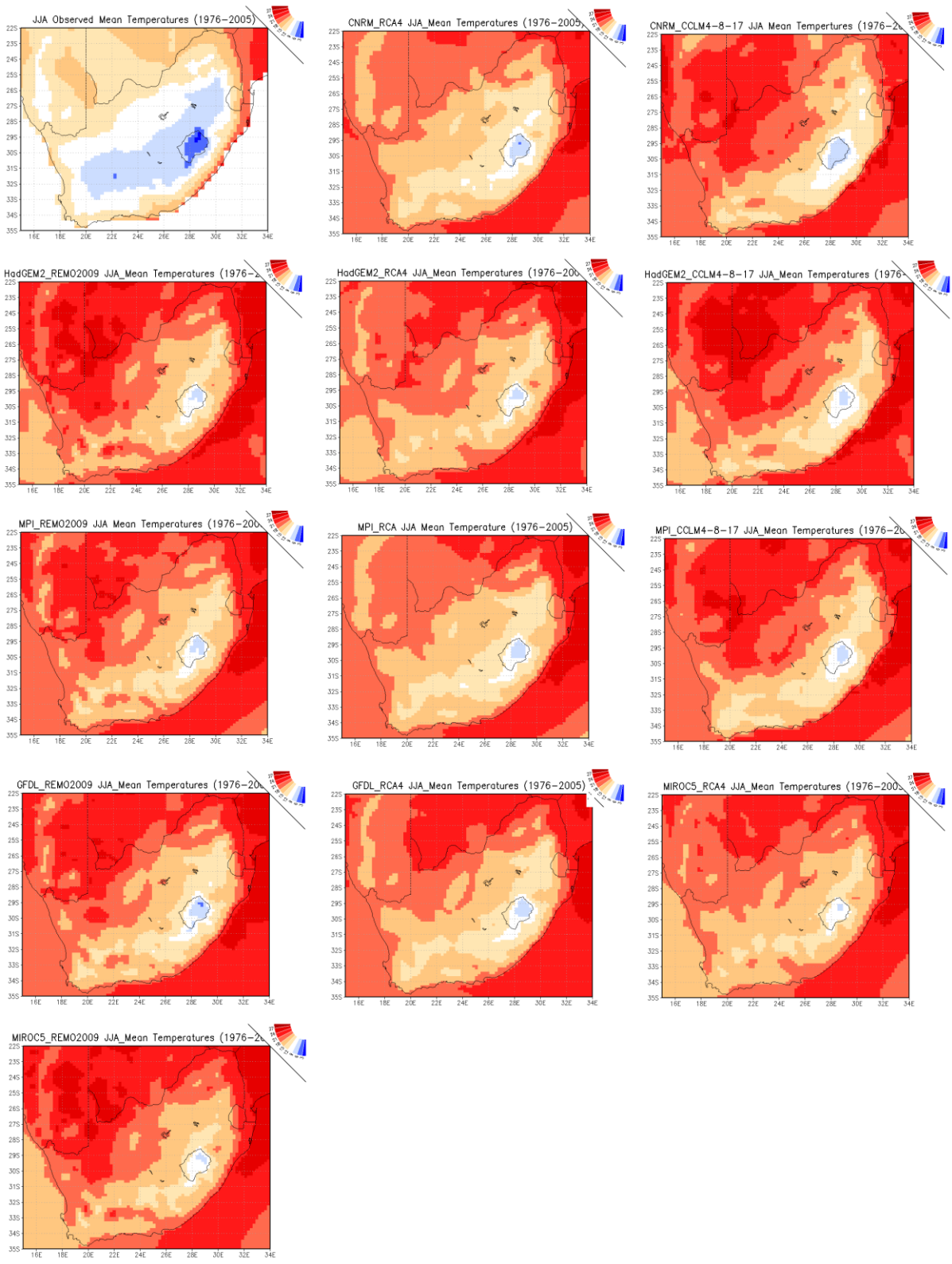

Figure 4. 15 Average of observed seasonal JJA, mean temperatures (°C), from the NOAA GHCN_CAMS Land Temperature Analysis (top-left), compared to 12 models (GCMs forcing RCMs) simulations from 1976-2005.

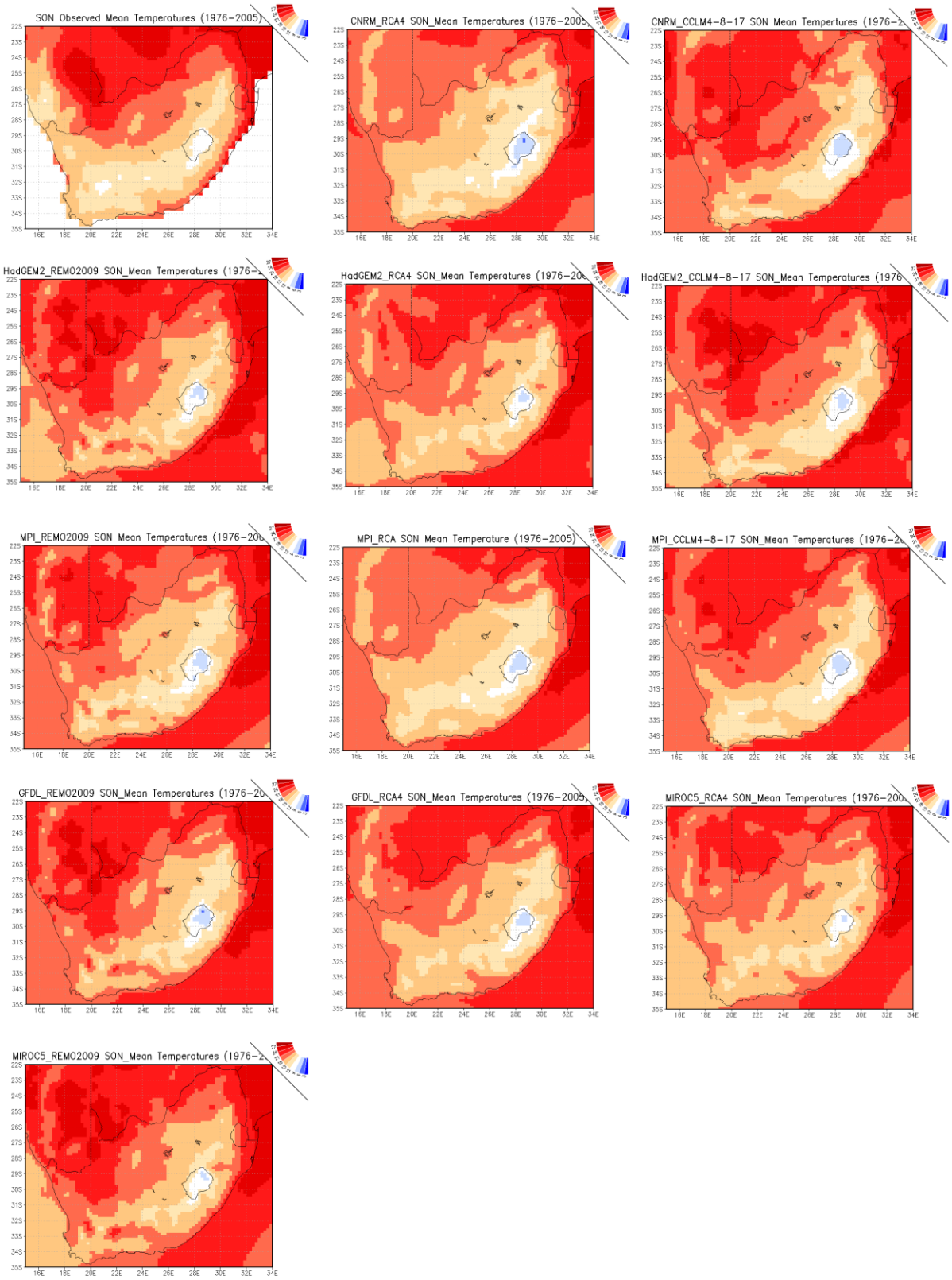

Figure 4. 16 Average of observed seasonal SON, mean temperatures (°C), from the NOAA GHCN_CAMS Land Temperature Analysis (top-left), compared to 12 models (GCMs forcing RCMs) simulations from 1976-2005.

CHAPTER 5: FUTURE PROJECTIONS

5.1 Introduction

Future projections are key in understanding climate change and to inform adaptation strategies and policies (Lazenby et al., 2018). This chapter is aimed at showing the variability in projections using some models whose present day climate simulations were discussed in the previous chapter. Due to the unavailability of some model data, future projections are limited to CCLM4-8-17 model forced with all three GCMs (MPI, CNRM and HadGEM2), and RCA4 nested within HadGEM2, and finally REMO2009 nested within MPI. The projections are considered for both RCP4.5 which is a high mitigation scenario and the low mitigation RCP8.5 emission scenario. The focus of the chapter then is to analyze the variability and change of rainfall in terms of spatial extent, magnitude and time over the domain of South Africa. Most of the current studies show a lower percentile, the median and a higher percentile to show the uncertainty associated with the projections. In this study, we will like to see the source of the uncertainties in the projections and therefore the actual projection from the models listed above are displayed. Future changes in rainfall are expressed as percentages whilst the temperature changes are in °C and calculated in relation to the baseline period (1976-2005). The first part of this chapter discusses the near future (2006-2035) rainfall (and other supporting variables) projections, under both RCP scenarios mentioned above. Far future (2036-2065) projections are then discussed later. Far future projections that usually the period ending in 2100 are not discussed in this study.

5.2 Annual mean rainfall change (Near Future)

Some of the most recent climate change studies (e.g. IPCC, 2014; Engelbrecht et al., 2015; Davis and Vincent, 2017) have focused on projected rainfall changes and found them to be associated with a larger uncertainty compared to other variables such as surface air temperature, and other large scale variables. CCLM4-8-17 projections are found here to be associated with pockets of increasing rainfall amounts over different parts of the country for each projection. For example, the projection nested within MPI projects wetter conditions over the eastern parts of Limpopo, while the two other projections drier conditions in the same area. The RCA4 nested within HadGEM2 and REMO2009 nested within MPI also project drier conditions. This result suggests that the source of this increase is not the GCM (i.e. MPI) because it provides different pictures when used to force two different RCMs (Figure 5.1).

There seems to be some suggestion that the central parts of South Africa extending to the coast could expect an increase in rainfall. Although not consistently over the exact same area, at least the of the five projections seem slightly positive over this area in general. REMO nested within MPI projects a decrease in rainfall percentages over the whole of South Africa, with these changes being larger over the West coast and adjacent interior. Few studies (e.g. Reason and Smart, 2015; SAWS, 2017), found increasing values over the Atlantic west coast and suggested a relaxation of easterly winds along the equator and subsequently warming of SSTs along Angola-Benguela frontal zone. All the models project a drier Western Cape rainfall, with RCMs nested within MPI showing the largest changes. CCLM4-8-17 projects changes of less than 30% over parts of the Western Cape. CCLM4-8-17 nested within HadGEM2 projects the smallest decrease percentage wise over the Western Cape. There are differences in RCM projections nested within the same GCM, as well as with the same RCM nested within different GCMs.

5.3 Annual mean temperature change (Near Future)

Global temperature projections tend to be more robust than of precipitation (Engelbrecht et al., 2015). Future projected changes of mean annual temperature were positive for both RCP4.5 and RCP8.5 over South Africa, though at different magnitudes (Figure 5.2). All the models projected increasing temperatures across South Africa with higher values in the western interior. Air temperature increases over the adjacent oceans are much smaller (<1°C). Such findings are consistent with IPCC (2014); Davis and Vincent (2017), who projected higher temperatures increases over terrestrial areas than oceans under both scenarios. REMO2009 nested within MPI projected greater increases (1.5°C) than any other model over the Northern and Western Cape under RCP4.5 scenario (Figure 5.2). Simulations conducted with the RCP8.5 scenario forcing are generally found to be associated with either a larger increase in temperature, or an increase in area associated with higher temperature increases. Furthermore, MPI model is associated with a pool of increasing temperatures (2°C) under RCP8.5, stretching from south of Botswana towards North West of South Africa (Figure 5.3). It may be noted that models generally perform better when predicting temperature compared to rainfall. The spread in temperature projections are always smaller and therefore the uncertainty associated with temperature is smaller than that associated with precipitation. For example, the rainfall projections were associated with both positive and negative changes where over some areas, one projection would indicate an increase in rainfall while another shows a large projected decrease in rainfall. In the case of temperature, the sign of the change is the same (i.e. positive) except in the case of REMO2009 nested with MPI, which indicated negative changes over the western coast.

5.4 Seasonal mean_ rainfall and temperature change (Near Future)

5.4.1 December-January-February (DJF)

South Africa's summer rainfall seasons are characterized by high variability between wet and dry events, modulated by ENSO (Archer et al., 2017) and adjacent oceans. DJF is the most important rainfall season for most parts of central and northern interior of South Africa (Landman et al., 2012). Mixed signals of rainfall projections amongst models over the northeastern parts of South Africa are projected under RCP4.5 scenario. CCLM4-8-17 nested within MPI projected extensive drying (-20%) over parts of Mpumalanga and eastern Limpopo and neighboring Mozambique (Figure 5.4) compared to the rest of the other models, which projected increasing values over the same areas. Projections of drying by CCLM4-8-17 forced on MPI were also consistent under RCP8.5, though with increased intensity and coverage (Figure 5.5). By contrast, rainfall over east coast and central interior areas is projected to consistently increase under both scenarios and models (except CCLM4 nested on MPI). This suggest that there still exist huge uncertainties amongst models in rainfall projections. Few studies (e.g. Engelbrecht *et al.,* 2009; Hewitson *et al.*, 2014) have also projected slightly similar increases in rainfall over the east coast.

Temperature projections were variable under RCP4.5 and RCP8.5 scenarios (Figure 5.6 and Figure 5.7) amongst models. Conspicuously, REMO2009 nested within MPI projected consistent decreasing temperature values (-0.5°C) along Western Cape and western coast towards south of Namibia under both scenarios contrasting the rest of the models. The area associated with a decrease in temperature is projected to experience large decreases in rainfall and therefore an increase in cloud cover does not explain the projected temperature increase. CCLM4-8-17 forced by HadGEM2 projected reduced average temperatures over the Kalahari Desert under the RCP8.5 scenarios. Such findings contradict with most previous works that projecting parts of Kalahari Desert to warm at a faster rate than the surrounding areas, under the "business as usual" emission scenario.

5.4.2 March-April-May (MAM)

All the models are projecting a decrease in rainfall over most of the country, with some areas, mostly the central parts of the country projected to increase during the March-April-May (MAM) season. Under RCP4.5 scenario, REMO2009 and CCLM4-8-17 nested within MPI projected an extensive drying along the Western Cape and along the south coast "all year rainfall region" (Figure 5.8). The MAM season is an important season for rainfall in the south Western Cape of South Africa. The CCLM4-8-17 forced with HadGEM2, projected drier conditions over northern parts of the country. However, CCLM4-8-17 forced with CNRM is associated with substantial

gradient of increasing values from central interior towards the eastern coast of South Africa, compared to other models. Projections under RCP8.5 (Figure 5.9) were somewhat similar to RCP4.5, though slight decreases over the eastern coast were projected by RCA4 nested within HadGEM2. Insignificant pockets of increasing values are projected by CCLM4-8-17 forced with both HadGEM2 and MPI over northwest and some parts of Botswana and Namibia, agree with Daron, (2014), who linked the dryness to the strengthening westerly waves.

Temperatures over the western parts of the country are projected to increase by at least 0.5°C on all model combinations. The two models nested within MPI have patches of projected temperatures being between 1 and 1.5°C with the RCP4.5 scenario. Under the RCP8.5 scenario the picture is similar to RCP4.5, however the extent of the area where increases of over 0.5°C is expected is larger with three of the projections (Figure 5.10 and Figure 5.11). As with DJF, a tongue of 1.5°C is projected to strengthen from south of Botswana towards of central interior of South Africa, by MPI-CCLM4-8-17 under RCP8.5.

5.4.3 June-July August (JJA)

The austral winter season is characterized by dry and cold conditions over most interior parts of South Africa (Tadross and Johnston, 2012; Du Plessis and Schloms, 2017; Phakula, 2017). It is the rainy season over the Western Cape and rain also occurs over the Cape South Coast and the KwaZulu-Natal coastal areas due to ridging anticyclones against the escarpment. REMO2009 is once again associated with projected drying along the Western Cape and south coast similar to DJF and MAM under both scenarios (Figure 5.12). CCLM4-8-17 projects a similar picture especially over the Western Cape. Such changes are likely to result in severe water scarcity in the affected areas. A shorter winter rainfall season is projected and also in agreement with other studies (e.g. DEADP, 2011). An increase in rainfall is projected by both models, that is, CCLM4-8-17 and REMO2009 nested within MPI in areas around Lesotho, however the areas do not match completely. Those nested within HahGEM2 project increases along the south east coast and adjacent ocean area (Figure 5.12). There seems to be some general agreement amongst projections nested within the same GCM. The rainfall increase in CCLM4-8-17 nested within CNRM are seen over the north eastern parts of the country. IPCC, (2013) suggested a decrease in frontal systems because of the strengthening Hardley Cell. However, all models agree in projecting extensive drying over the northern interior. There is agreement in projections for the two scenarios (Figure 5.13).

There is variability amongst the models in projecting winter temperatures. MPI-REMO2009 projected cooling (0 to -0.5°C) temperatures along the eastern coast and over the south tip of the country under RCP4.5 (Figure 5.14). Also, a similar belt of warming (~2°C) along the west coast was projected to have intensified from MAM season. Under RCP8.5 (Figure 5.15), a homogenous increase of ~1°C over the entire country was projected by RCA4 forced on HadGEM2.

5.4.4 September-October-November (SON)

The degree of rainfall changes are highly variable with different scenarios over South Africa during the spring season. Under RCP4.5, REMO2009 and CCLM4-8-17 nested within MPI, projected substantial decreases over the entire country, with the south coast projected severe drying than most parts of the country (Figure 5.16). RCMs forced with HadGEM2, projected a tendency of wetting over the eastern coast and into the adjacent interior than any other models. Such increases along the coast are consistent with Daron (2014) who projected a wet belt towards northeastern parts of the country. However, under RCP85, the eastern coastal areas were projected to become drier (Figure 5.17) by the rest of the models, except CCLM4-8-27 nested within HadGEM2. This may point to a late onset and reduced length of the growing season with serious implications on the agricultural sector (Lazenby, 2016) such as sugar cane plantation over Kwa-Zulu Natal. The SON season is also the burning or fire season in most parts such that drying during this season may also imply a longer fire season.

During the spring, all the models projected resilient increases in temperature from JJA season, ranging from 1.0 °C–1.5 °C in a large part of the inland to 0.5 °C over adjacent oceans. CCLM4-8-17 nested within CNRM exhibited a substantial increase from RCP45 (Figure 5.18) to RCP8.5 (Figure 5.19) over the central interior of South Africa. This may suggest that much of the drying and warming in the north are occurring during the austral spring.

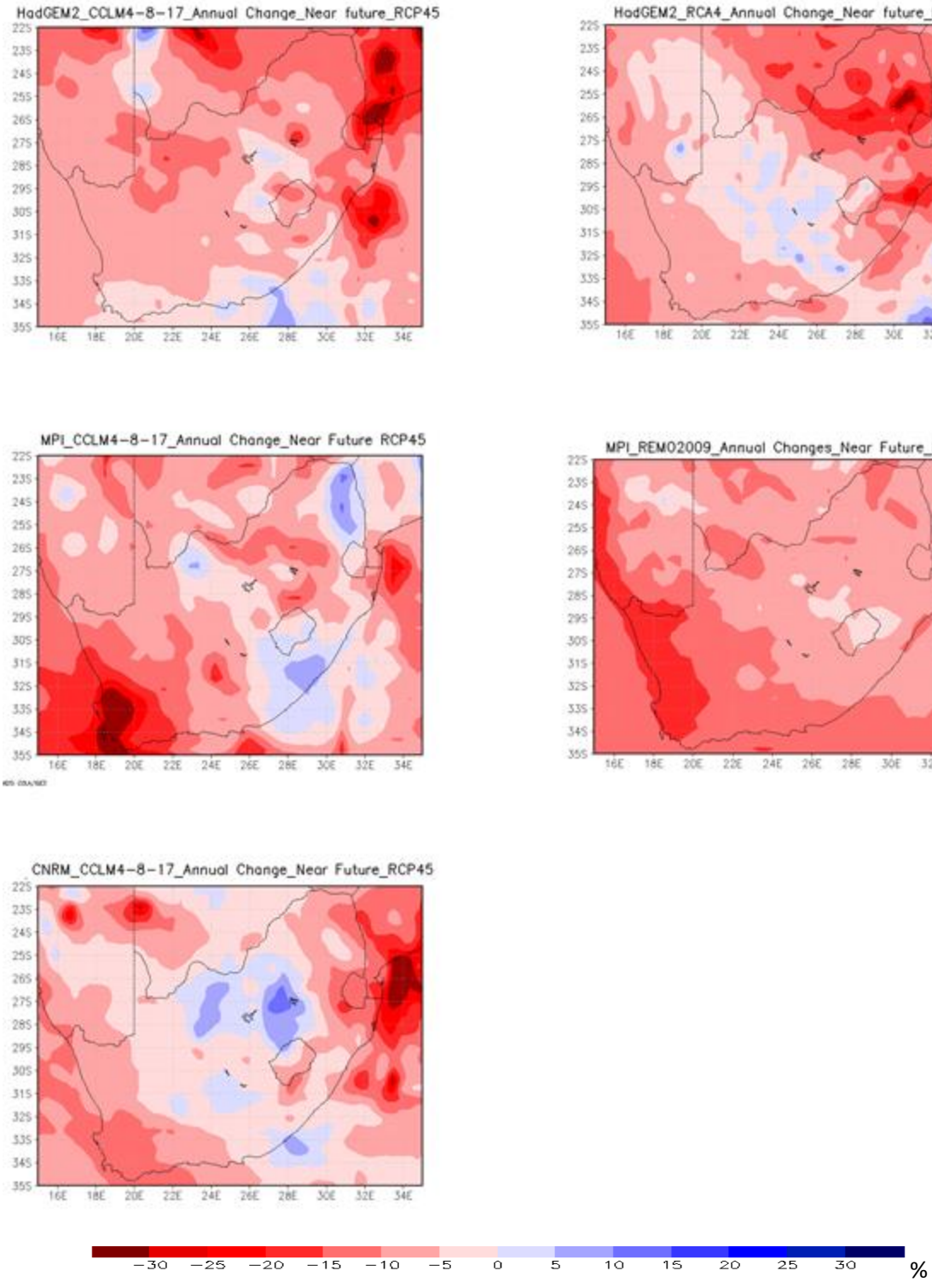

Figure 5. 1 Annual rainfall percentage projected for Near-Future (2006-2035), relative to present climate (1976-2005), under conditions of the RCP45.

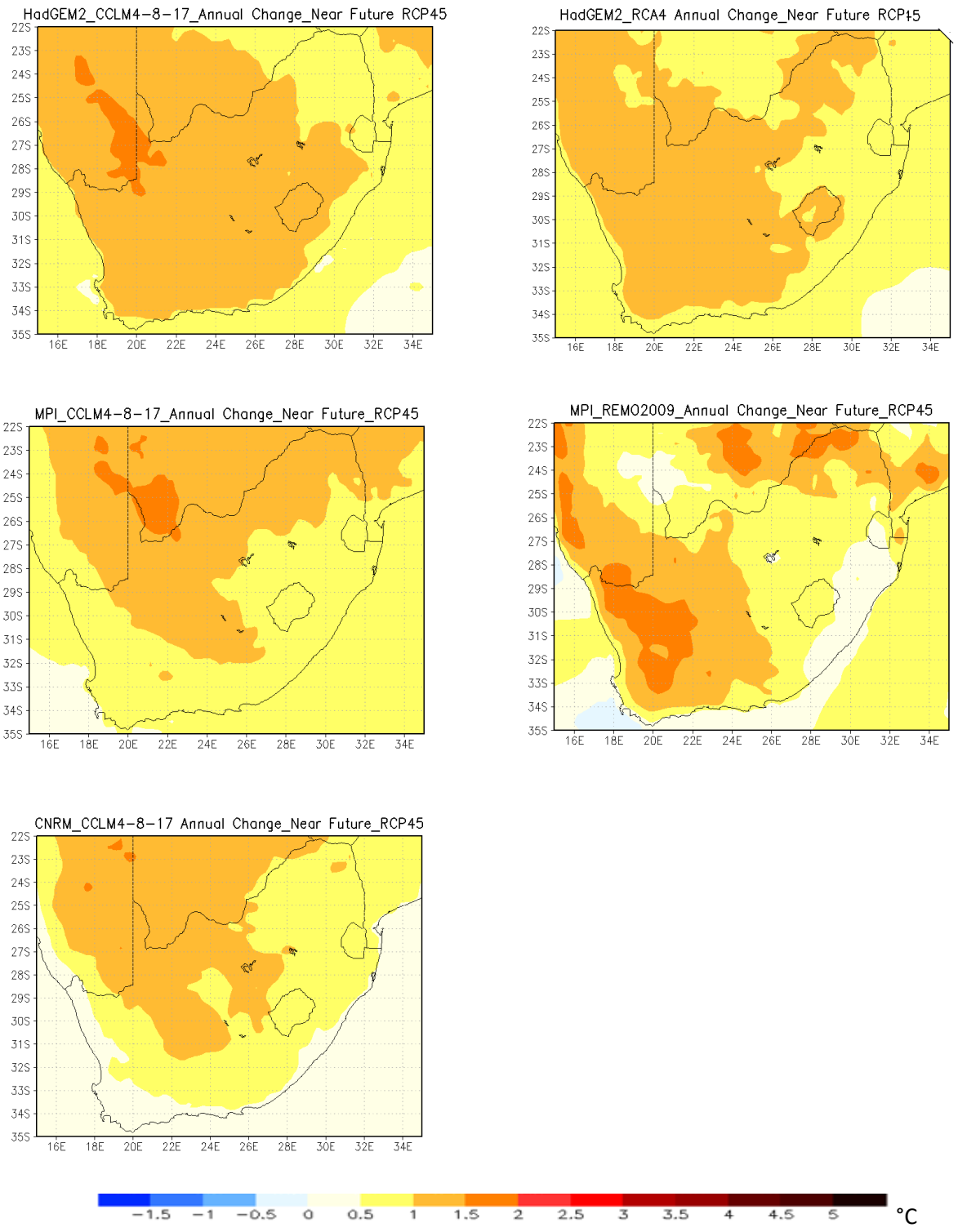

Figure 5. 2 Annual mean temperature change projection for Near-Future (2006-2035), relative to present climate (1976-2005), under conditions of the RCP45.

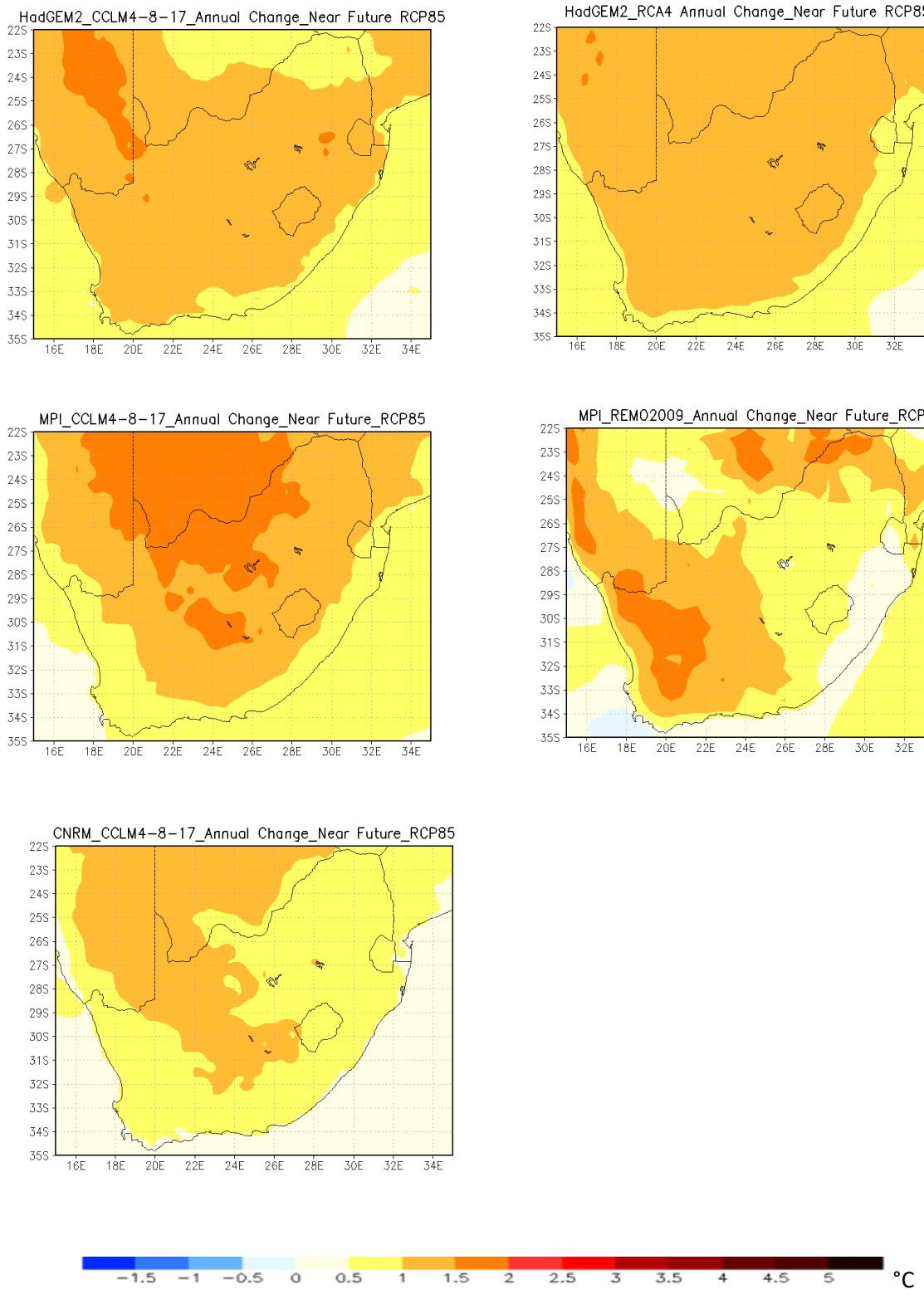

Figure 5. 3 Annual mean temperature change projection for Near-Future (2006-2035), relative to present climate (1976-2005), under conditions of the RCP85.

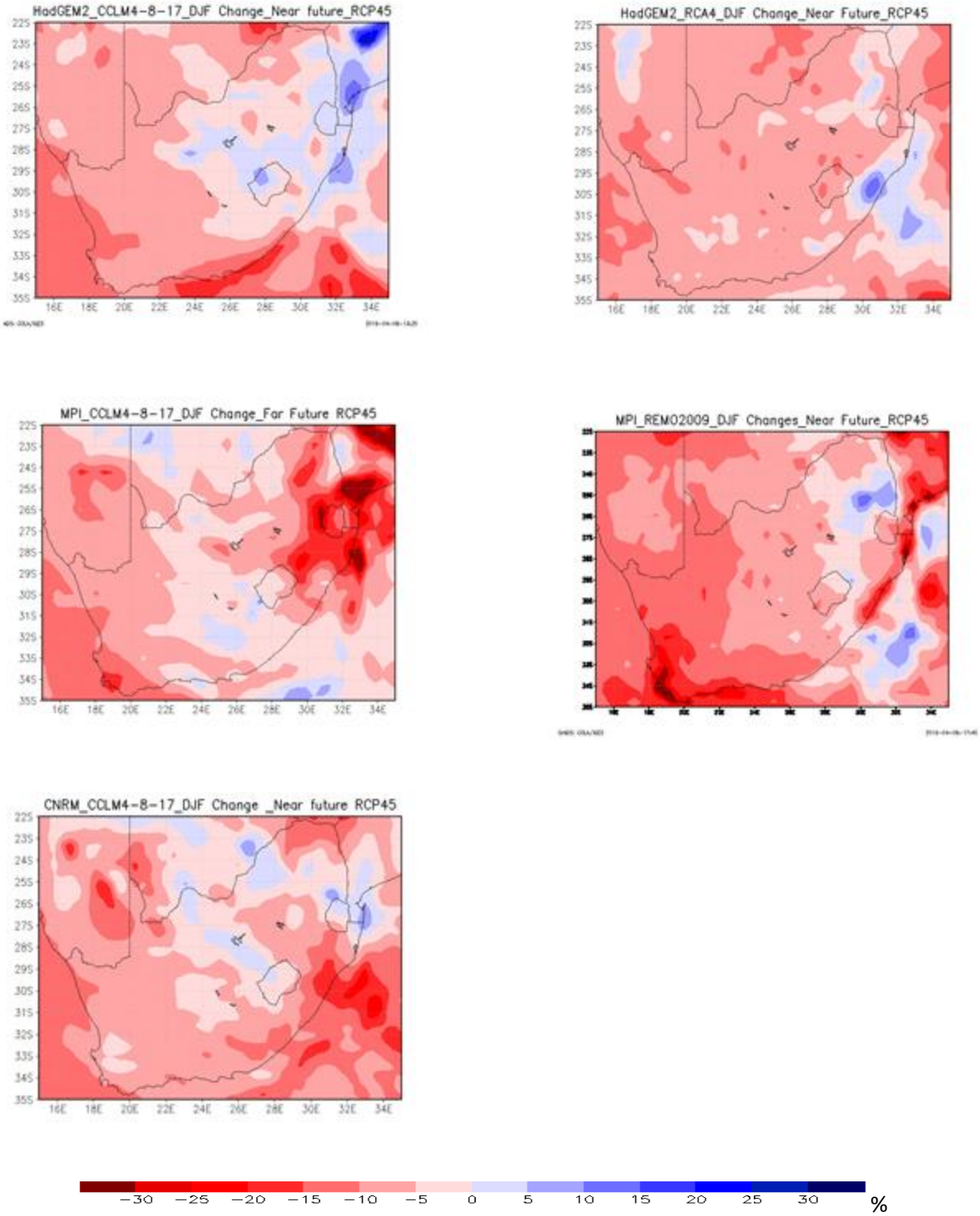

Figure 5. 4 DJF mean rainfall change projection, for Near-Future (2006-2035), relative to present climate (1976-2005), under conditions of the RCP45.

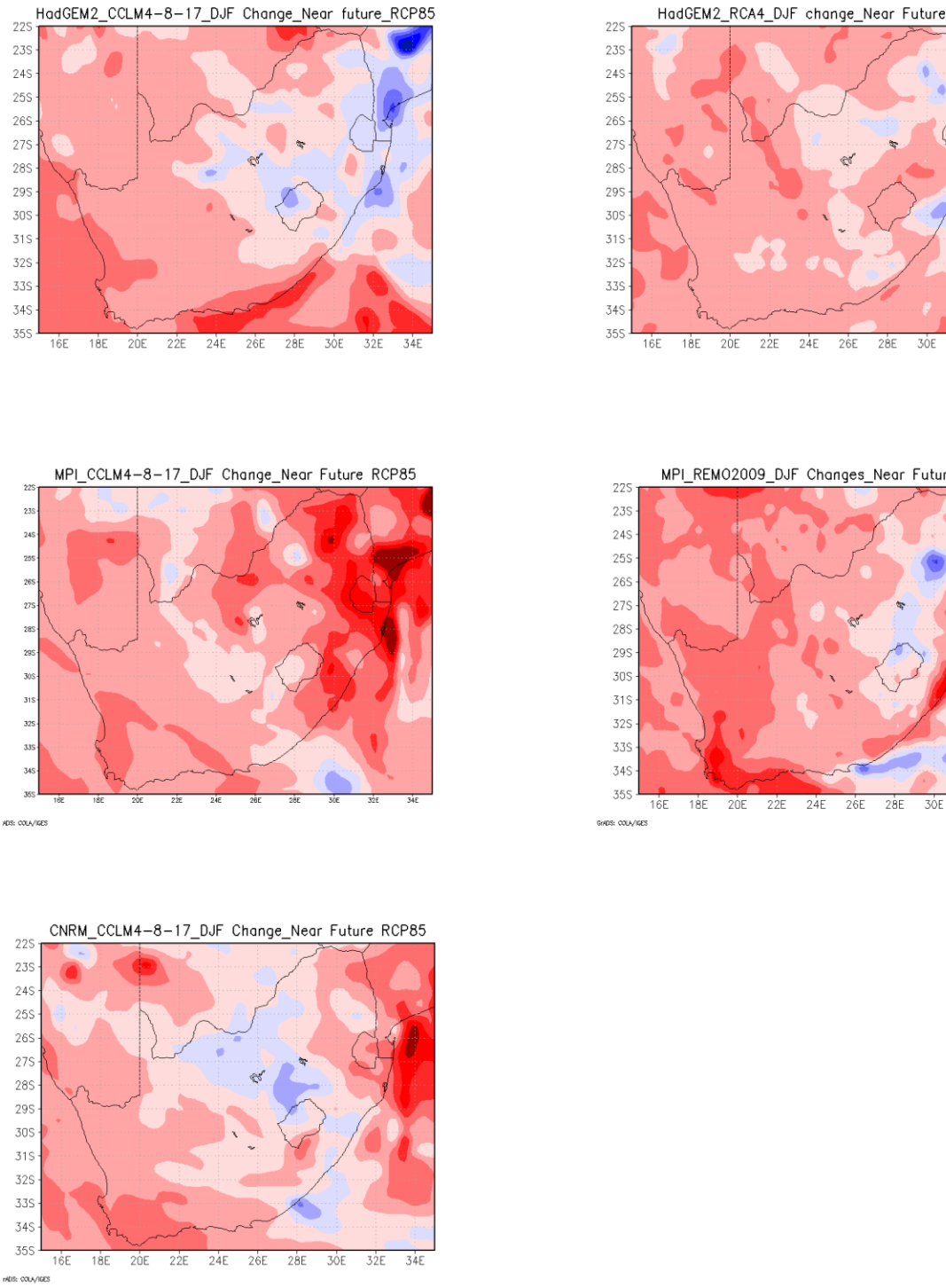

Figure 5. 5 DJF mean rainfall change projection, for Near-Future (2006-2035), relative to present climate (1976-2005), under conditions of the RCP85.

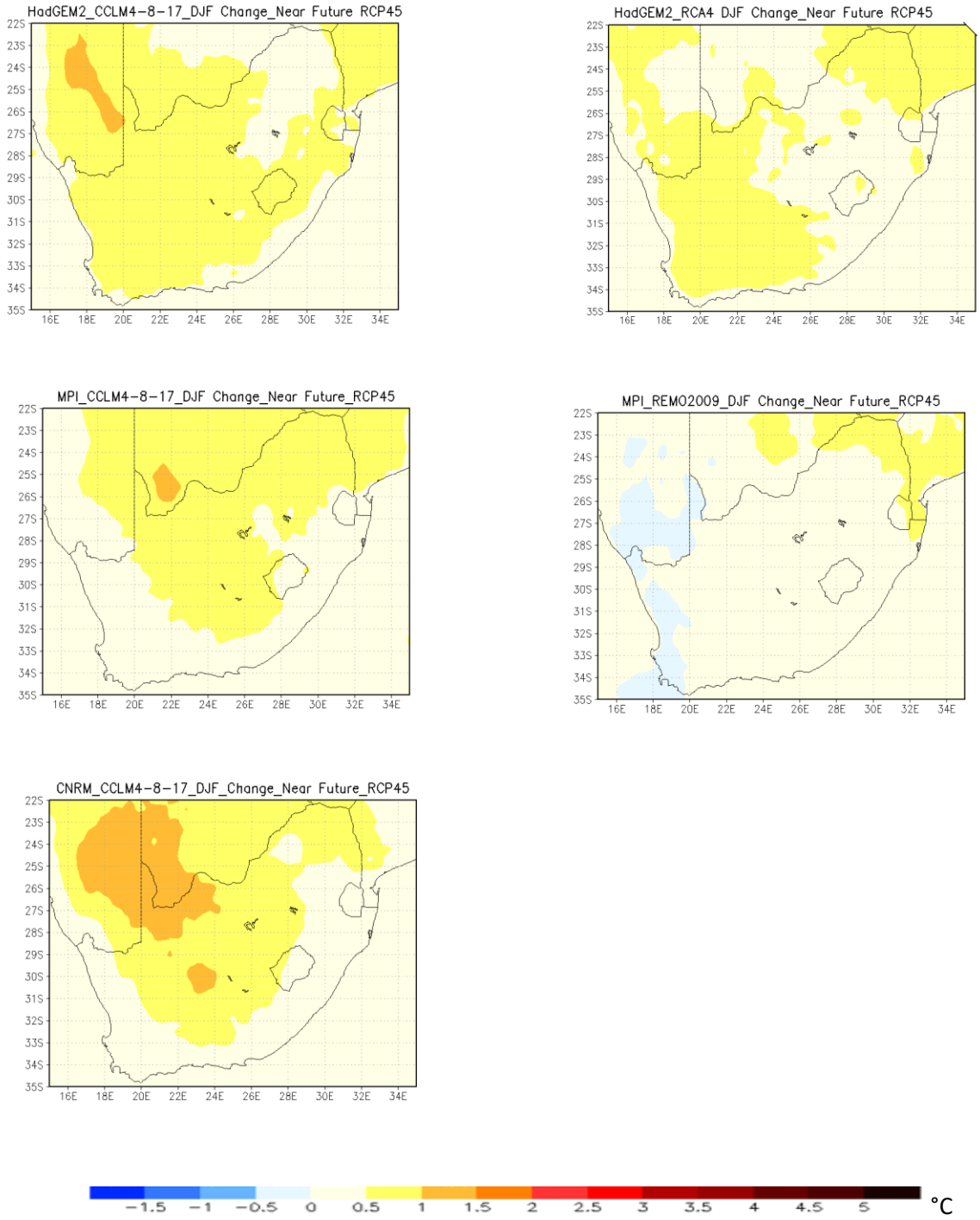

Figure 5. 6 DJF mean temperature change projection, for Near-Future (2006-2035), relative to present climate (1976-2005), under conditions of the RCP45.

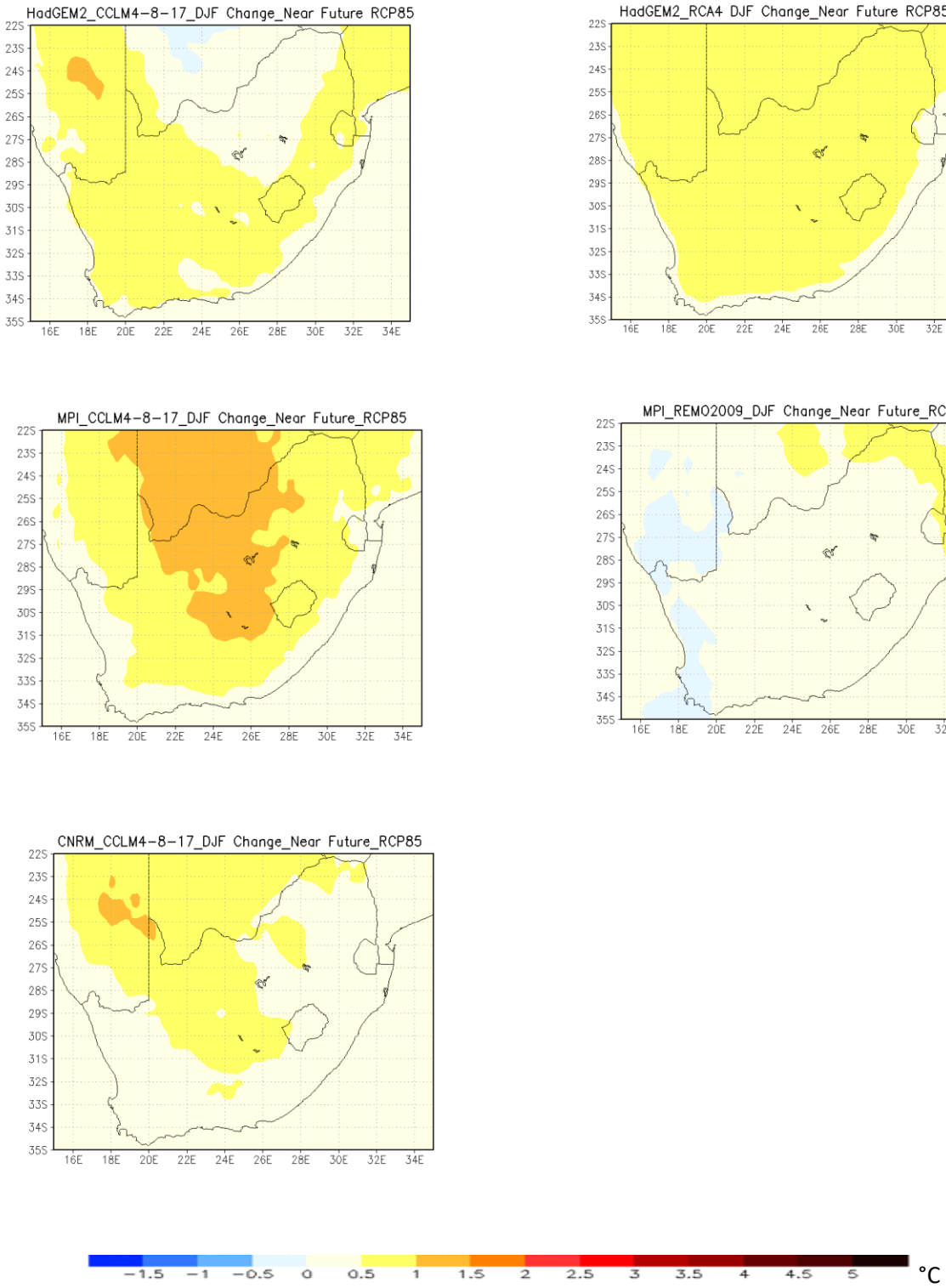

Figure 5. 7 DJF mean temperature change projection, for Near-Future (2006-2035), relative to present climate (1976-2005), under conditions of the RCP85.

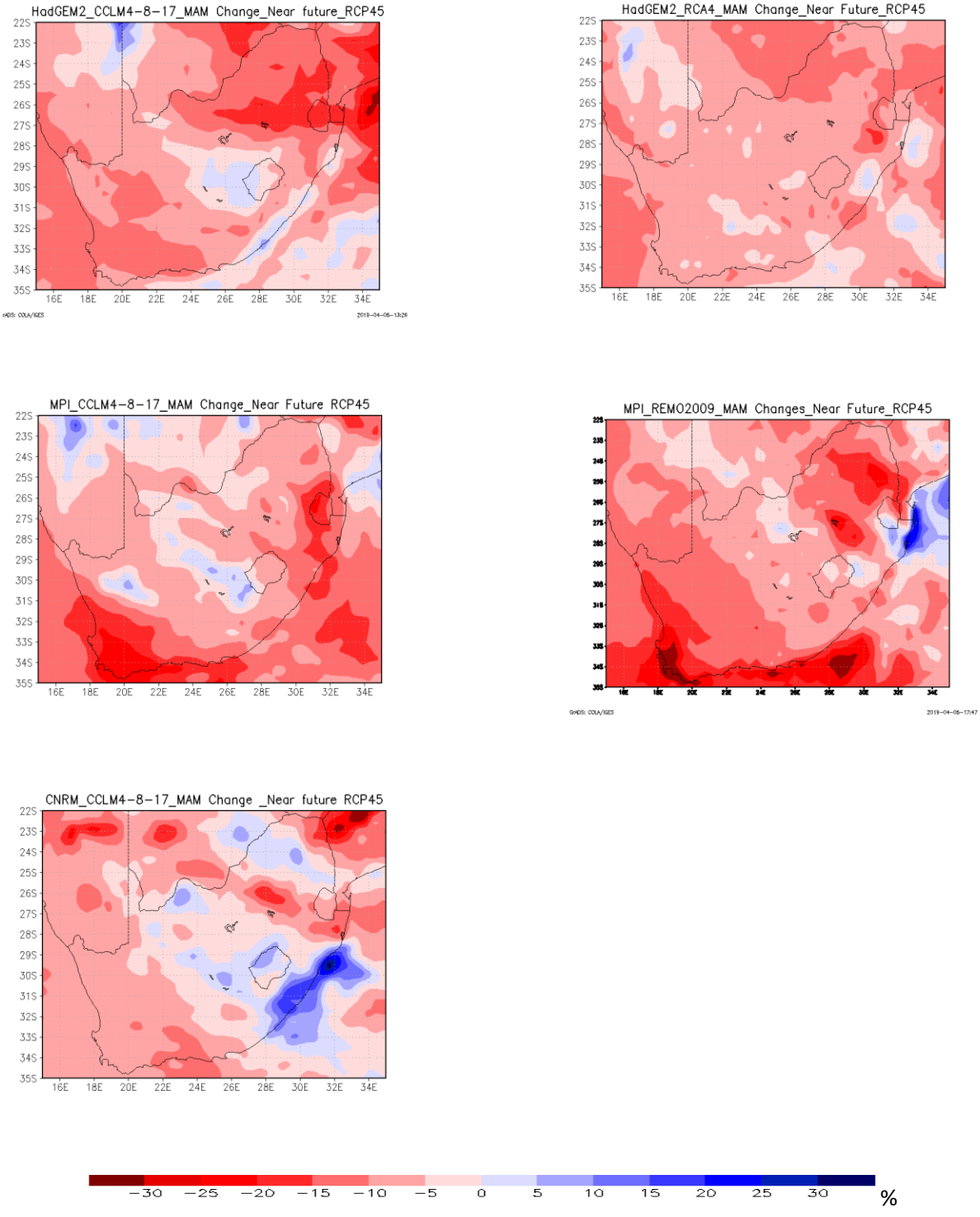

Figure 5. 8 MAM mean rainfall change projection, for Near-Future (2006-2035), relative to present climate (1976-2005), under conditions of the RCP45.

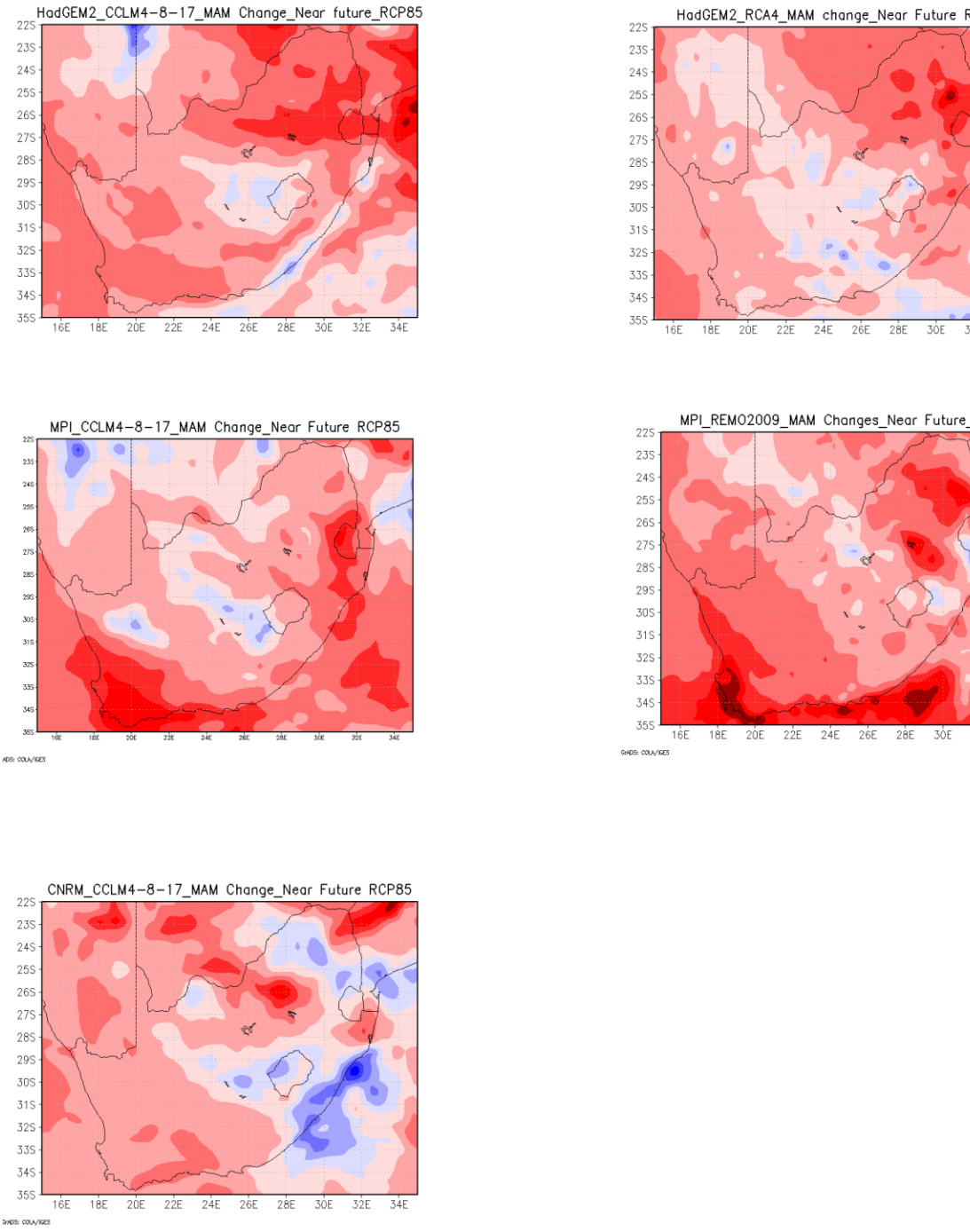

Figure 5. 9 MAM mean rainfall change projection, for Near-Future (2006-2035), relative to present climate (1976-2005), under conditions of the RCP85.

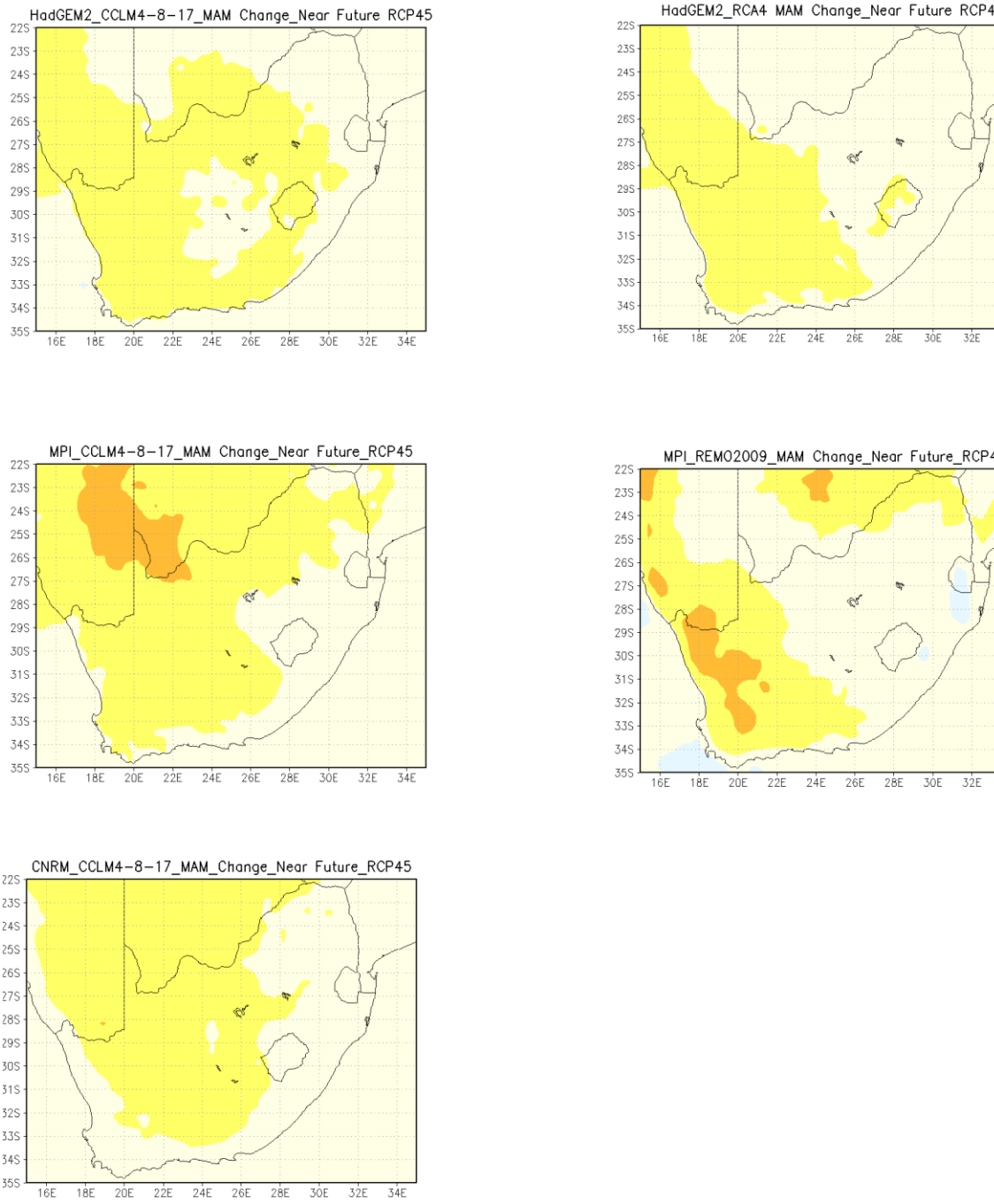

Figure 5. 10 MAM mean temperature change projection, for Near-Future (2006-2035), relative to present climate (1976-2005), under conditions of the RCP45.

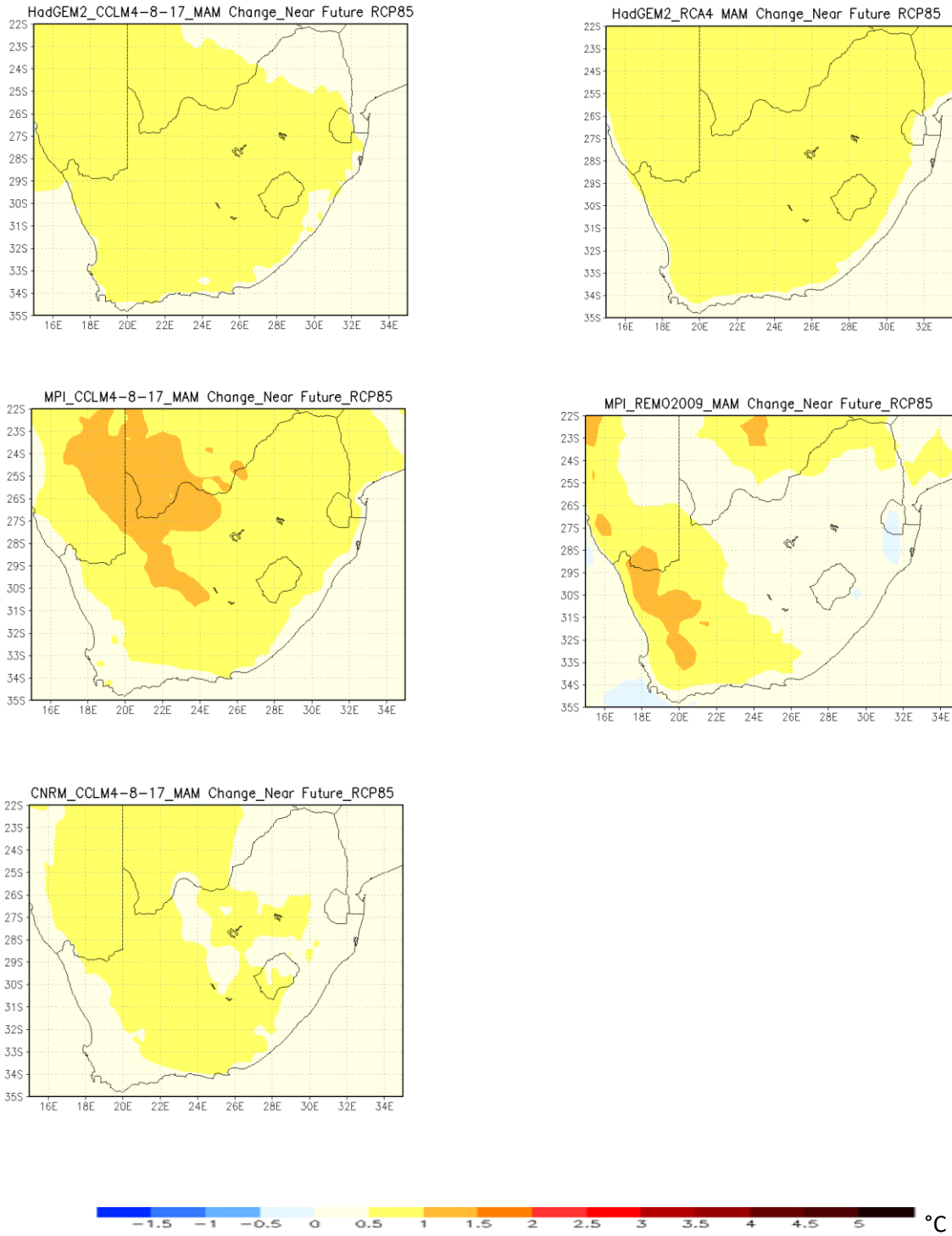

Figure 5. 11 MAM mean temperature change projection, for Near-Future (2006-2035), relative to present climate (1976-2005), under conditions of the RCP85.

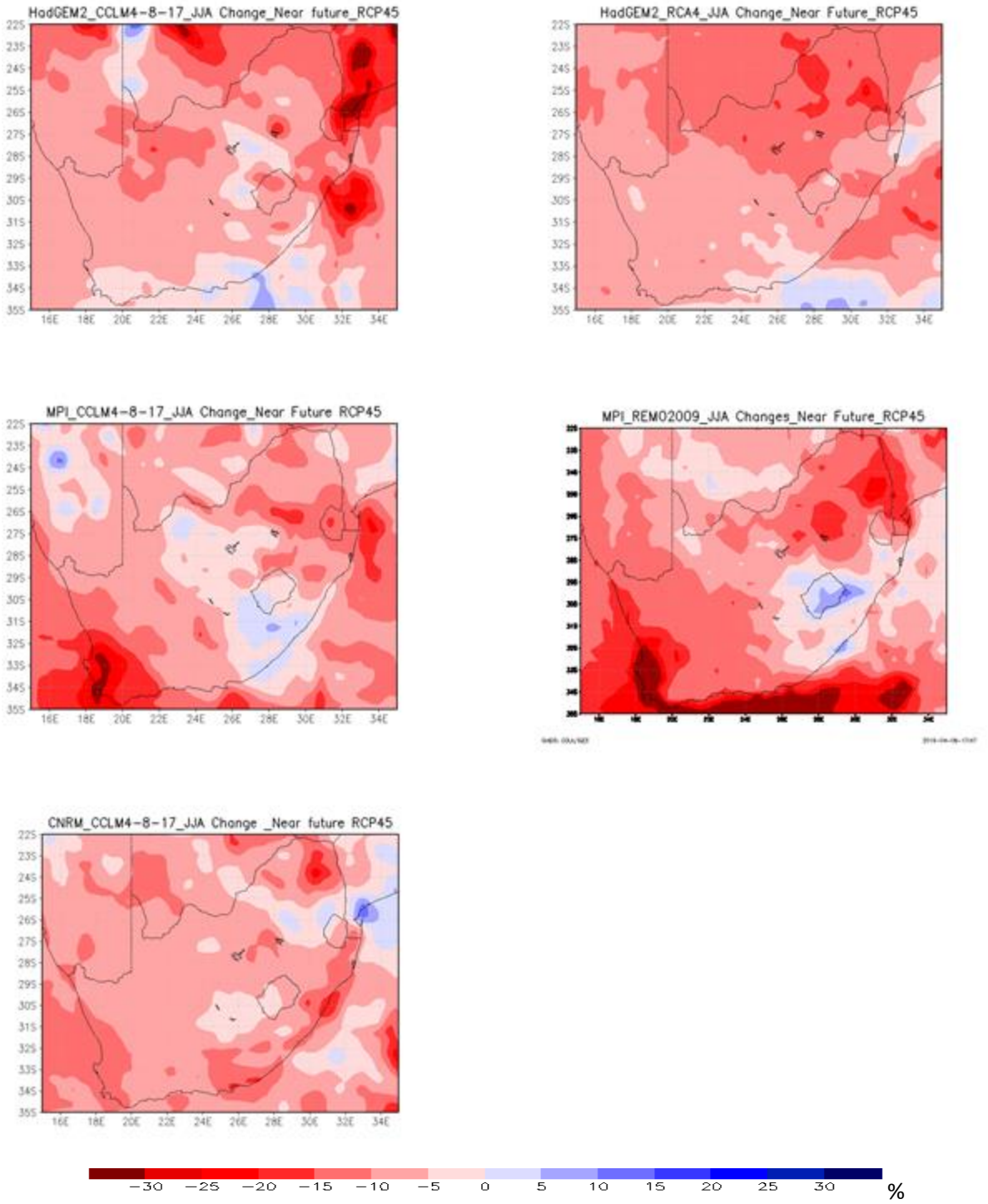

Figure 5. 12 JJA mean temperature change projection, for Near-Future (2006-2035), relative to present climate (1976-2005), under conditions of the RCP45.

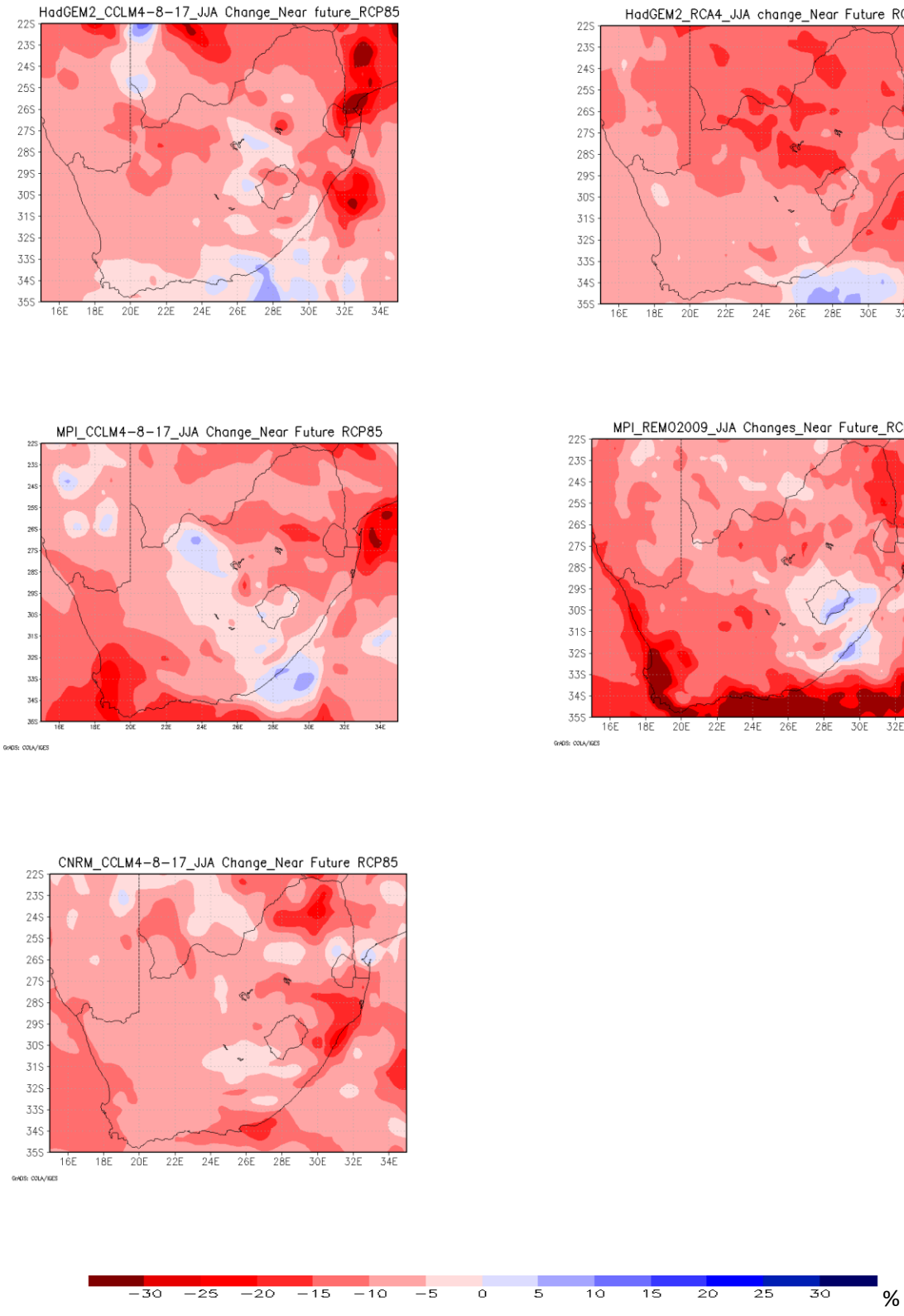

Figure 5. 13 JJA mean temperature change projection, for Near-Future (2006-2035), relative to present climate (1976-2005), under conditions of the RCP85.

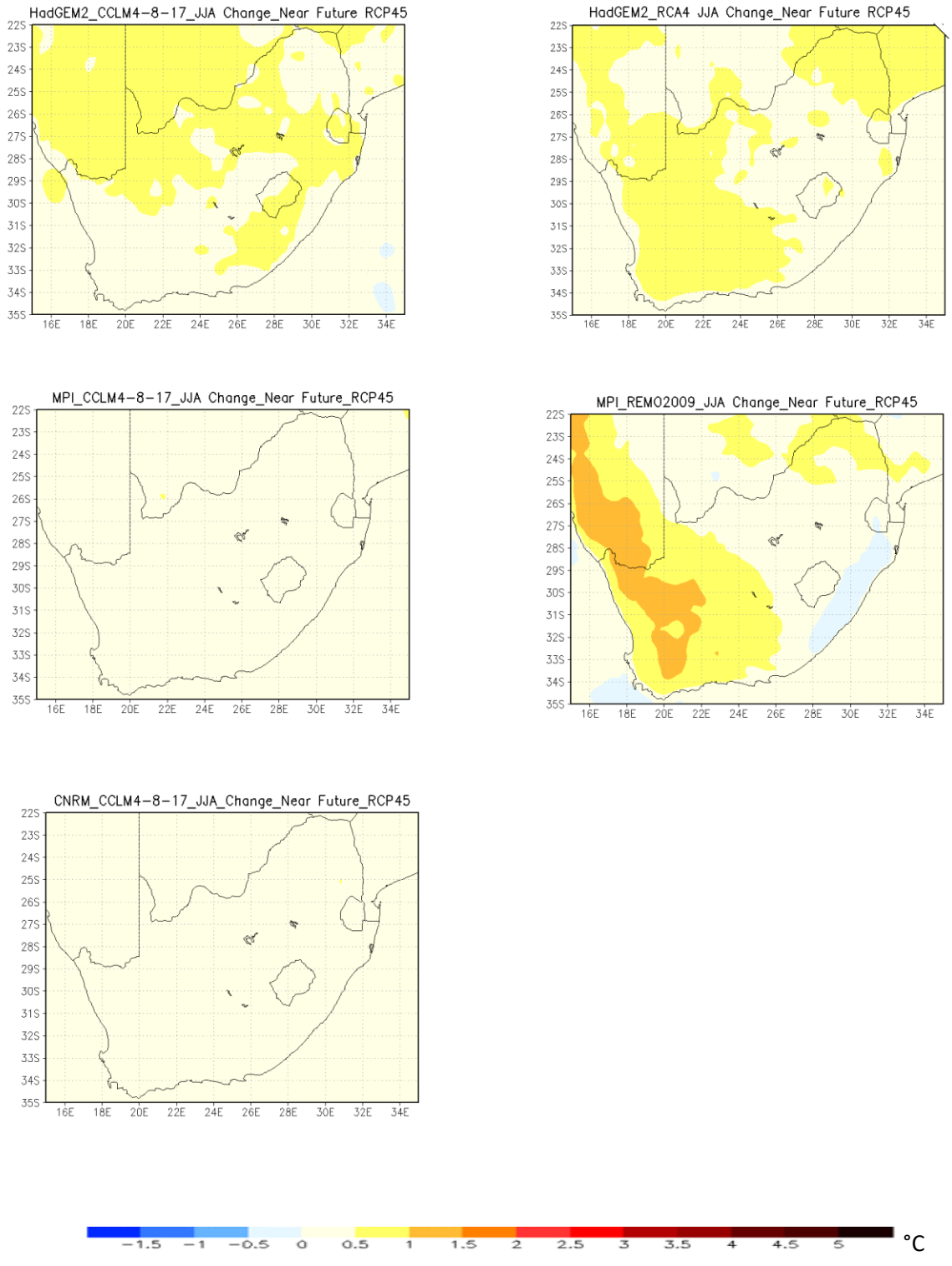

Figure 5. 14 JJA mean temperature change projection, for Near-Future (2006-2035), relative to present climate (1976-2005), under conditions of the RCP45.

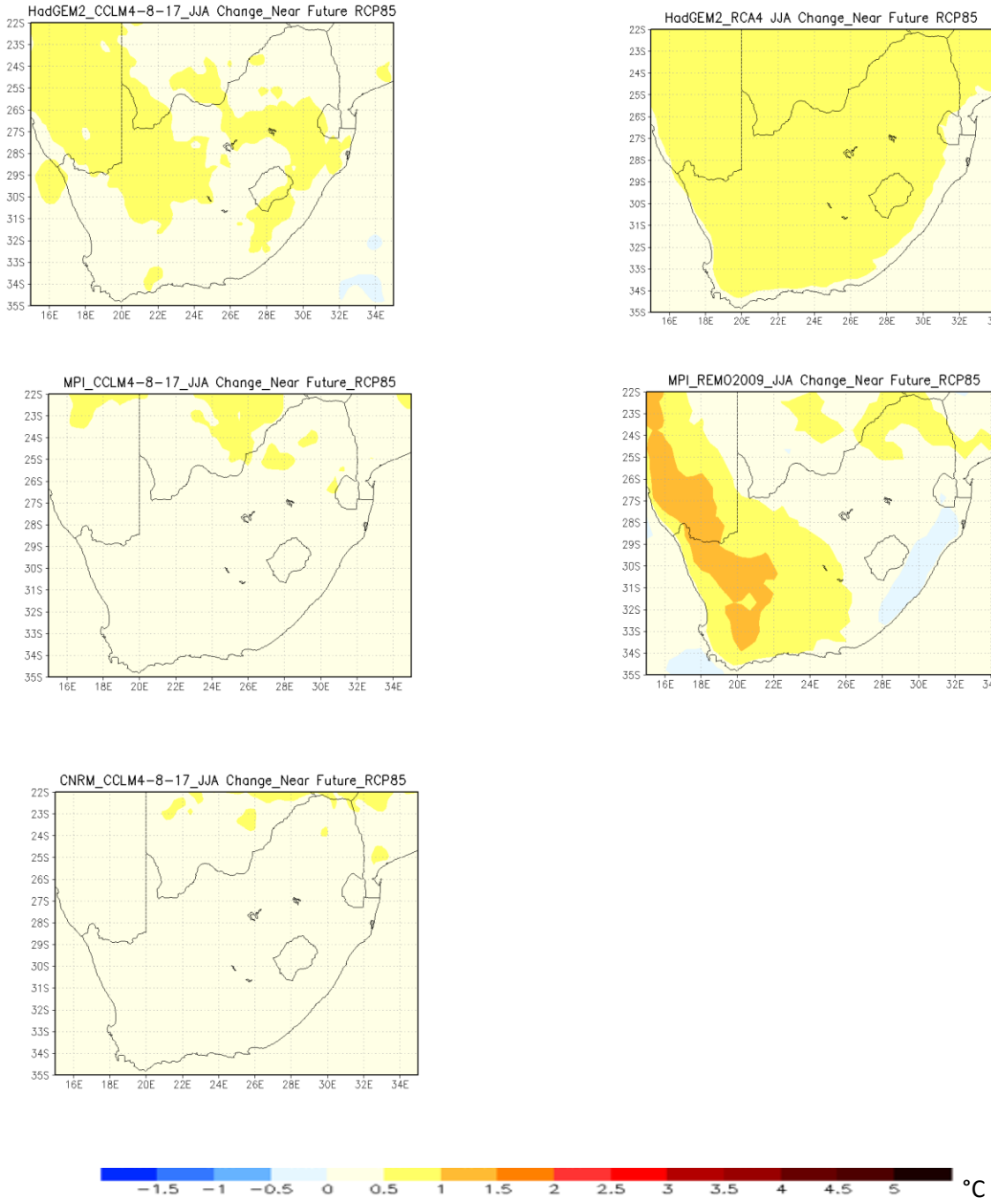

Figure 5. 15 JJA mean temperature change projection, for Near-Future (2006-2035), relative to present climate (1976-2005), under conditions of the RCP85.

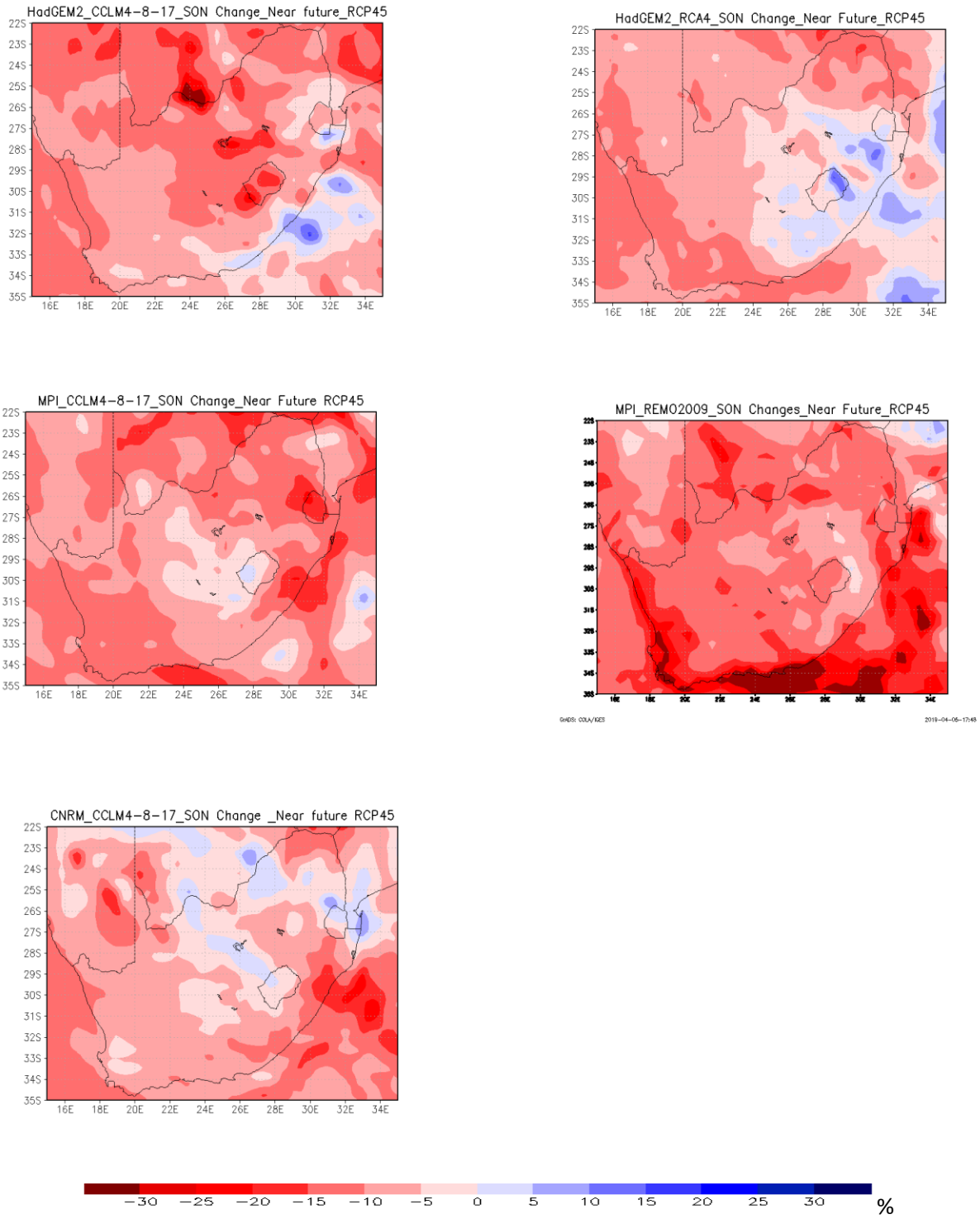

Figure 5. 16 SON mean rainfall change projection, for Near-Future (2006-2035), relative to present climate (1976-2005), under conditions of the RCP45.

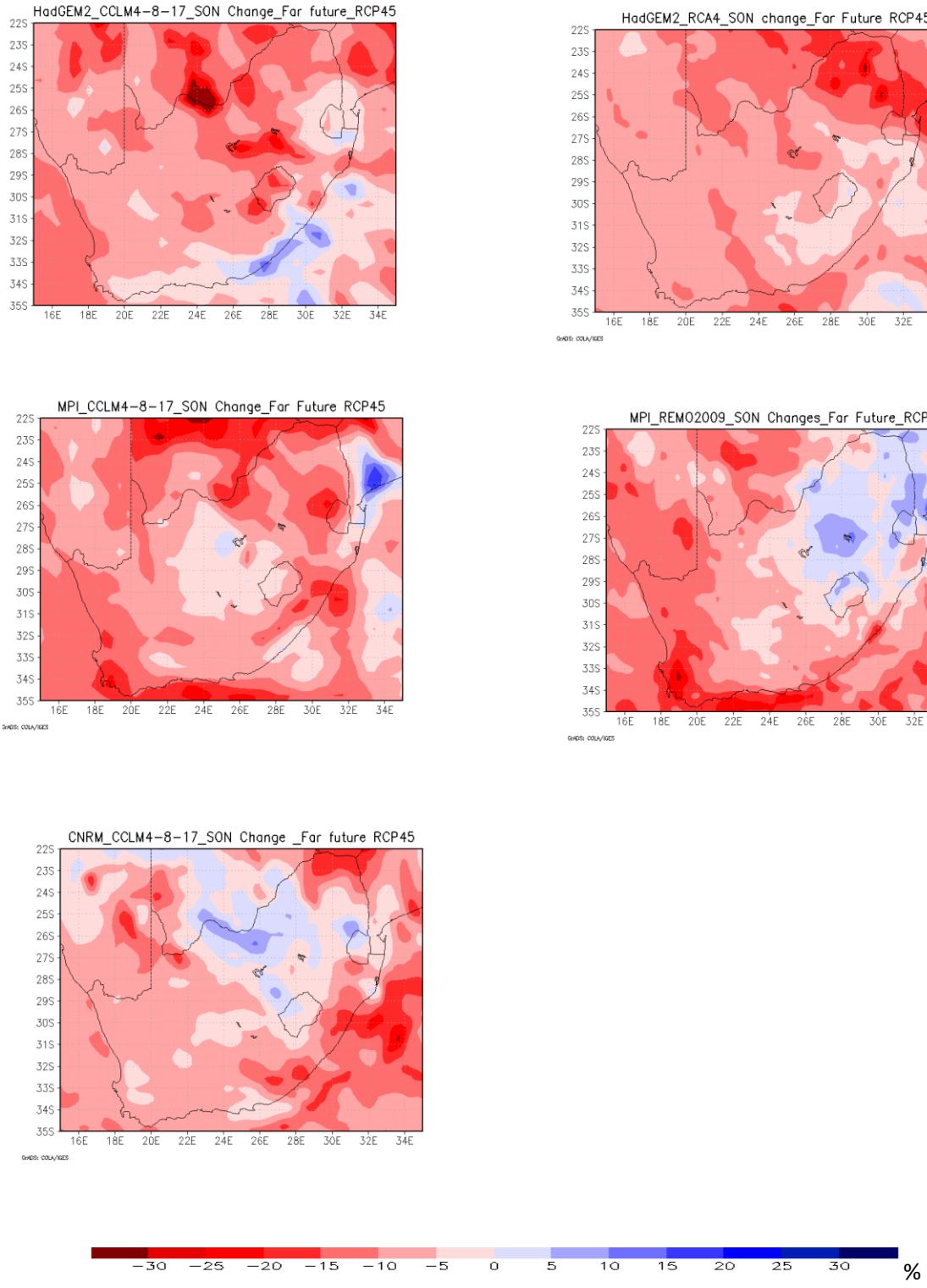

Figure 5. 17 SON mean rainfall change projection, for Near-Future (2006-2035), relative to present climate (1976-2005), under conditions of the RCP85.

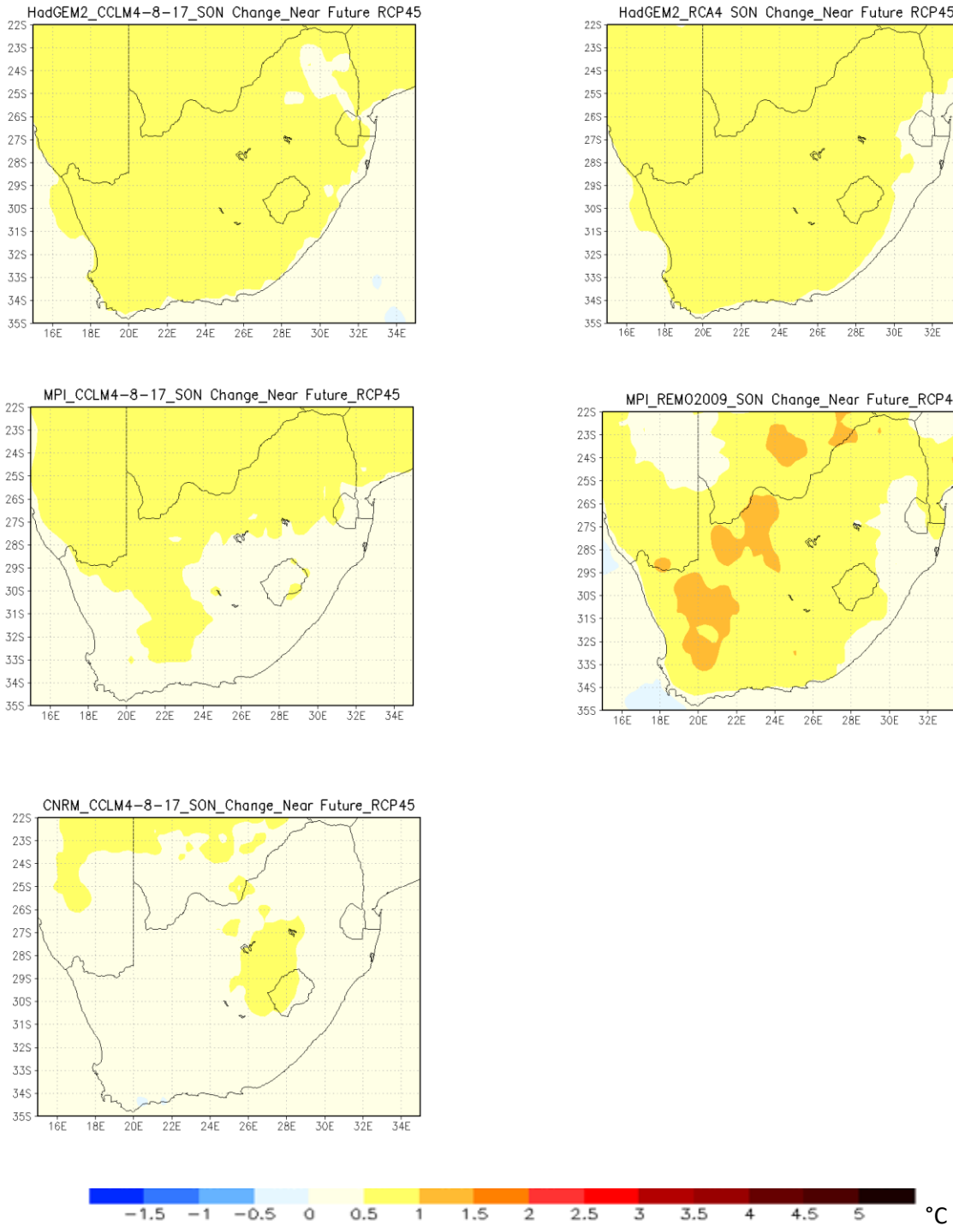

Figure 5. 18 SON mean temperature change projection, for Near-Future (2006-2035), relative to present climate (1976-2005), under conditions of the RCP45.

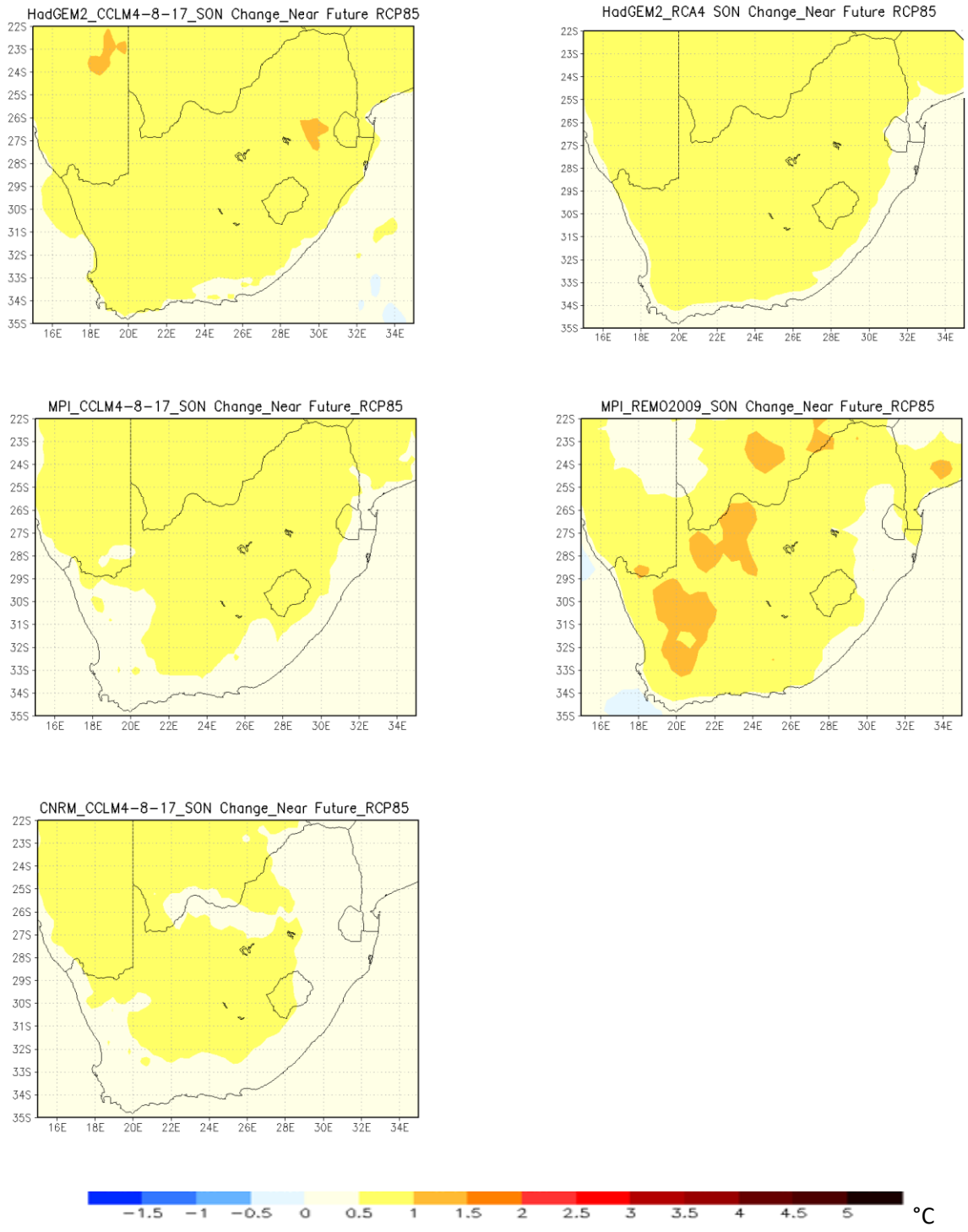

Figure 5. 19 SON mean temperature change projection, for Near-Future (2006-2035), relative to present climate (1976-2005), under conditions of the RCP85.

5.5 Annual rainfall change (Far Future)

A decrease in rainfall is projected for far future, similar to the near future with some patches of rainfall increases. The patches that indicate an increase in rainfall are smaller than those found in the near future projections (Figure 5.20). The projected increase in rainfall is found along the east coast and adjacent interior. For two of the projections made with CCLM4-8-17, nested within MPI and CNRM, the positive picture is also seen over the central interior. The two RCMs, that is, REMO2009 and CCLM4-8-17 nested within MPI project substantial decreases in total rainfall over the Western Cape, as was seen in the near-future projections as well. The REMO2009 projected drying, extends across the whole Western coast, again similar to the near-future projections. RCMs nested within HadGEM2 show some increases in rainfall over very small areas in the north eastern parts of the country, as well as over parts of the east coast. These increases do not extend into the interior. Most of low-lying areas such on the northeastern and eastern coast of South Africa are projected by all the models to receive considerable below average rainfall. Such findings agree with, UK Met Office (2011) who also suggested climate change to pose minor impacts on water resources beyond 2030s over the Limpopo low-lying areas. Moreover, other studies (e.g. Daron, 2014; IPCC, 2014; Garland et al., 2015) also projected less rainy days with high rainfall amounts in far future suggesting a possible increase in extreme rainfall events.

5.6 Annual mean temperature change (Far Future)

Further increases are projected for far future with these ranging from 2°C to 2.5°C over the central interior and at most 1.5°C for the coastal areas (Figure 5.21,). This is with the exception of REMO2009 nested within MPI, which projected consistently lower temperature than other models as was also the case for the near future projections. RCP8.5 projected pockets of intense heating (at most over western “arid” parts of South Africa including neighboring deserts (Figure 5.22). Several studies (e.g. Engelbrecht et al., 2015, Garland et al., 2015) have projected surfaces to heat up at a faster rate than the rest of the globe over these western parts of southern Africa, linked to the intensified subsidence of dry compressed hot air. In general, lower annual temperature increases are more likely under a low emissions scenario and higher temperature increase are more likely under a high emissions scenario as well-defined by several studies (e.g. Tadross et al, 2011; IPCC, 2014). The combination of increased temperatures and dry spells may result in frequent future wildfires over large areas in South Africa particularly in spring. This implies that the projected regional climate-change signal in temperature is determined by enhanced anthropogenic forcing. Engelbrecht et al., (2015) maintained that high-fire danger days would be

consistent with more frequent heat wave days. High ambient temperatures can directly impact human health through heat related diseases (Wright et al., 2015).

5.7 Seasonal mean rainfall and temperature changes (Far Future)

5.7.1 December-January-February (DJF)

All the models project a decrease in temperature in general over most of the country. CCLM4-8-17 nested within HAdGEM2 and CNRM and REMO2009 forced on MPI projected slightly increasing values (above 5%) over the central interior under RCP4.5, than RCA4 nested within HadGEM2 (Figure 5.23). Areas that are projected to experience increases in rainfall are almost similar to those in the near future climate. However, a tongue of extremely decreasing values (-25%) over the eastern parts of the country along south of Mozambique, tend to be consistently projected by RCMs forced by MPI and CCLM4-8-17 nested on CNRM under RCP8.5 scenarios (Figure 5.24). This may suggest the season was governed by the El Nino phase. A gradual increase of terrestrial temperature is projected over the western parts of the country from RCP4.5 (Figure 5.25) to RCP8.5 (Figure 5.26) by CCLM4-8-17 model nested within three GCMs, with MPI exhibiting the largest increase over the central interior of South Africa. However, REMO2009 nested within MPI, contradicted with other models and projected decreasing values (up to -0.5°C) along the western coast and adjacent interior of South Africa under both scenarios, similar to near future projections.

5.7.2 March-April-May (MAM)

All models similarly projected a drying trend over the low-lying areas of Limpopo Valley, under both scenarios, with CCLM4-8-17 nested within HadGEM2 showing great magnitude compared to the rest of the models. RCMs nested within MPI have projected a strong decreasing trend of rainfall over the Western Cape throughout the seasons, than any other models (Figure 5.27). However, RCP8.5 projected slight wetting over the central interior towards western parts of the country (Figure 5.28). Rainfall spatially varies prominently over South Africa in the same season (e.g. Nikulin, et al., 2012; Dedekind et al., 2016).

On the other hand, evidence of prolonged drier spells is supported by amplified surface temperature increase of 2°C from normal state over northwest and central interior are projected by CCLM4-8-17 model within three GCMs for both scenarios, with RCP85 having higher intensity (Figure 5.29). However, REMO2009 within MPI projected similar lower values than the rest of the models, the projections are however slightly different to the annual mean and DJF were lower

temperatures were projected over the Western parts of the country. For MAM, the highest temperature changes are projected over the western parts of the country. (Figure 5.30).

5.7.3 June-July August (JJA)

As already seen for most of the rainfall projections discussed here, all the models are projecting lower rainfall amounts for most of the country during JJA. A concentration of increasing values was projected by all the models under RCP45 over the eastern coast and the adjacent interior (Figure 5.31), with RCA4 nested within HadGEM2 and REMO2009 forced on MPI exhibiting significant wetting over the neighboring Lesotho Eastern Highlands. Importantly, over the Cape south coast and parts of Western Cape, models had a tendency of variability on rainfall projection. Projections driven by MPI are consistent in projecting extreme drying over the Western Cape and south coast similar to near future. Such findings agree with previous studies (e.g. Engelbrecht et al., 2009; Stager et al., 2012) projecting displacement of the rain producing mid latitude cyclones and westerlies farther south into the ocean. This would imply that the rainfall that would have fallen over the Western Cape will now occur south of the continent. CCLM4-8-17 nested within HadGEM2 projected a significant wetting over the south coast and Western Cape. All the models are consistent in projecting a general decrease in rainfall, due to changed circulation patterns characterized by suppressed rainfall as a result subsidence, as suggested by Dedekind et al (2016), over Limpopo Valley and some parts of western interior under RCP8.5 (Figure 5.32). All the models projected surface temperatures to be consistent with the previous season (MAM) for both scenarios (Figure 5.33 and Figure 5.34), hence some studies (e.g. IPCC, 2014) agree that there is high confidence of decrease (increase) in cold (warm) days and nights over southern Africa.

5.7.4 September-October-November (SON)

Predictions of rainfall change in South Africa displayed potential increases and decreases for both scenarios. A tendency of general wetting almost the entire central Highveld projected by CCLM4-8-17 nested within CNRM and REMO2009 forced on MPI, extending towards low-lying areas over Limpopo (Figure 5.35). The remaining models projected fairly decreasing values (-10%) over the same low-lying areas. The models projected significant below present day total rainfall values along the west coast. Previous other studies (e.g. Engelbrecht et al., 2009; Lumsden et al., 2009) projected similar decreasing values along the west coast and proximity interior areas and suggested a strengthening of the anticyclonic circulation and displacement of westerly winds. In contrast, SAWS (2017), projected wetter patterns over the west coastal areas.

Projections under RCP8.5 (Figure 5.36.) scenario are associated with larger temperature changes compared to RCP45, for all the models. RCMs nested with MPI model projected large increases of surface temperatures at most 2°C, with highest values noted over northwest parts of South Africa (Figure 5.37). The models also projected amplified warming (~3.5°C) under RCP8.5 with greater coverage towards much of the entire country in the far future (Figure 5.38). Such changes could trigger frequent heat waves and associated diseases Garland et al., 2015). However, REMO2009 nested within MPI projected lower temperature increases across all the seasons and annually. This may be due to the model (s) physics.

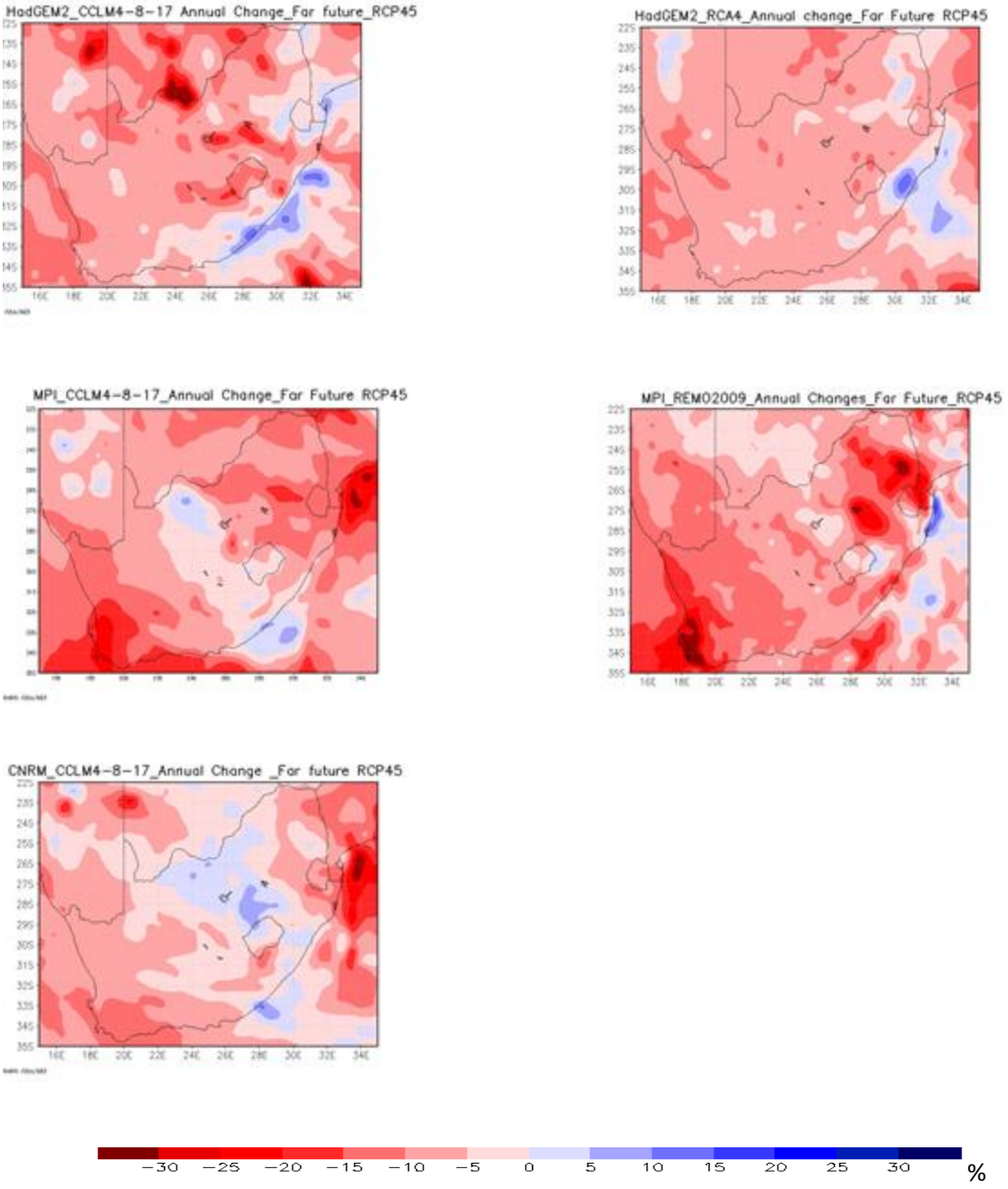

Figure 5. 20 Annual mean rainfall change projection, for Far-Future (2036-2065), relative to present climate (1976-2005), under conditions of the RCP45.

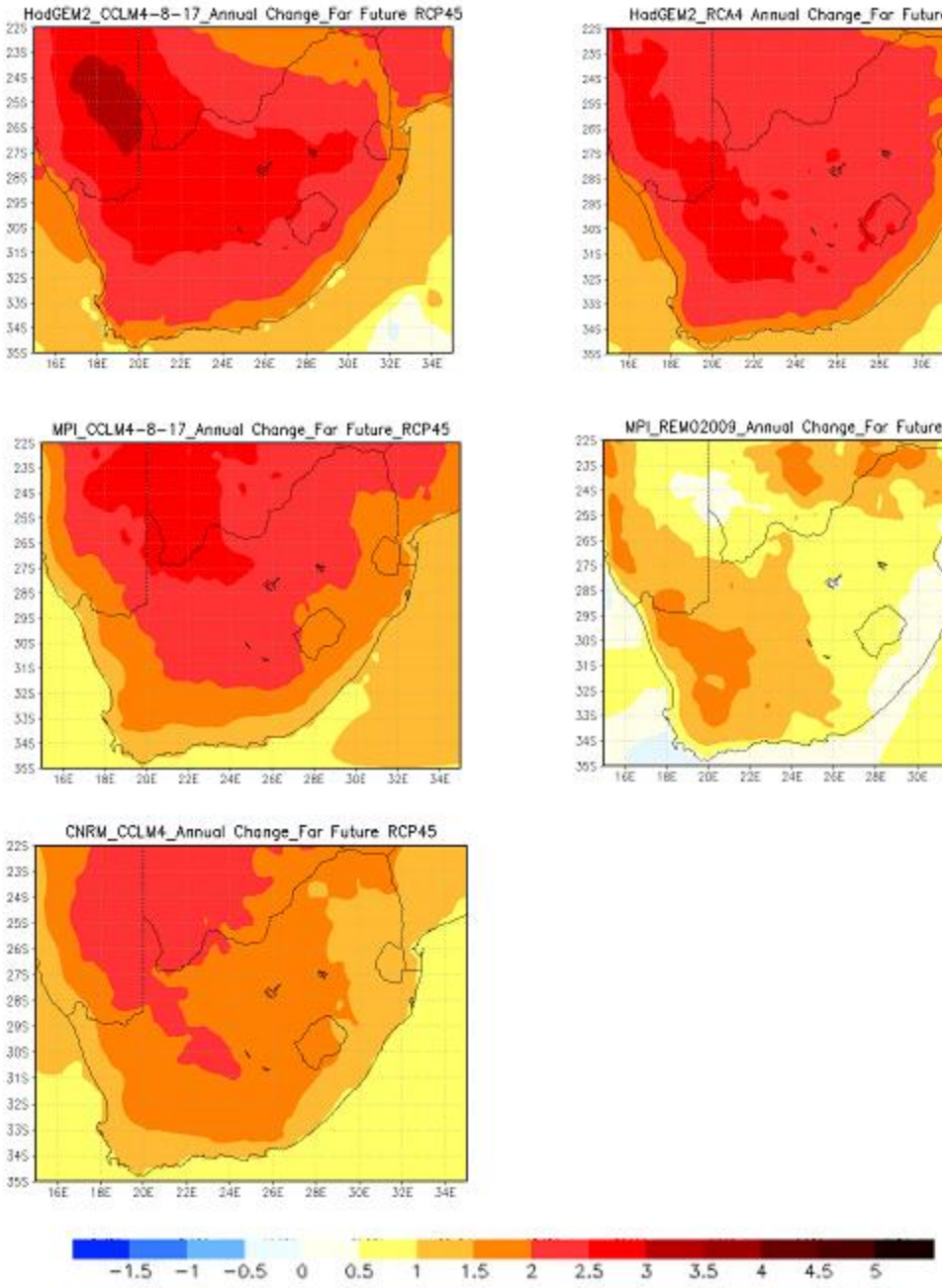

Figure 5. 21 Annual mean temperature change projection, for Far-Future (2036-2065), relative to present climate (1976-2005), under conditions of the RCP45.

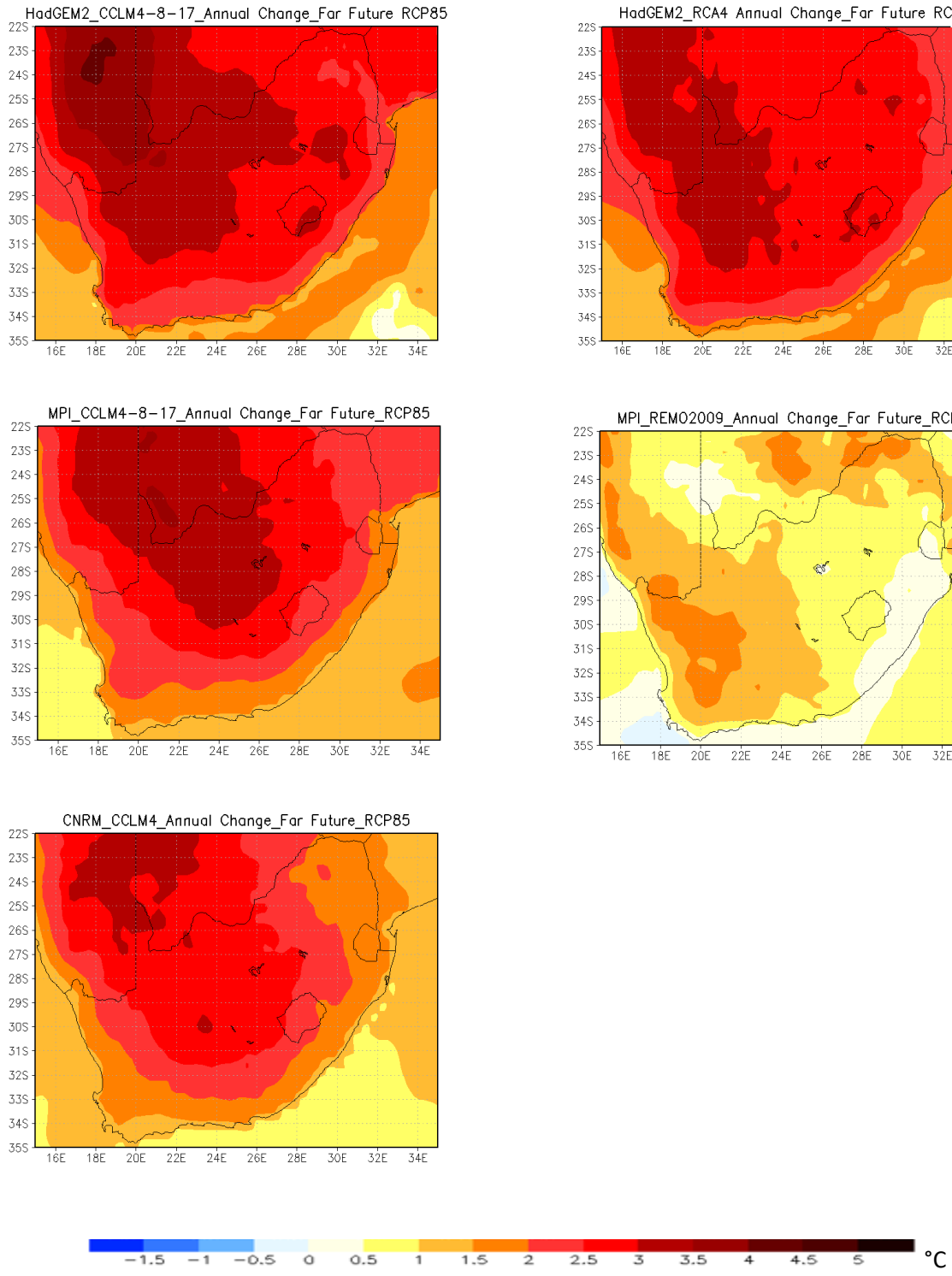

Figure 5. 22 Annual mean temperature change projection, for Far-Future (2036-2065), relative to present climate (1976-2005), under conditions of the RCP85.

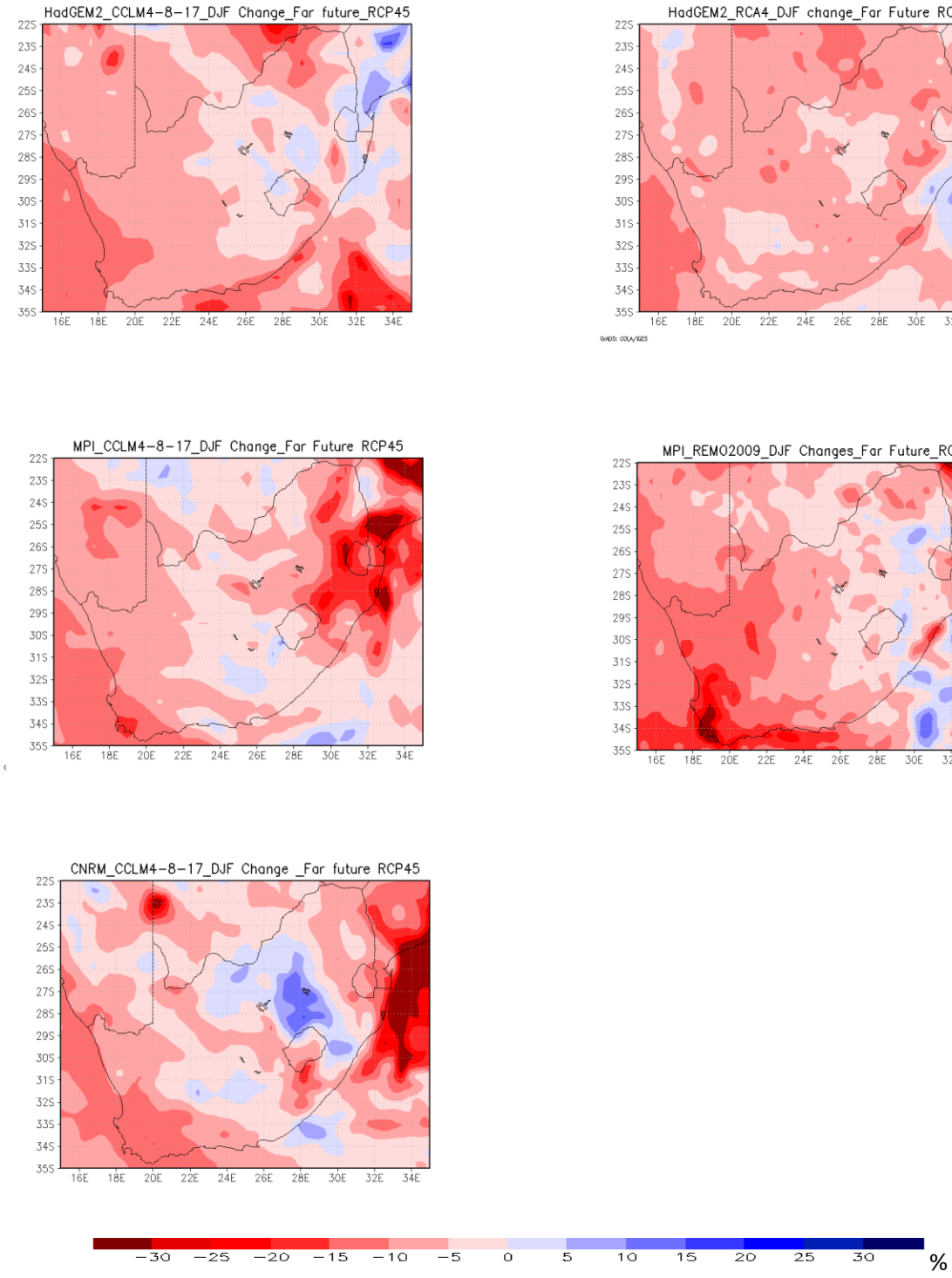

Figure 5. 23 DJF mean rainfall change projection, for Far-Future (2036-2065), relative to present climate (1976-2005), under conditions of the RCP45.

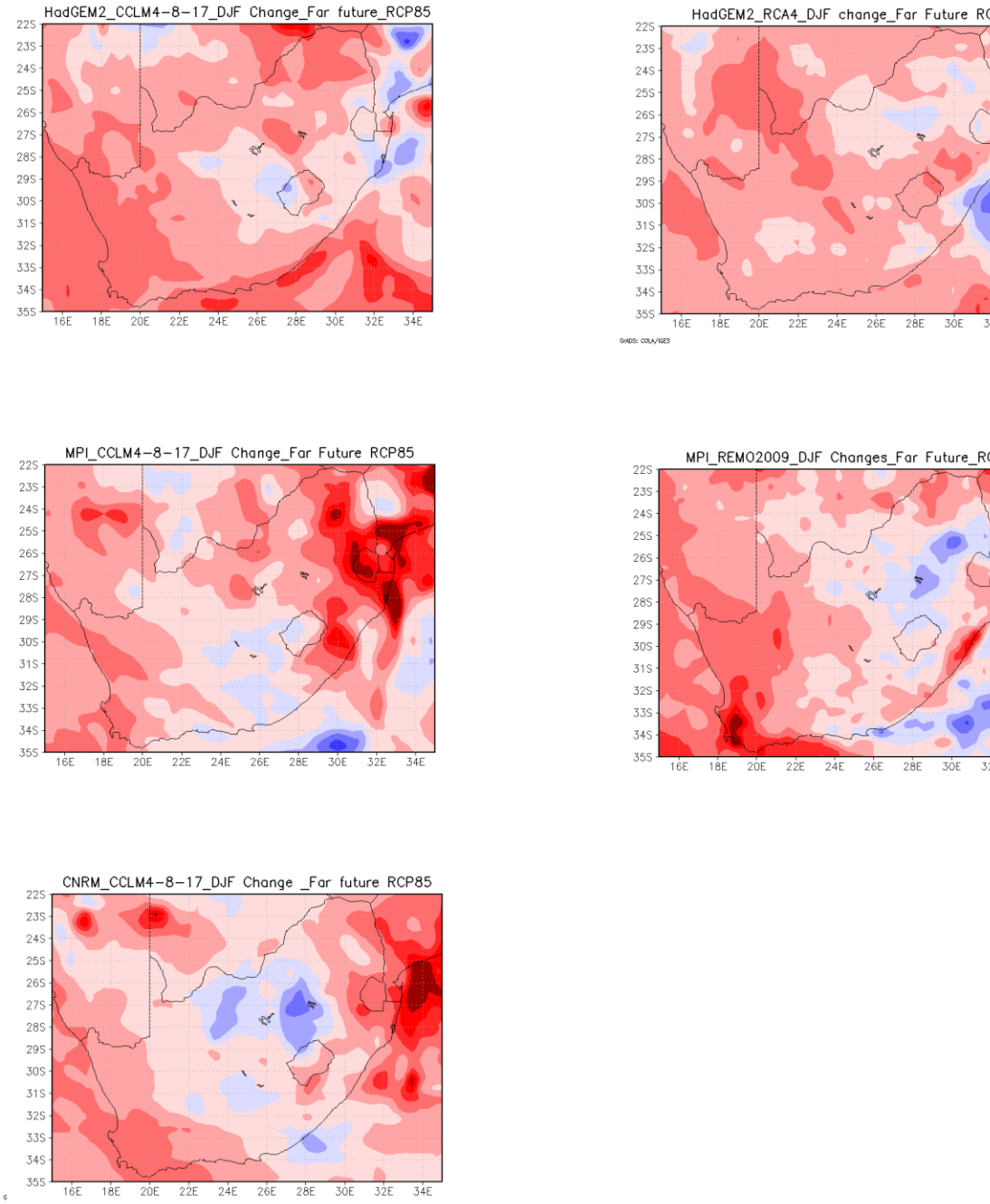

Figure 5. 24 DJF mean rainfall change projection, for Far-Future (2036-2065), relative to present climate (1976-2005), under conditions of the RCP85.

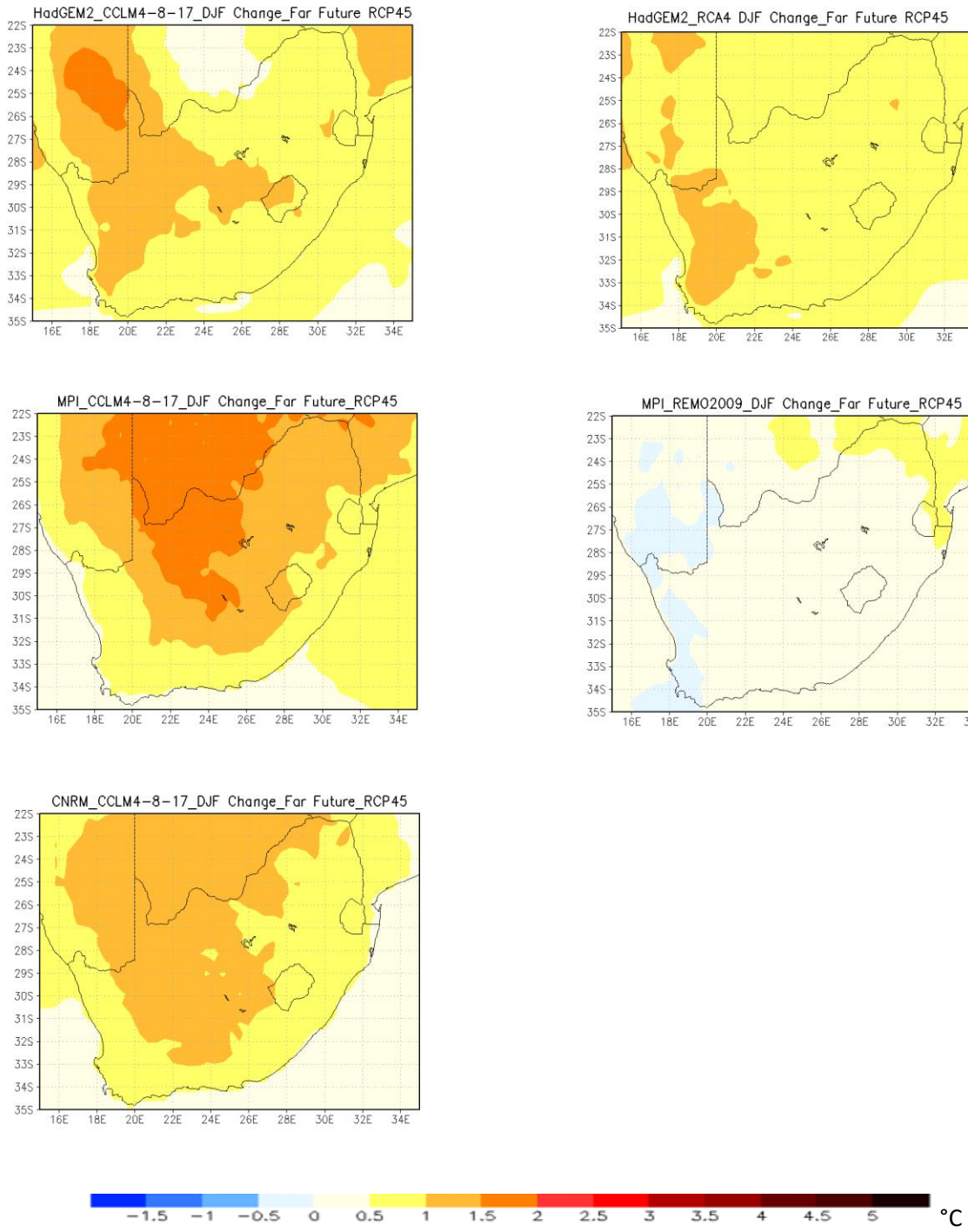

Figure 5. 25 DJF mean temperature change projection, for Far-Future (2036-2065), relative to present climate (1976-2005), under conditions of the RCP45.

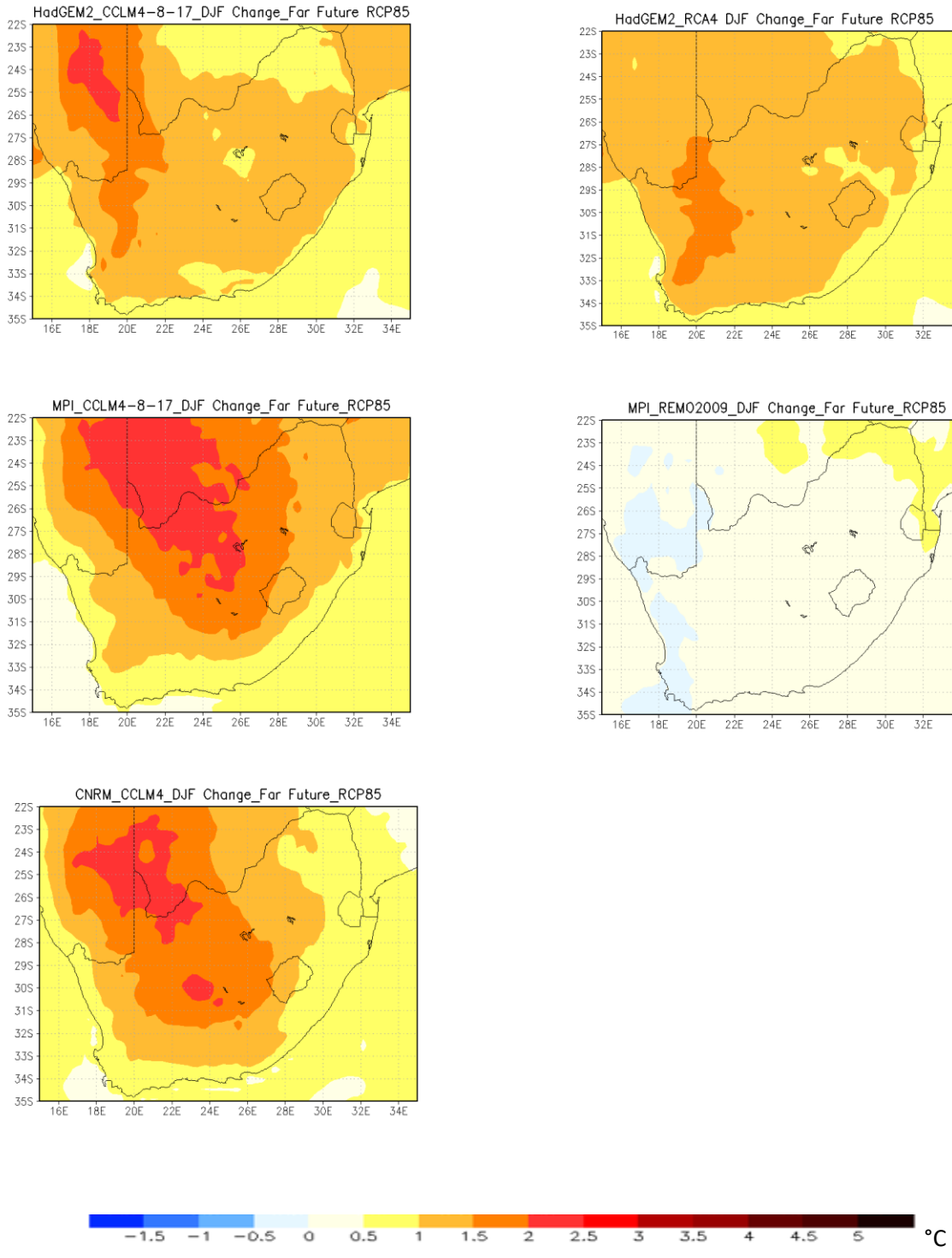

Figure 5. 26 DJF mean temperature change projection, for Far-Future (2036-2065), relative to present climate (1976-2005), under conditions of the RCP85.

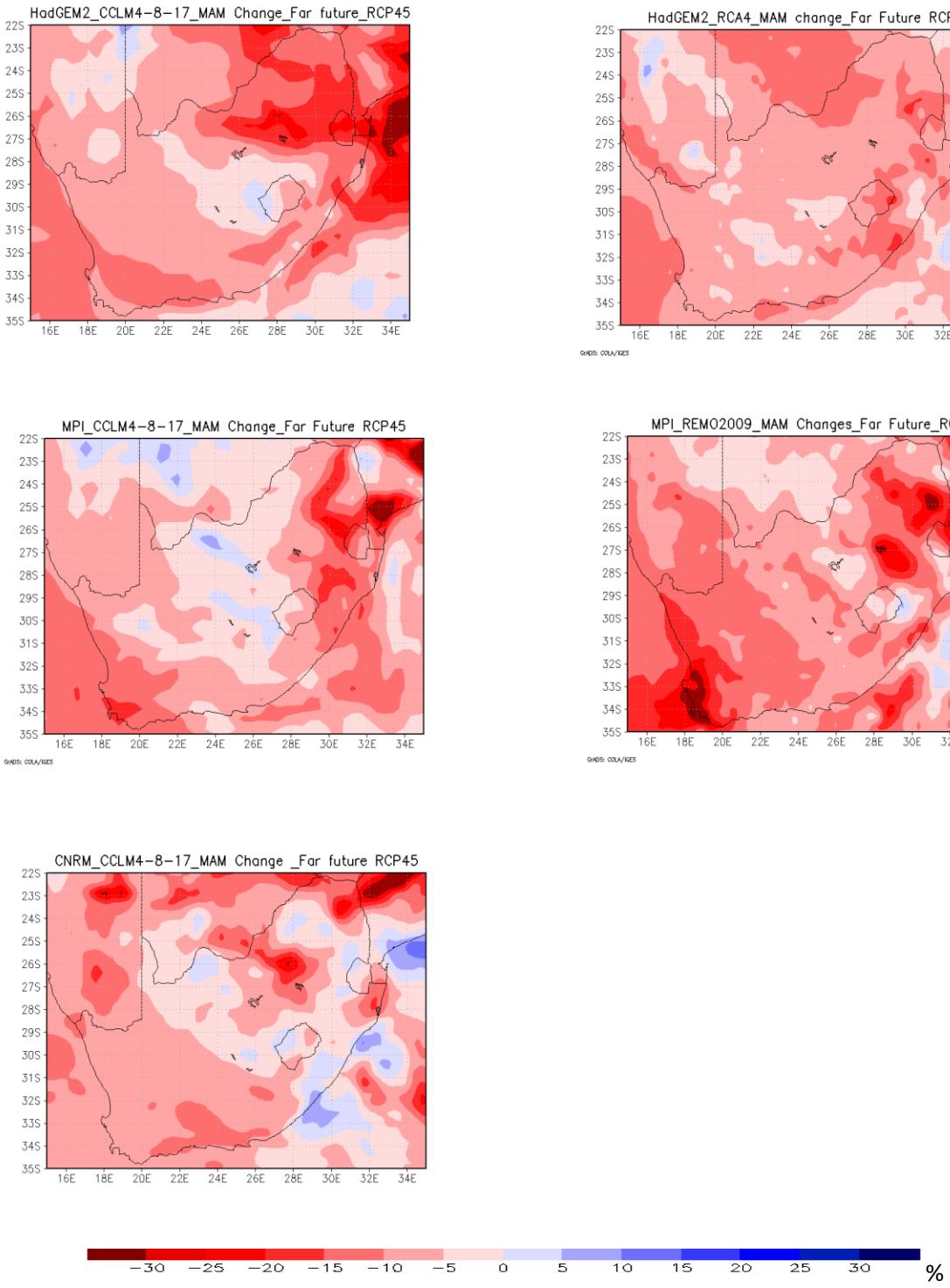

Figure 5. 27 MAM mean rainfall change projection, for Far-Future (2036-2065), relative to present climate (1976-2005), under conditions of the RCP45.

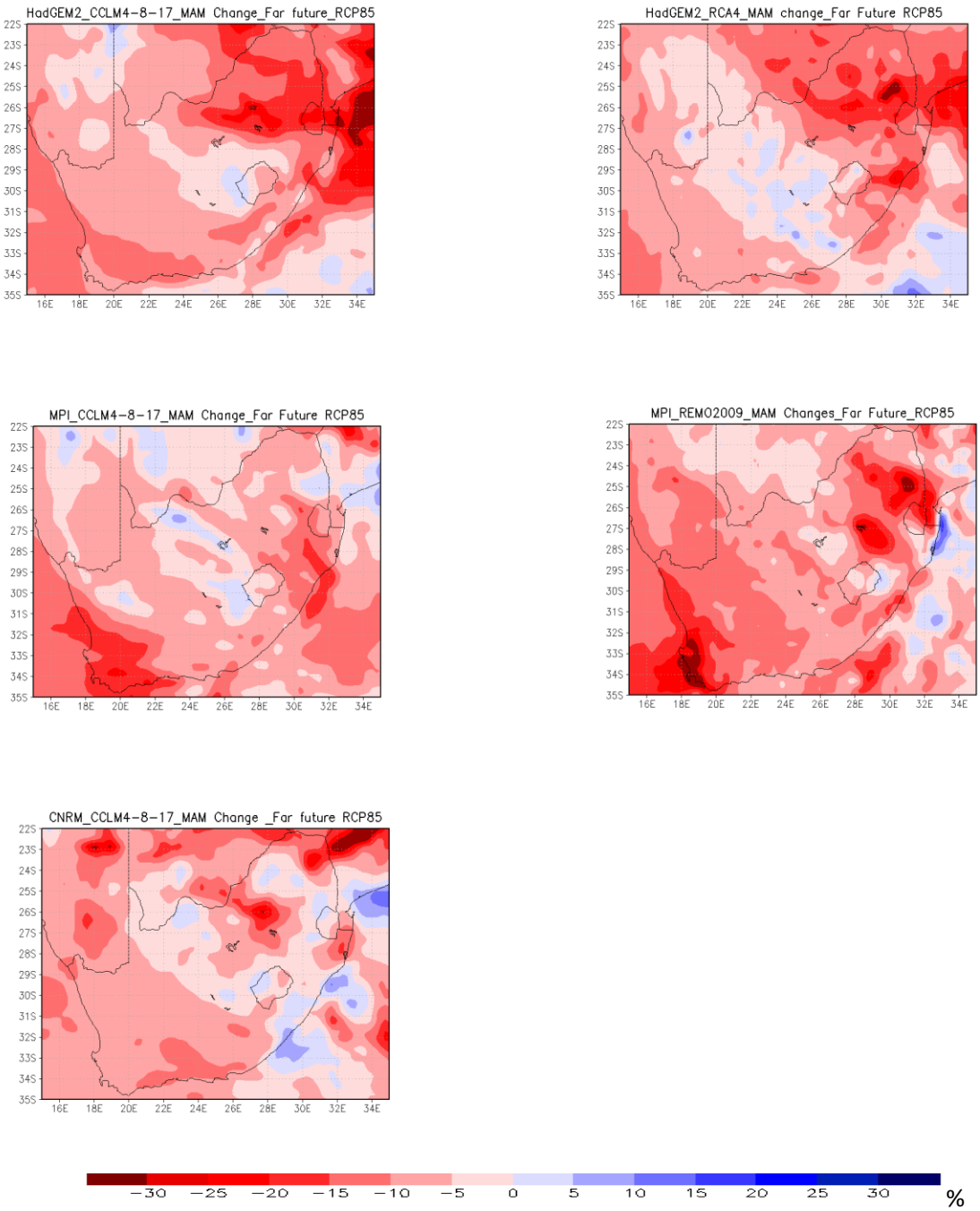

Figure 5. 28 MAM mean rainfall change projection, for Far-Future (2036-2065), relative to present climate (1976-2005), under conditions of the RCP85.

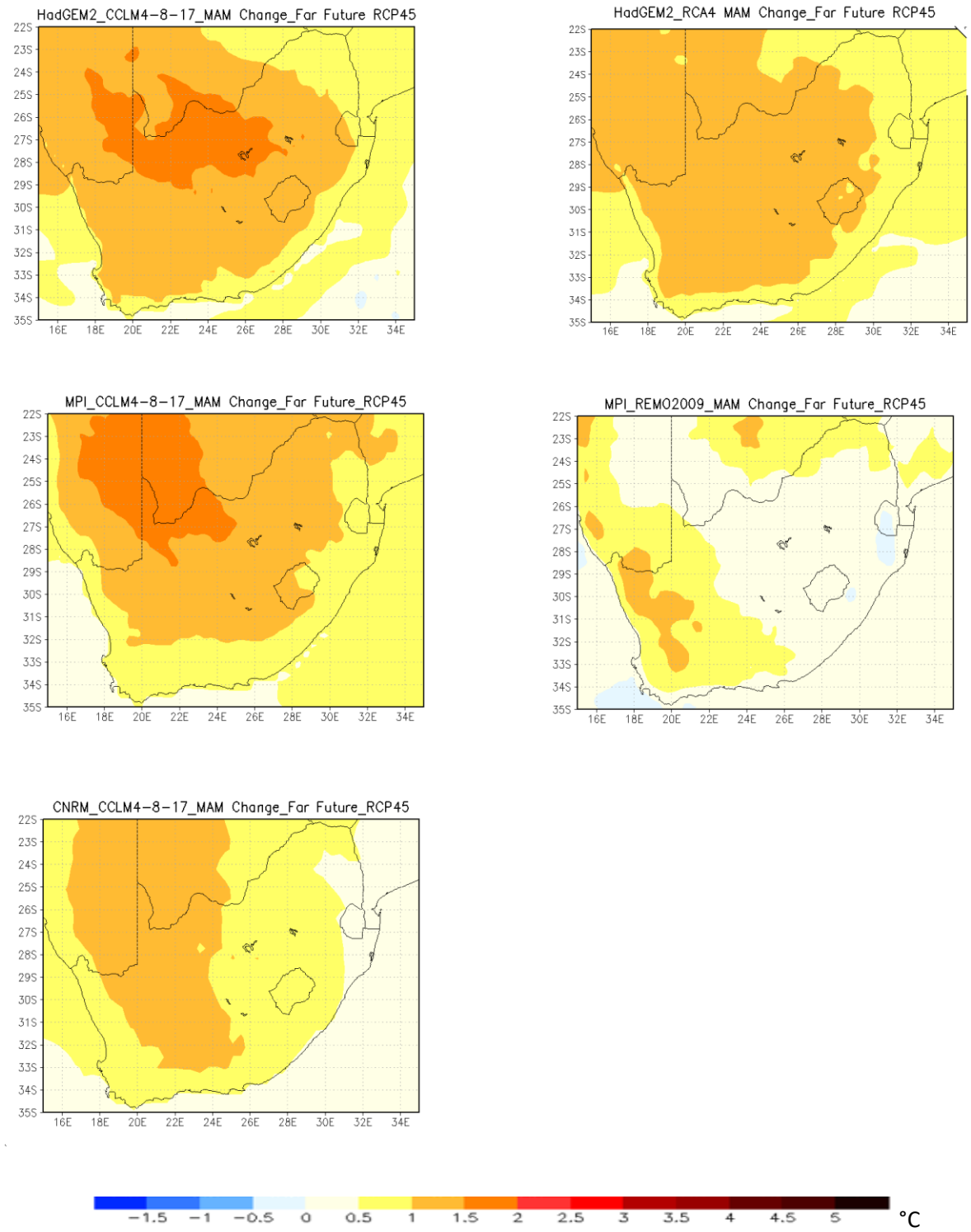

Figure 5. 29 MAM mean temperature change projection, for Far-Future (2036-2065), relative to present climate (1976-2005), under conditions of the RCP45.

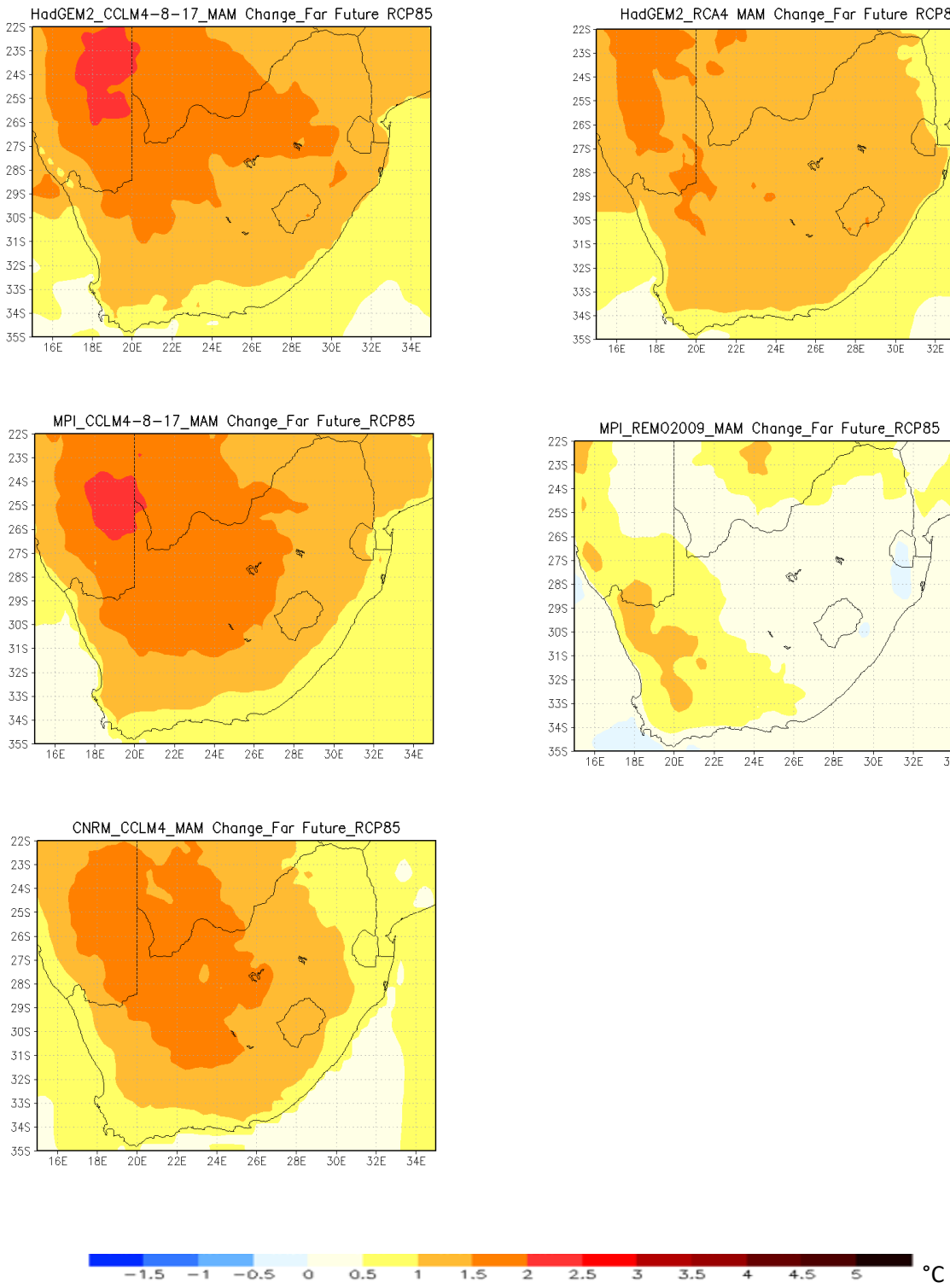

Figure 5. 30 MAM mean temperature change projection, for Far-Future (2036-2065), relative to present climate (1976-2005), under conditions of the RCP85.

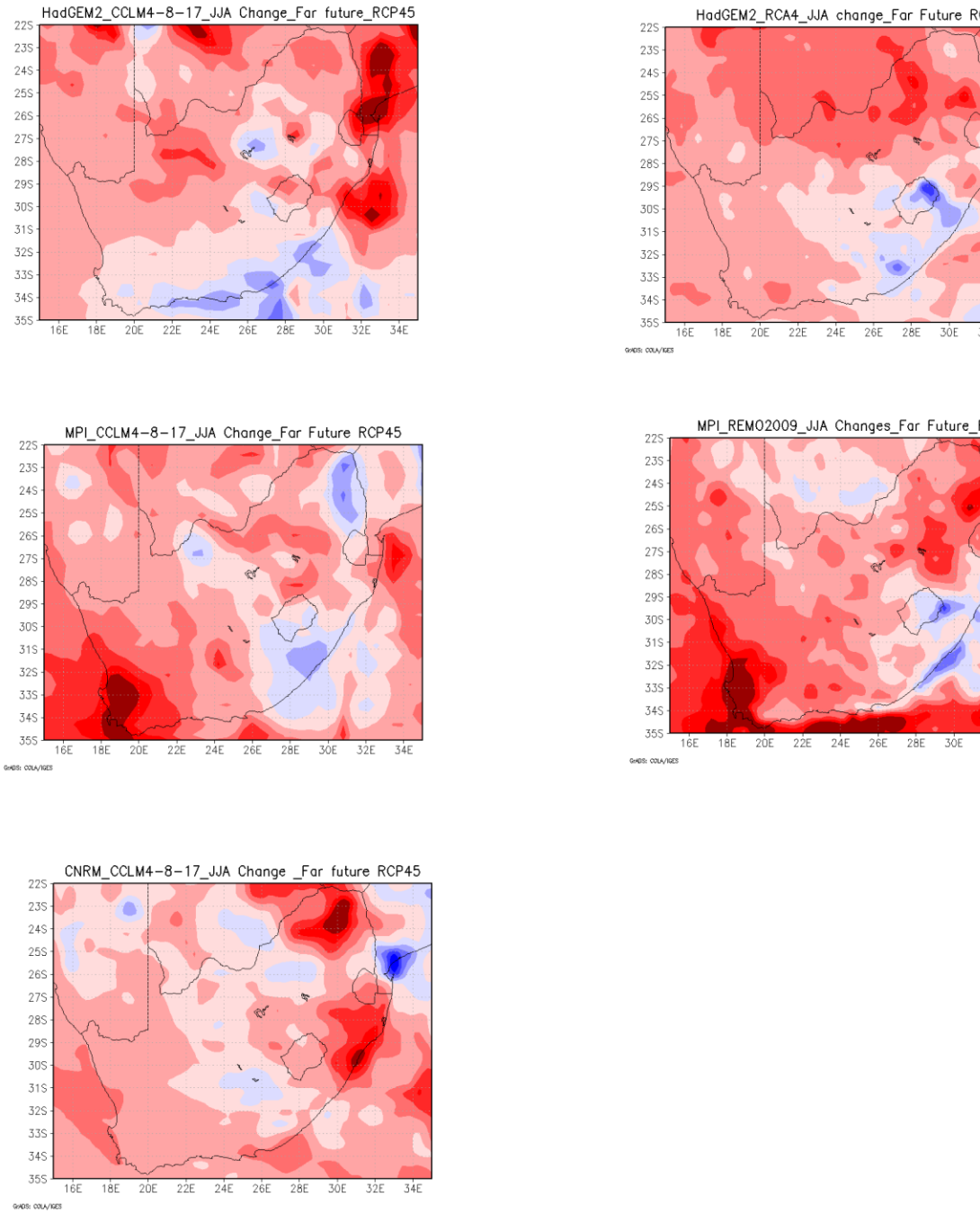

Figure 5. 31 JJA mean rainfall change projection, for Far-Future (2036-2065), relative to present climate (1976-2005), under conditions of the RCP45.

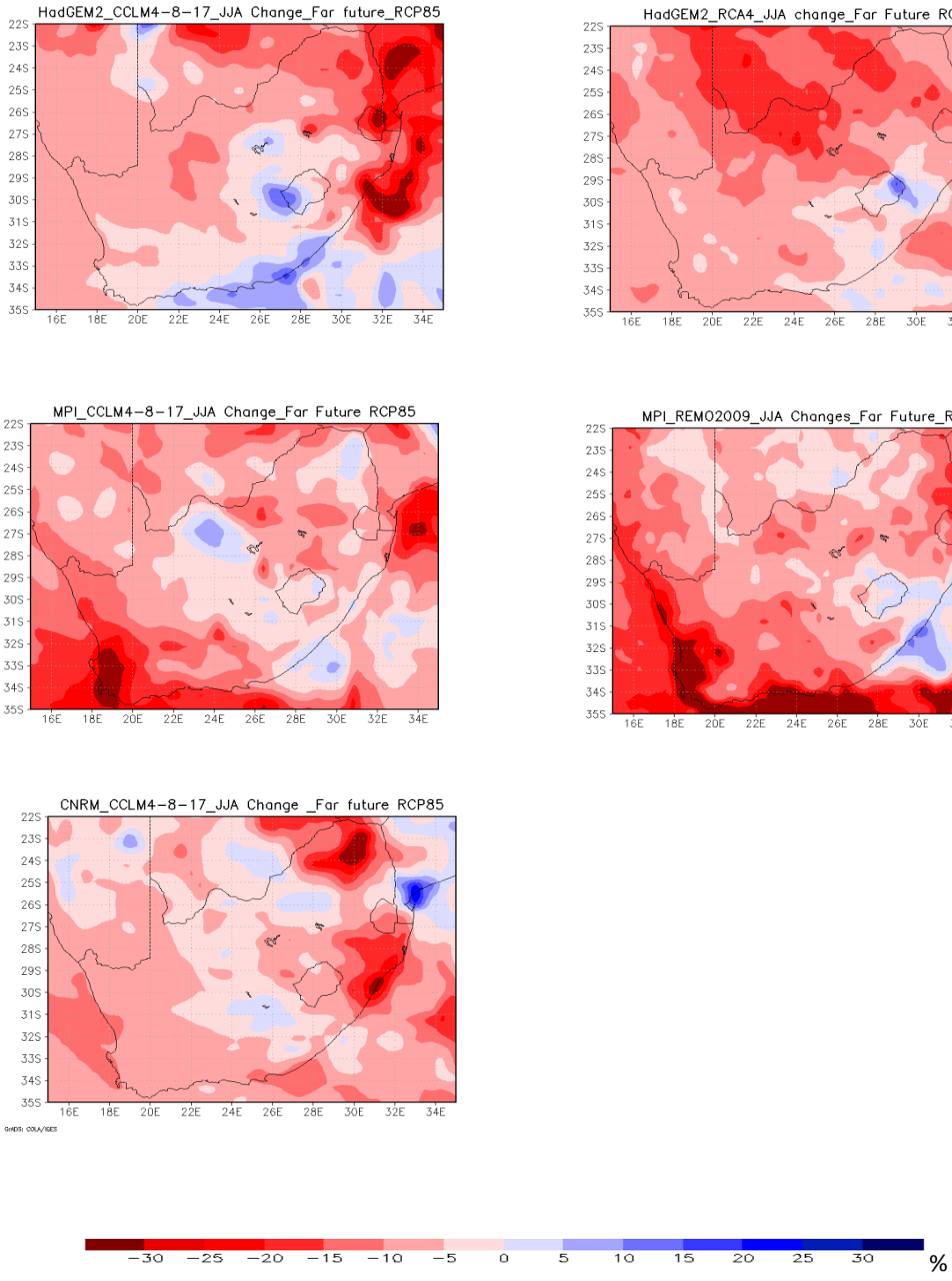

Figure 5. 32 JJA mean rainfall change projection, for Far-Future (2036-2065), relative to present climate (1976-2005), under conditions of the RCP85.

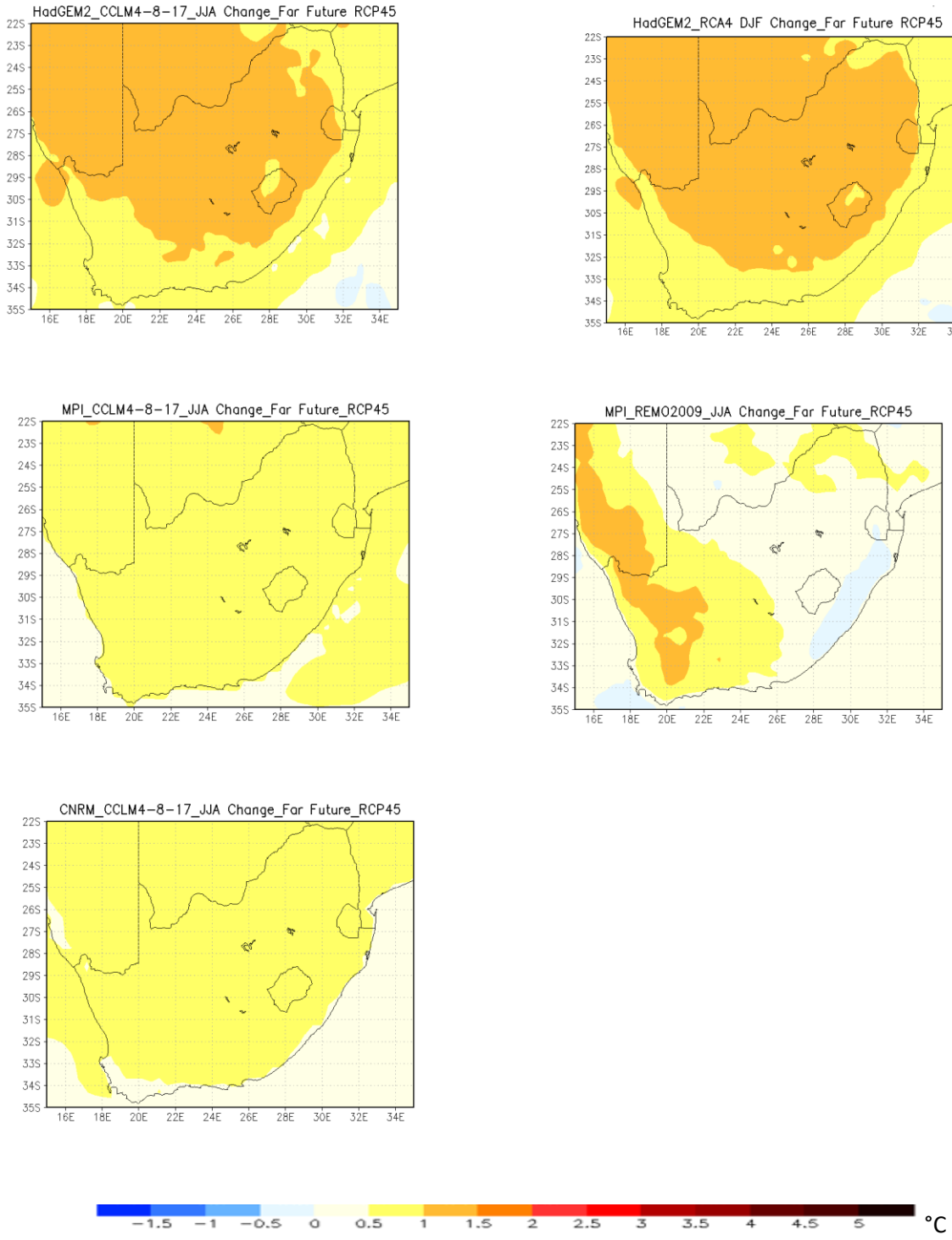

Figure 5. 33 JJA mean temperature change projection, for Far-Future (2036-2065), relative to present climate (1976-2005), under conditions of the RCP45.

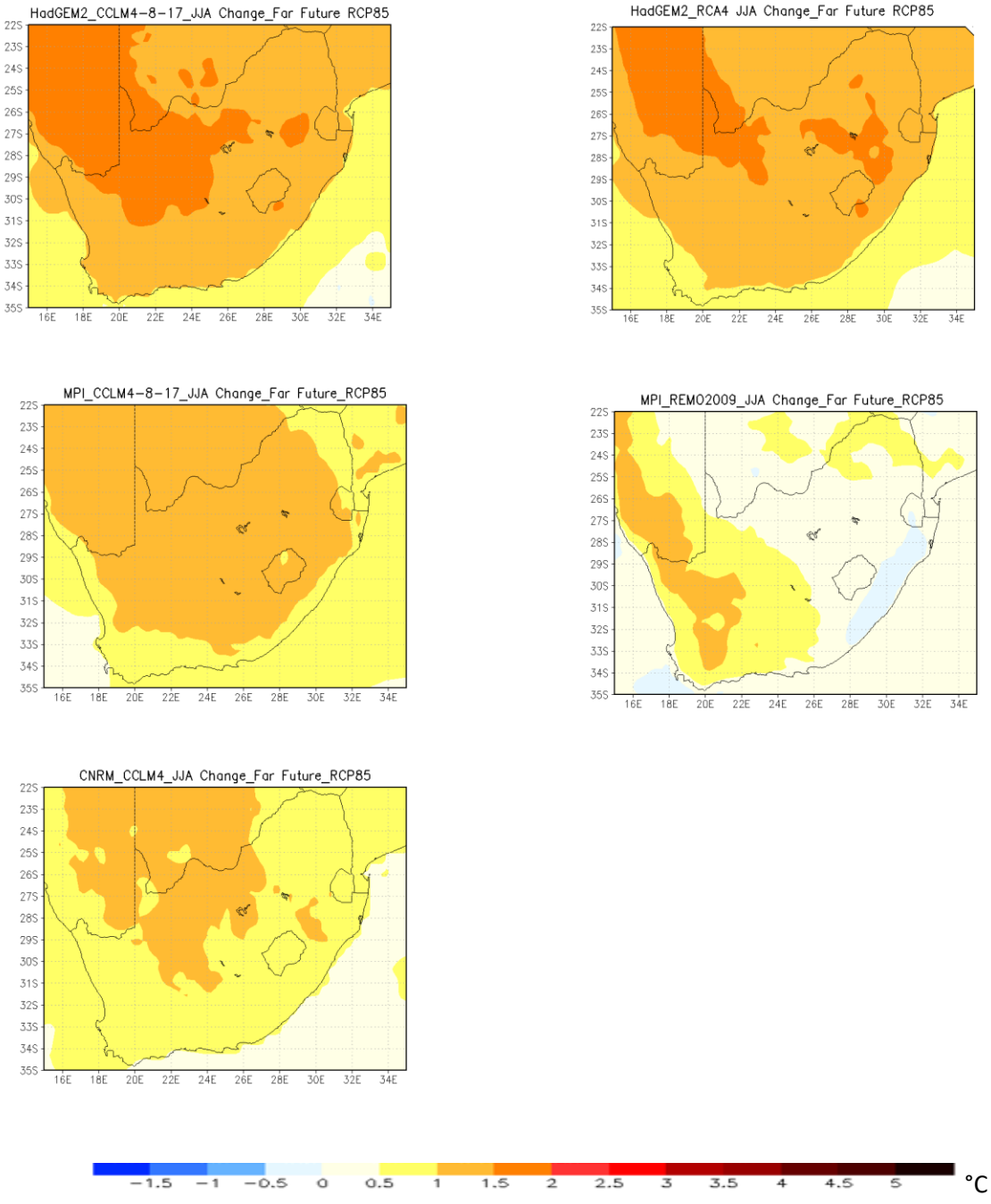

Figure 5. 34 JJA mean temperature change projection, for Far-Future (2036-2065), relative to present climate (1976-2005), under conditions of the RCP85.

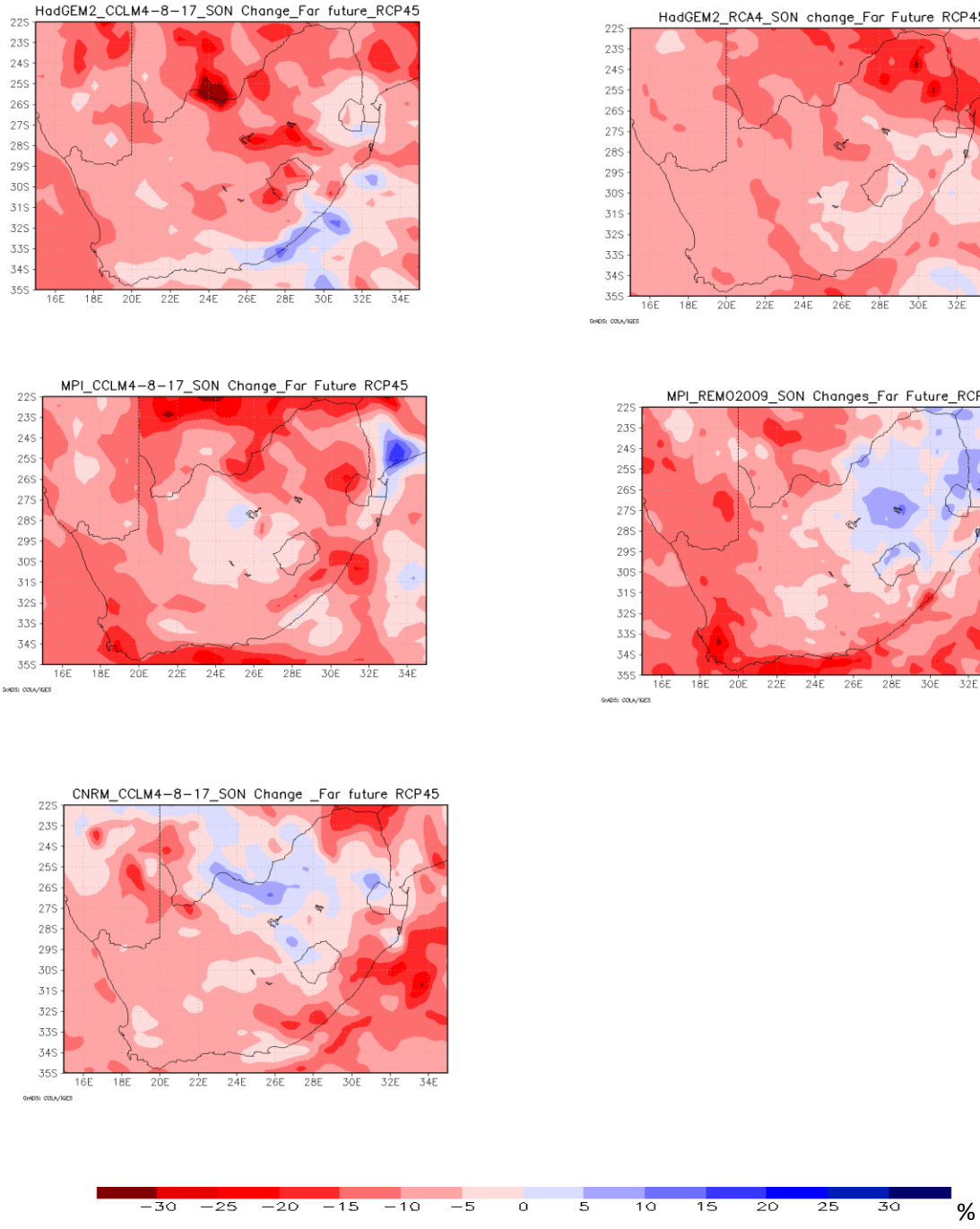

Figure 5. 35 SON mean rainfall change projection, for Far-Future (2036-2065), relative to present climate (1976-2005), under conditions of the RCP45.

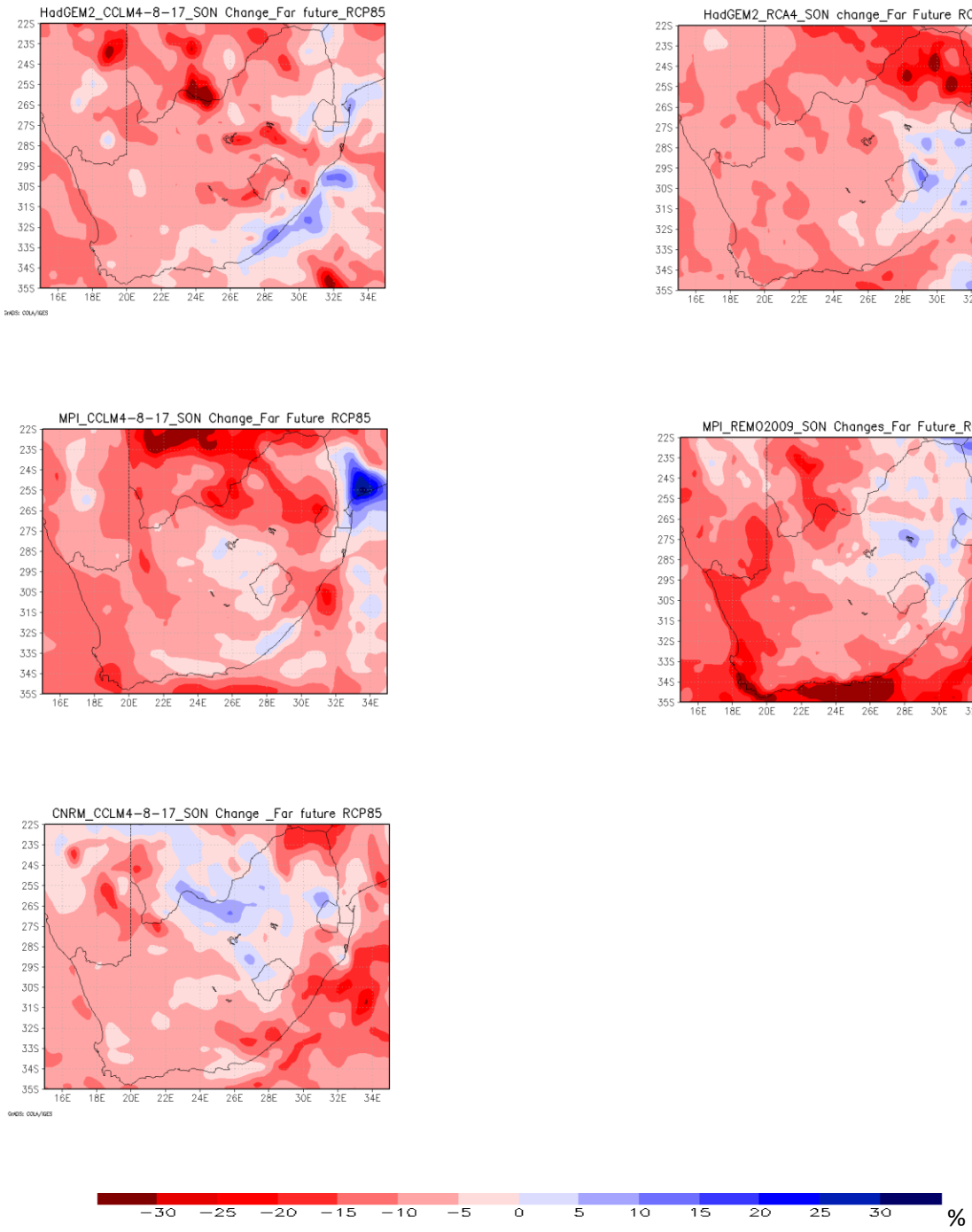

Figure 5. 36 SON mean rainfall change projection, for Far-Future (2036-2065), relative to present climate (1976-2005), under conditions of the RCP85.

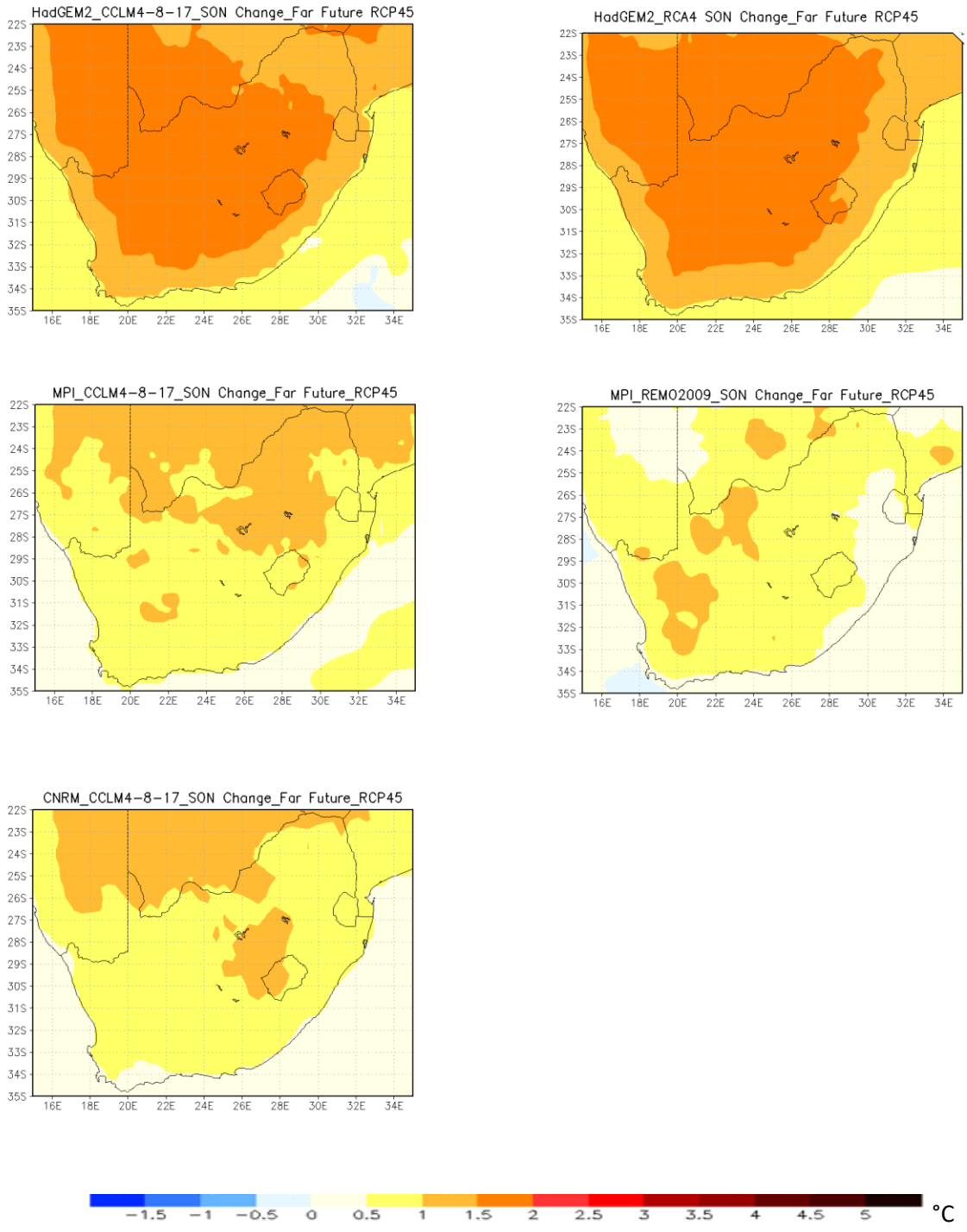

Figure 5. 37 SON mean temperature change projection, for Far-Future (2036-2065), relative to present climate (1976-2005), under conditions of the RCP45.

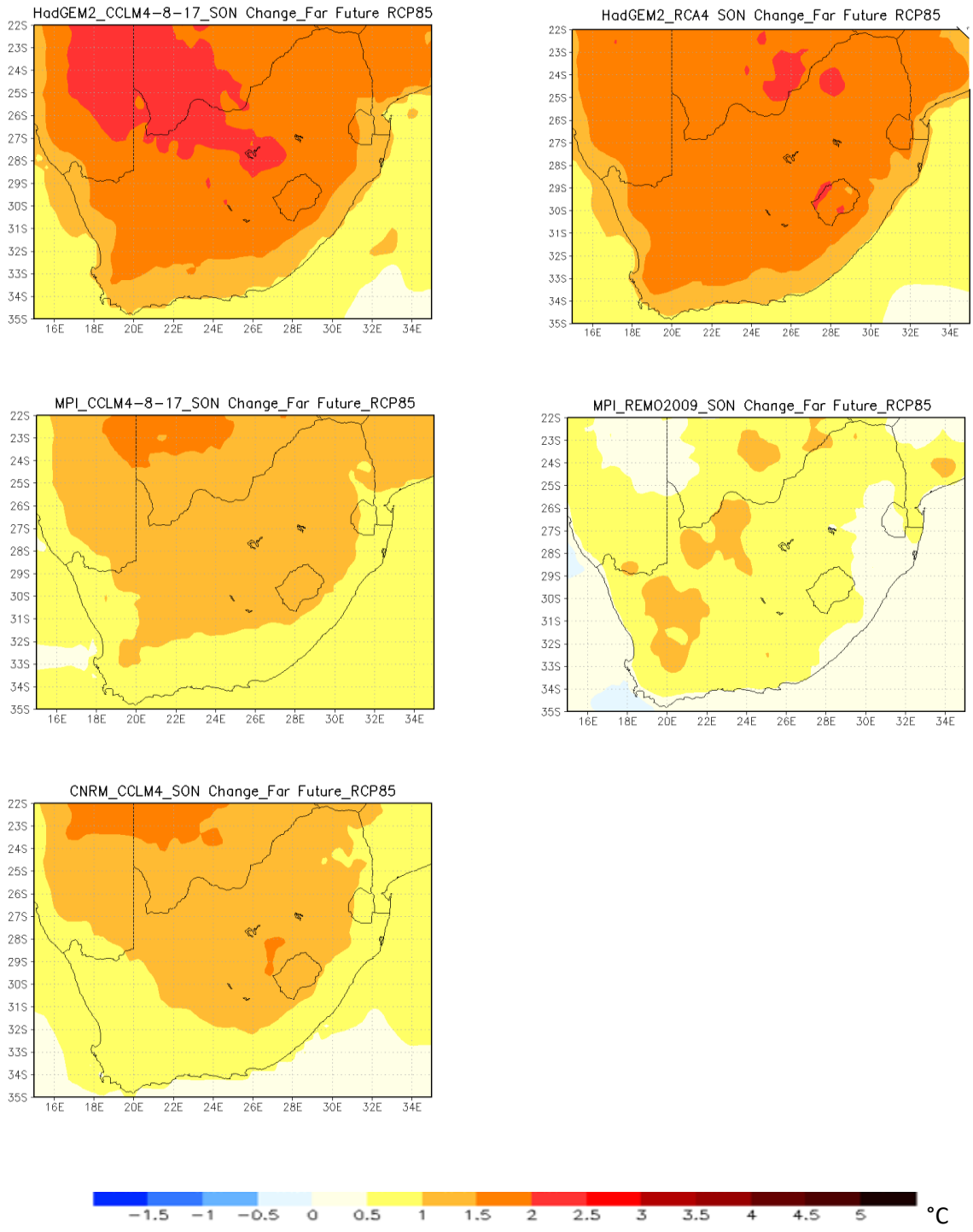

Figure 5. 38 SON mean temperature change projection, for Far-Future (2036-2065), relative to present climate (1976-2005), under conditions of the RCP85.

5.8 Annual mean evaporation change

Several studies have projected warming due to increased concentration of GHGs in the atmosphere (Tadross et al., 2005; Engelbrecht et al., 2015; Henderson et al., 2015). An anticipated consequence is the intensification of the global hydrological cycle manifested specifically as an enhancement of atmospheric moisture transport (Laîné et al., 2014). Increased air temperatures will change the surface and atmospheric heat fluxes, causing variations in spatial and temporal distributions of evaporation (Brutsaert and Parlange, 1998). Soil moisture availability and heat are some of the preconditions for evaporation to take place (Lu et al., 2016). Mixed signals of pan evaporation changes over the tropics are recently under debate and thorough research is still needed. According to Figure 5.39, under both scenarios, despite a warming climate, the model displayed a general decreasing trend in evaporation, though the magnitudes varied.

Over adjacent interior (Figure 5.40), a general reduction of evaporation is projected with lowest (-0.15 mm) over northeast, northwest parts and south coastal parts of South Africa, under RCP8.5, though an insignificant pool of increasing values are projected over the central interior towards northwest under RCP4.5. Some studies are in agreement, having found similar decrease to be associated with drier soil conditions (e.g. Laîné et al., 2014). Despite declines in evaporation over the land, this study projected increasing value (0.15-2 mm) over tropical South Western Indian Ocean (SWIO) and Atlantic Ocean under both scenarios at 50th percentile value distribution. Such findings are in line with Laîné et al., (2014), who found strengthening of trades and westerlies winds to govern over the oceans. Furthermore, some studies (e.g. DEADP, 2016) also projected a rising actual evapotranspiration trend over Western Cape, due to projected increase of temperatures. Thus, observed and projected declines are inconsistent with the rapidly rising surface air temperatures. This might explain that the model is projecting a decrease due to reduced water availability. This phenomenon has been termed the “evaporation paradox” which has been detected in several regions across the globe. Some studies have linked such phenomenon to the continuous GHG emissions, subsequently disrupting the normal hydrological cycle (e.g. Brutsaert and Parlange, 1998; Cong et al., 2009).

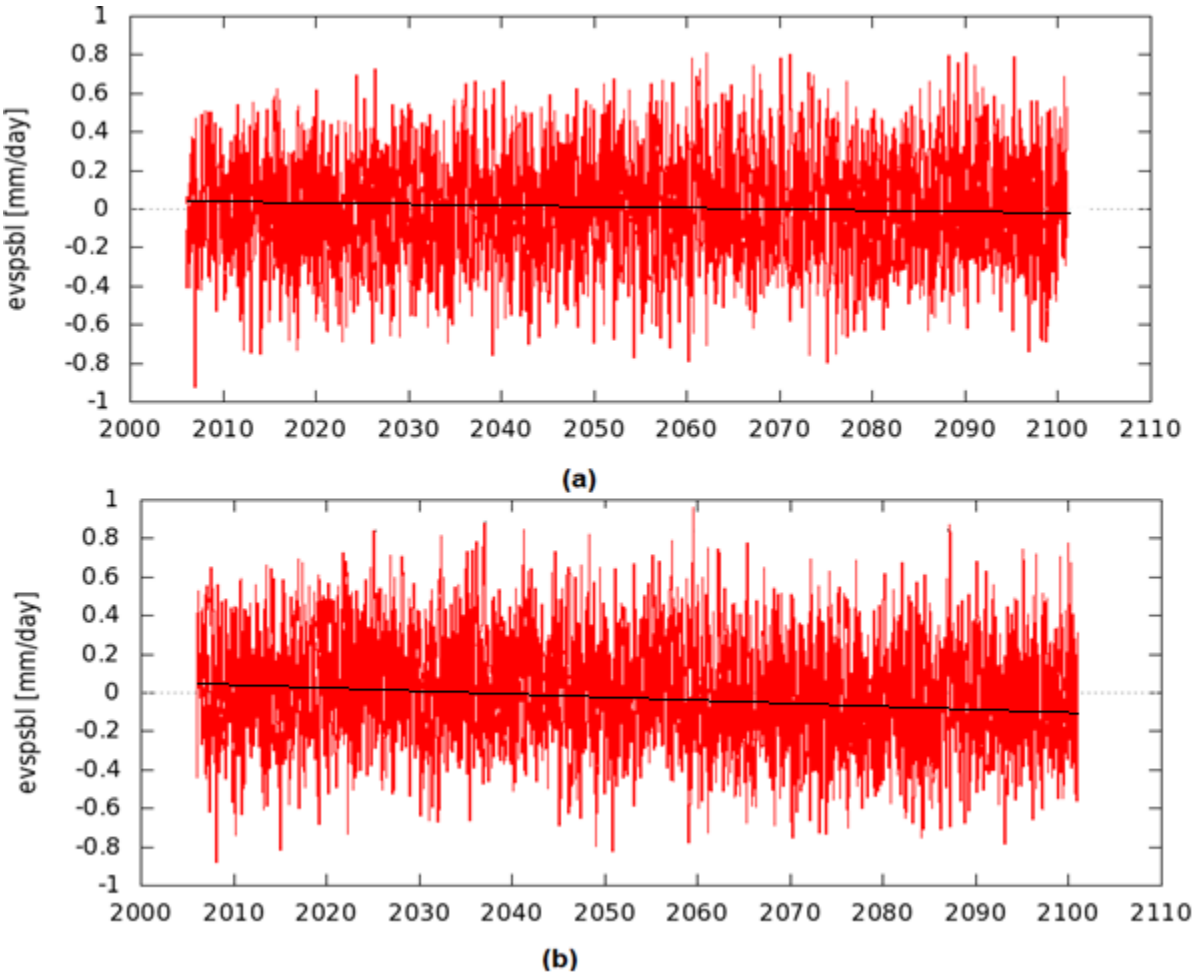

Figure 5. 39 Mean actual evapotranspiration projections for MPI_GCM (a) RCP45 and (b) RCP85, over South Africa_ 22-35°S and 15-35°E.

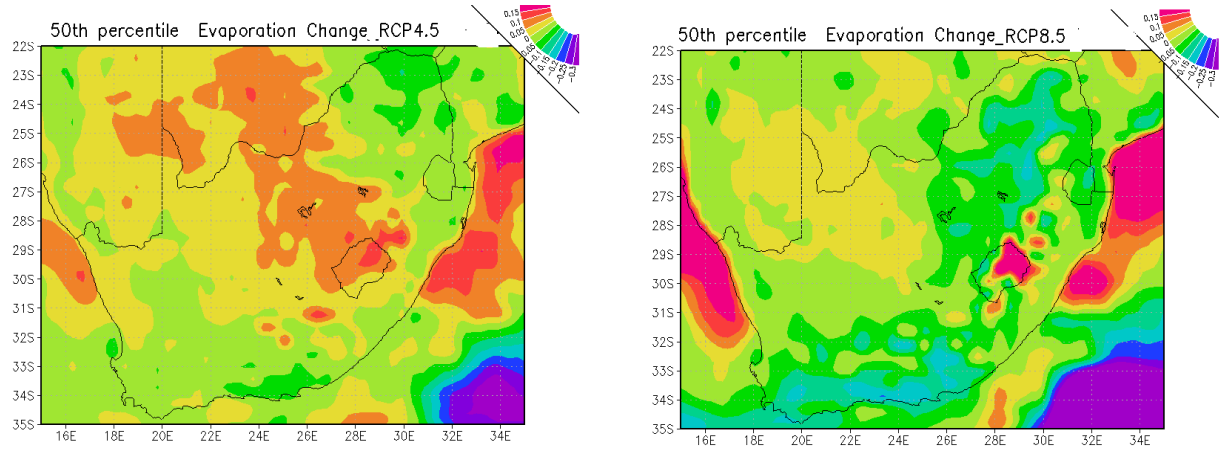

Figure 5. 40 Annual mean actual evapotranspiration change for MPI, under RCP4.5 and 8.5 for 50th percentile over South Africa (from 2006-2065), in relation to 1976-2005.

5.9 Summary

In this chapter projection of two periods, near future (2006-2035) and far future (2036-2065) under the RCP 4.5 and RCP 8.5 emission scenarios were compared to the present day climate defined as 1976-2005. The majority of the models project a general decrease in rainfall over most of the country with wetting patches over some area. In general, all the models projected slightly similar pattern of annual rainfall distribution on both future climate, indicated plausible wetter conditions over the east coasts and central interior of South Africa. One of the RCMs, REMO2009 model distinctively projecting drying elements over much of the interior. The RCMs nested within MPI projected far drier conditions for the Western Cape and south coast for all seasons and in both periods that were considered. Over north of South Africa parts, the projected near-future decrease in rainfall are small in amplitude. An exception is northwest and east coast region, greater uncertainty surrounds RCMs and this shows that rainfall is less robust to project over South Africa. There is high confidence amongst the models that mean and annual surface temperatures are projected to increase in future, unlike, trends in precipitation which are still less coherent. This is with the exception of REMO2009 model nested within MPI which projected smaller temperature increases and in some cases, a decrease in temperature over most seasons. The smallest decreases in this projection were different depending on the season being considered, with some showing a decrease or smaller increase over the west, while the others showed this over the east. A general reduction of evaporation was projected with lowest over northeast, northwest parts and south coastal parts of South Africa, though a small tongue if increasing values over tropical South Western Indian Ocean (SWIO) and Atlantic Ocean was projected under both scenarios.

CHAPTER 6: CONCLUSION AND RECOMMENDATIONS

6.1 Introduction

South Africa consists of diverse climate regions and receives most of its rainfall during austral summer (Kruger, 2017). The study has investigated the variability and change of future rainfall (2006-2065) over South Africa, relative to present-day climate (1976-2005). Rainfall was displayed and analyzed on long-term mean annual and seasonal timescales under RCP 4.5 and RCP 8.5 emission scenarios. This chapter provides a discussion and synthesis of key findings of this work, mainly from Chapter 4-5. Recommendations and implications for future work on modelling future rainfall are also offered.

6.2 Discussion and synthesis of key findings

6.2.1 Present-day (1976-2005)

Different cases (1991/92 dry and 1999/00 wet DJF seasons) of extreme events, were used to assess the capability of model (s) to reasonable match the present-day. Rainfall as the primary data understudy, was also studied at inter-annual timescale to determine its variability with respect to models and GPCC. Therefore, it is important to note the following fundamental findings from chapter 4. Each regional climate models displayed different signature on simulations, rainfall in particular because this is a variable that is affected most by sub-grid process. In the RCM, REMO2009 consistently simulated the largest amount of rainfall during all the seasons and also produced rainfall over the Western Cape throughout the year. RCA4 was characterized by scattering high rainfall (dark blue) noticeable over the north-eastern highlands of Lesotho and on the Highveld. CCLM4-8-17 was associated with least amount of simulated rainfall. Simulations nested within CNRM produced the least amount of rainfall across all seasons. The interannual variability of both rainfall and temperature is underestimated in all the models, with high temperature peaks in DJF, and low temperatures in JJA not well captured by all models. Simulations nested within MIROC generally result in more precipitation than simulations forced with other GCMs. HadGEM2 large scale patterns generally resembles the observations.

6.2.2 Future variability and change projections (2006-2065)

In the near future annual rainfall projections, CCLM4-8-17 projections are found here to be associated with pockets of increasing rainfall amounts over different parts of the country for each projection. For example, the projection nested within MPI projects wetter conditions over the eastern parts of Limpopo, while the two other projections drier conditions in the same area. All

the models project a drier Western Cape annual rainfall, with RCMs nested within MPI showing the largest changes. The spatial differences in temperature projections were smaller and therefore the model uncertainty associated with temperature is robust than that of precipitation. Temperature, the sign of the change is the same (i.e. positive) except in the case of REMO2009 nested with MPI, which indicates very small changes over the eastern coast. For DJF season, areas associated with a decrease in temperature are projected to experience large decreases in rainfall and therefore an increase in cloud cover does not explain the projected temperature increase. CCLM4-8-17 forced by HadGEM2 projected below average temperatures over the Kalahari Desert under the RCP8.5 scenarios. During JJA season, REMO2009 once again was associated with drying along the Western Cape and south coast similar to DJF and MAM under both scenarios, with CCLM4-8-17 projecting a similar picture. During the spring, all the models projected resilient increases in temperature from JJA season, ranging from 1.0 °C–1.5 °C in a large part of the inland to 0.5 °C over adjacent oceans.

In the far future climate, REMO2009 model distinctively projected drying elements over much of the interior. The RCMs nested within MPI projected far drier conditions for the Western Cape and south coast for all seasons and in both periods that were considered. Over north of South Africa parts, most of the models projected rainfall decrease, though in small amplitude. An exception is northwest and east coast region, greater uncertainty surrounds RCMs and this shows that rainfall is less robust to project over South Africa. There is high confidence amongst the models that mean and annual surface temperatures are projected to increase in future, unlike, trends in precipitation which are still less coherent. This is with the exception of REMO2009 model nested within MPI which projected smaller temperature increases and in some cases, a decrease in temperature over most seasons. The smallest decreases in this projection were different depending on the season being considered, with some showing a decrease or smaller increase over the west, while the others showed this over the east.

6.3 Implications for future work

The ability for African countries to mitigate climate change tends to be of hinderance due to several factors such as political instability, widespread poverty, lack of infrastructure and continuous unsustainable development actions to catch up developed countries with modernization and industrialization. Therefore, the development and application of climate models capable to project rainfall is still primitive and requires thorough attention. A number of climate change models project that some regions will experience an increase in temperature and a general decrease in rainfall amounts (though some also contradict on rainfall). This indicates

that there will be an increase in climate uncertainties and challenges in the future. A better consideration is the development of more high-resolution climate models (e.g. CCAM_8km resolution from CSIR) that are exceptional on physical processes. Changes and trends over South Africa, may prove to be very useful in developing sustainable mitigation and adaptive measures to deal with changing climate. Focus could lead to negative implications for quality of life, economic well-being and growth of Africa at large.

The study presented a detailed long-term mean annual and seasonal assessment of rainfall variability using medium to low and high mitigation scenarios. They were presented on spatial maps. Generally, at regional scales, future projections were mainly based on dynamic model applications which use laws of physics applied to the earth system with a set of complex partial differential equations. Dynamic Regional Climate Models (RCMs) from CORDEX were key in obtaining detailed projections of the climate in South Africa. They were applied at very high-resolution for regions of interest. This reasoning and understanding allowed for future projections using a combination high resolution RCMs from CORDEX and low resolution CMIP5 GCMs.

6.4 Conclusions

A clear distinction is that this study presented future projections of rainfall (and other supporting variables such as temperature) variability and change over South Africa. Majority of the models findings are in agreement with other previous works, projecting a prolonged future drying over South Africa (e.g. IPCC, 2014; Engelbrecht et al., 2015). This study adds knowledge few existing literatures with new different model approaches and results It is also apparent that climate change may have evolving influences on mean circulations largely modulating rainfall (e.g. Tadross and Johnston, 2012; Engelbrecht et al., 2015; SAWS, 2017).

In relation to the research objectives, the study managed to validate the models in respect to the observations / reanalysis. RCMs nested within REMO2009 model, presented relatively weak correlation, higher standard deviation and RMSE than the rest of the models. With RCA4_HadGEM2 closer to the observations, during annual and DJF seasonal timescales. There was not much comparison between raw GCM and RCM output to determine the greatest source of uncertainty. The projected changes suggest that, continuous emission of GHG, may intensify uncertainties amongst models on projections over South Africa and global at large. Since rainfall projections are regarded as ambiguous at local and global scales, there is need for thorough development of better models, research and to apply sustainable mitigation measures in practice.

REFERENCES

Akerman, J. 1975. Evaporation and Evapotranspiration - a review. 10.13140/RG.2.1.3932.8886.

Archer, E.R.M., Landman, W.A., Tadross, M.A., Malherbe, J., Weepener, H., Maluleke, P and Marumbwa, F.M., 2017. Understanding the evolution of the 2014–2016 summer rainfall seasons in southern Africa: Key lessons. *Clim Risk Manag*, 16:22-28.

Asuero, A.G., Sayago, A and Gonzalez, A.G., 2006. The correlation coefficient: An overview. *Crit. Rev. Anal. Chem, 36*:41-59.

Banacos, P.C and Schultz, D.M., 2005. The use of moisture flux convergence in forecasting convective initiation: Historical and operational perspectives. *Weather and Forecasting*, *20*:351-366.

Barrett, E.C., Doodge J, Goodman, M. Janowiak, J, Smith E and Kidd C. 1994. The First WetNet Precipitation Intercomparison Project (PIP-1). *Remote Sensing Review*, 11: 49 - 60.

Beck, C., Grieser, J and Rudolf, B. 2005. A New Monthly Precipitation Climatology for the Global Land Areas for the Period 1951 to 2000. DWD, Klimastatusbericht 2004

Becker, A., Schneider, U., Meyer-Christoffer, A., Ziese, Ms., Finger, P and Rudolf, B. 2012. A description of the 1951-2000 monthly global land-surface climatology of the Global Precipitation Climatology Centre and its derivative global products providing use case tailored reference in-situ precipitation reanalysis data sets.

Bellprat, O., Kotlarski, S., Lüthi, D, et al., C. 2016. Objective calibration of regional climate models: application over Europe and North America. *J. Climate*, *29*:819-838.

Behera, S.K. and Yamagata, T. 2001. Subtropical SST dipole events in the southern Indian Ocean. *Geophys. Res. Lett*, *28*:327-330.

Bhaktawar, N., Van Niekerk, L. 2012. South Africa Yearbook 2012/13. Government Communication and Information System (GCIS)

Bohm, U., M. Kücken, W. Ahrens, A. Block, D. Hauffe, K. Keuler, B. Rockel, and A. Will .2006. CLM-the climate version of LM: Brief description and long-term applications, COSMO Newsletter

Chakraborty, A and Krishnamurti, T.N. 2003. A coupled model study on ENSO, MJO and Indian summer monsoon rainfall relationships. *Meteorol Atmos Phys*, *84*:243-254.

Chai, T and Draxler, R.R. 2014. Root mean square error (RMSE) or mean absolute error (MAE)?–Arguments against avoiding RMSE in the literature. *Geosci. Model Dev, 7*:1247-1250.

Chaturvedi, R.K., Joshi, J., Jayaraman, M., Bala, G and Ravindranath, N.H. 2012. Multi-model climate change projections for India under representative concentration pathways. Current Science, pp.791-802.

Chikoore, H. 2005. Vegetation feedback on the boundary layer climate of Southern Africa. Doctoral dissertation, University of Zululand.

Chikoore, H. and Jury, M.R., 2010. Intraseasonal variability of satellite-derived rainfall and vegetation over Southern Africa. *Earth Interact*. *14*:1-26.

Chikoore, H, Vermeulen J.A and Jury M.R. 2015. Tropical cyclones in the Mozambique Channel: January–March 2012. *Nat Haz* 77: 2081-2095

Cimbala, J.M., 2014. Basic Statistics

Clarke, L., Edmonds, J., Jacoby, H., Pitcher, H., Reilly, J., Richels R. 2007. Scenarios of greenhouse gas emissions and atmospheric concentrations. US Department of Energy Publications, University of Nebraska-Lincoln, USA

Collins, W.J., Bellouin, N., Doutriaux-Boucher, M., Gedney, N., Halloran, P., Hinton, T., Hughes, J., Jones, C.D., Joshi, M., Liddicoat, S and Martin, G. 2011. Development and evaluation of an Earth-System model–HadGEM2. *Geosci. Model Dev*, *4*:1051-1075.

Cong, Z.T., Yang, D.W. and Ni, G.H., 2009. Does evaporation paradox exist in China*? Hydrol Earth Syst Sci.* 13: 357-366.

Cook, C., Reason, C.J.C and Hewitson, B.C. 2004: Wet and dry spells within particularly wet and dry summers in the South African summer rainfall region, *Climate Res*, 26:17-31.

Cox, P. M., Betts, R. A., Jones, C. D., Spall, S. A and Totterdell, I. J. 2000. Acceleration of global warming due to carbon-cycle feedbacks in a coupled climate model, Nature 408:184–187, doi: 10.1038/35041539,

CORDEX, 2015. Coordinated Regional Climate Downscaling Experiment. Available at: http://wcrp-cordex.ipsl.jussieu.fr/

Cretat J.Y, Richard B, Pohl M, Rouault C, Reason and Fauchereau N. 2010. Recurrent daily rainfall pattern over South Africa and associated dynamics during the core of the austral summer, *Int. J. Climatol.* doi: 10.1002/joc.2266.

Crowe, S., Cresswell, K., Robertson, A., Huby, G., Avery, A. and Sheikh, A. 2011. The case study approach. *BMC medical research methodology*, *11*:100.

Dams, J., Nossent, J., Senbeta, T.B., Willems, P. and Batelaan, O. 2015. Multi-model approach to assess the impact of climate change on runoff. *J. Hydrol.* 529:1601-1616.

Daron, J.D. 2014. Regional Climate Messages: Southern Africa. Scientific report from the CARIAA Adaptation at Scale in Semi-Arid Regions (ASSAR) Project, December 2014

Davis, C. 2011. Climate risk and vulnerability: A handbook for southern Africa (1st Edition). Pretoria, South Africa: Council for Scientific and Industrial Research.

Davis, C. Engelbrecht, F. Tadross, M. Wolski, P. Archer van Garderen, E. 2017. Future climate change over Southern Africa.

DEA&DP, 2011. White Paper on Sustainable Energy. Department of Environmental Affairs and Development Planning. Western Cape Government.

DEA&DP, 2016. Western Cape Climate Change Response Strategy Biennial Monitoring & Evaluation Report 2015/16, Cape Town: Western Cape Government.

Dedekind, Z., Engelbrecht, F.A and Van der Merwe, J. 2016. Model simulations of rainfall over southern Africa and its eastern escarpment. *Water SA*, 42: 129-168.

Delworth, T.L., Broccoli, A.J., Rosati, A., Stouffer, R.J., Balaji, V., Beesley, J.A., Cooke, W.F., Dixon, K.W., Dunne, J., Dunne, K.A. and Durachta, J.W. 2006. GFDL's CM2 global coupled climate models. Part I: Formulation and simulation characteristics. *J. Climate*., *19*:643-674.

Dilmahamod, A.F., 2014. Links between the Seychelles-Chagos thermocline ridge and large scale climate models and primary productivity; and the annual cycle of chlorophyll. Doctoral dissertation, University of Cape Town.

Dosio, A., 2017. Projection of temperature and heat waves for Africa with an ensemble of CORDEX Regional Climate Models. *Clim Dyn*, 49:493-519.

Driver, P.M. 2014. Rainfall variability over southern Africa.

Dunne, J.P., John, J.G., Adcroft, A.J., Griffies, S.M., Hallberg, R.W., Shevliakova, E., Stouffer, R.J., Cooke, W., Dunne, K.A., Harrison, M.J. and Krasting, J.P., 2012. GFDL's ESM2 global coupled climate–carbon earth system models. Part I: Physical formulation and baseline simulation characteristics. *J. Climate*. *25:*6646-6665.

Dunne, J.P., Stouffer, R.J. and John, J.G. 2013. Reductions in labor capacity from heat stress under climate warming. *Nat Clim Chang*, 3:.563.

Du Plessis, J.A., Schloms, B. 2017. An investigation into the evidence of seasonal rainfall pattern shifts in the Western Cape, South Africa. J. S. Afr. Inst. Civ. Eng.:59(4), Art. #1281, 9 pages. http://dx.doi.org/10.17159/2309-8775/2017/v59n4a5.

Dyson, L. L. and van Heerden, J. 2001, The heavy rainfall and floods over the northeastern interior of South Africa during February 2000, *S. Afr. J. Sci.* 97, 80–86.

Edwards, P.N., 2011. History of climate modeling. *Wiley Interdisciplinary Reviews: Climate Change*, *2*:128-139.

Edwards, J. M., Falloon, P. D., Gedney, N. *et al.*, 2011. The HadGEM2 family of Met Office Unified Model Climate configurations, *Geosci. Model Dev.* Discuss., 4:765–841.

Engelbrecht, F. A., McGregor, J.L. and Engelbrecht, C.J. 2009. Dynamics of the Conformal-Cubic Atmospheric Model projected climate-change signal over Southern Africa. *Int J Climatol,* 29: 1013–1033.

Engelbrecht, F.A., Landman, W.A., Engelbrecht, C.J., Landman, S., Bopape, M.M., Roux, B., McGregor, J.L. and Thatcher, M. 2011. Multi-scale climate modelling over Southern Africa using a variable-resolution global model. *Water SA*, *37*:647-658.

Engelbrecht, F., Adegoke, J., Bopape, M.J., Naidoo, M., Garland, R., Thatcher, M., McGregor, J., Katzfey, J., Werner, M., Ichoku, C. and Gatebe, C. 2015. Projections of rapidly rising surface temperatures over Africa under low mitigation. *Environ. Res. Lett.,* 10:.085004.

Evans, J.P., Ekström, M., and Ji, F. 2012. Evaluating the performance of a WRF physics ensemble over South-East Australia, *Clim Dynam* 39:1241–1258.

Fan, Y. and van den Dool, H. 2007. A global monthly land surface air temperature analysis for 1948-present.

Fan, Y. and Van den Dool, H. 2008. A global monthly land surface air temperature analysis for 1948–present. J Geophys Res-Atmos *113*(D1).

Favre, A., Philippon, N., Pohl, B., Kalognomou, E.A., Lennard, C., Hewitson, B., Nikulin, G., Dosio, A., Panitz, H.J. and Cerezo-Mota, R. 2016. Spatial distribution of precipitation annual cycles over South Africa in 10 CORDEX regional climate model present-day simulations. *Clim Dyn*, *46*:1799-1818.

Fauchereau, N., Trzaska, S., Rouault, M. and Richard, Y. 2003. Rainfall variability and changes in southern Africa during the 20th century in the global warming context. *Nat Hazards, 29*:139-154.

Feser, F., Rockel, B., von Storch, H., Winterfeldt, J. and Zahn, M., 2011. Regional climate models add value to global model data: a review and selected examples. *92*:1181-1192. *Bull. Amer. Meteor. Soc*. 92:1181–1192.

Flato, G., J. Marotzke, B. Abiodun, P. Braconnot, S.C, *et al.* 2013. Evaluation of Climate Models. In: Climate Change 2013: The Physical Science Basis. Contribution of Working Group I to the Fifth Assessment Report of the Intergovernmental Panel on Climate Change [Stocker, T.F., D. Qin, G.-K. Plattner, M. Tignor, S.K. Allen, J. Boschung, A. Nauels, Y. Xia, V. Bex and P.M. Midgley (eds.)]. Cambridge University Press, Cambridge, United Kingdom and New York, NY, USA.

Fujino, J., Nair, R., Kainuma, M., Masui, T., Matsuoka, Y. 2006. Multigas mitigation analysis on stabilization scenarios using aim global model. The Energy Journal Special issue, 3:343–354.

Garland, R.M., Matooane, M., Engelbrecht, F.A., Bopape, M.J.M., Landman, W.A., Naidoo, M., Merwe, J.V.D. and Wright, C.Y., 2015. Regional projections of extreme apparent temperature days in Africa and the related potential risk to human health*. Int. J. Environ. Res. Public Health*, 12:12577-12604.

Giorgetta, M .2012. CMIP5 Simulations of the Max Planck Institute for Meteorology (MPI-M) Based on the MPI-ESM-LR Model: The 1pctCO2 Experiment, Served by ESGF, World Data Cent. for Clim, doi: 10.1594/WDCC/CMIP5.MXELc1, WDCC, DKRZ

Giorgetta, M.A., Jungclaus, J., Reick, C.H., Legutke, S., Bader, J., Böttinger, M., Brovkin, V., Crueger, T., Esch, M., Fieg, K. and Glushak, K., 2013. Climate and carbon cycle changes from 1850 to 2100 in MPI-ESM simulations for the Coupled Model Intercomparison Project phase 5. *J Adv Model Earth Sy, 5*:572-597.

Giorgi, F. and Mearns, L.O., 1991. Approaches to the simulation of regional climate change: a review. *Rev. Geophys,* 29:191-216.

Giorgi, F., Xue-Jie, Gao. 2018 Regional earth system modeling: review and future directions. *Atmos. Oceanic Sci. Lett*. 11: 189-197.

Giorgi, F., Jones, C., and Asrar, R.G. 2009. Addressing climate information needs at the regional level: the CORDEX framework, WMO *Bull*, 58:175-183

Guido, Z. 2010. El Niño–Southern Oscillations: The causes, impacts in the Southwest, and future. *Southwest Clim. Outlook*, 9:1-3.

Hagemann, S., Loew A. and. Andersson A. 2013. Combined evaluation of MPI-ESM land surface water and energy fluxes, *J. Adv. Model. Earth Syst.,* doi: 10.1029/2012MS000173.

Hall, G. 2015. Pearson's correlation coefficient. *1*(9).

Hansen, J., Sato, M. and Ruedy, R., 2012. Perception of climate change. *Proceedings of the National Academy of Sciences*, *109*: .E2415-E2423.

Hansingo, K., Reason, C.J.C. 2008. Modelling the atmospheric response to SST dipole patterns in the South Indian Ocean with a regional climate model. *Meteorol. Atmos. Phys.* 100:37–52.

Harrison, H., Birks, M., Franklin, R. and Mills, J., 2017, January. Case study research: foundations and methodological orientations. In *Forum Qualitative Sozialforschung/Forum: Qualitative Social Research* (Vol. 18, No. 1).

Hart, C. G., Reason, C and Fauchereau, N. 2013. Cloud bands over southern Africa: Seasonality, contribution to rainfall variability and modulation by the MJO. *Clim Dynamics.* 41. 10.1007/s00382-012-1589-4.

He, J., Lin, H. and Wu, Z., 2011. Another look at influences of the Madden-Julian Oscillation on the wintertime East Asian weather. *J Geophys Res Solid Earth-Atmos, 116*(D3).

Hewitson, B.C., Daron, J., Crane, R.G., Zermoglio, M.F. and Jack, C., 2014. Interrogating empirical-statistical downscaling. *Climatic change*, *122*:539-554.

Hijioka Y, Matsuoka Y, Nishimoto H, Masui T, Kainuma M .2008. Global GHG emission scenarios under GHG concentration stabilization targets. *J Glob Environ Eng,* 13:97–108

Hurtt, G. C., and Coauthors. 2009. Harmonisation of global land-use scenarios for the period 1500–2100 for IPCC-AR5. iLEAPS Newsletter, No. 7, iLEAPS International Project Office, Helsinki, Finland, 6–8

Ilyina, T., K. Six, J. Segschneider, E. Maier-Reimer, H. Li, and Nunez-Riboni, I. 2013. Global ocean biogeochemistry model HAMOCC: Model architecture and performance as component of the MPI-Earth System Model in different CMIP5 experimental realizations, *J. Adv. Model. Earth Syst*., doi: 10.1029/2012MS000178.

IPCC. 2000. Special Report on Emissions Scenarios, N. Nakicenovic (ed.), Cambridge, Cambridge University Press.

IPCC. 2001. Climate Change; The Scientific Basis, Contribution of Working Group I to the Third Assessment Report of the Intergovernmental Panel on Climate Change [Houghton, J.T., Y. Ding, D.J. Griggs, M. Noguer, P.J. van der Linden, X. Dai, K. Maskell, and C.A. Johnson (eds.)]. Cambridge University Press, Cambridge, United Kingdom and New York, NY, USA,

IPCC. 2007. Climate Change; Synthesis Report contribution of Working Groups I,II and III to the Fourth Assesement Reoprt of the Intergovernmental Panel on Climate change. Team, Pachauri RK and Reisinger a (Eds), Geneva, Switzerland, 104.

IPCC. 2013. Climate Change 2013: The Physical Science Basis. Contribution of Working Group I to the Fifth Assessment Report of the Intergovernmental Panel on Climate Change [Stocker, T.F., D. Qin, G.-K. Plattner, M. Tignor, S.K. Allen, J. Boschung, A. Nauels, Y. Xia, V. Bex and P.M. Midgley (eds.)]. Cambridge University Press, Cambridge, United Kingdom and New York, NY, USA, 1535 pp, doi: 10.1017/CBO9781107415324.

IPCC, 2014: Climate Change 2014: Synthesis Report. Contribution of Working Groups I, II and III to the Fifth Assessment Report of the Intergovernmental Panel on Climate Change [Core Writing Team, R.K. Pachauri and L.A. Meyer (Eds.)]. IPCC, Geneva, Switzerland, 151 pp.

Jones, C. 2018. Madden–Julian Oscillation.

Joubert, A.M., Katzfey, J.J., Mcgregor, J.L., Nguyen, K.C. 1999. Simulating midsummer climate over southern Africa using a nested regional climate model analyses 104:15–19.

Jungclaus, J. H., N. Fischer, H. Haak, K. Lohmann, J. Marotzke, D. Matei, U. Mikolajewicz, D. Notz, and J. S. von Storch (2013), Characteristics of the ocean simulations in MPIOM, the ocean component of the MPI-Earth System Model*, J. Adv. Model. Earth Syst*., doi:10.1002/jame.20023

Jury, M.R., 2018. Climate trends across South Africa since 1980. *Water SA*, *44*:.297-307.

Kalognomou, E.-A., Lennard, C., Shongwe, M., Pinto, I., Favre, A., Kent, M., Hewitson, B., Dosio, A., Nikulin, G., Panitz, H.-J., Büchner, M. 2013. Diagnostic Evaluation of Precipitation in CORDEX Models over Southern Africa. *J. Clim.* 26: 9477–9506.

Kane, R.P. 2009. Periodicities, ENSO effects and trends of some South African rainfall series: an update. *S. J Sci*, 105:199-207.

Katzfey, J.J. and Mcinnes, K.L. 1996. GCM simulations of eastern Australian cutoff lows. *J. Climate*., 9:2337-2355.

Ker ADR, Moorse MW, Watts ER, Gill BN. 1978. Agriculture in East Africa. Edward Arnold, London, UK

Keshavamurty, R.N. and Rao S.M. 1992. The Physics of Monsoons. Allied Publishers Ltd, New Delhi, 199.

Kjellström, E., Bärring, L., Nikulin, G., Nilsson, C., Persson, G. and Strandberg, G. 2016. Production and use of regional climate model projections–A Swedish perspective on building climate services. *Climate services*, *2*:15-29.

Kijazi A.L and Reason C.J.C. 2011: Intra-seasonal variability over the northeasten highlands of Tanzania, *Int. J. Climatol.,* DOI: 10.1002/joc.2315.

Knapp, P.A. and YIN, Z.Y. 1996. Relationships between geopotential heights and temperature in the south-eastern us during wintertime warming and cooling periods. *Int. J. Climatol*. *Q. J. Royal Meteorol. Soc*, *16*:195-211.

Knutti, R., Masson, D. and Gettelman, A. 2013. Climate model genealogy: Generation CMIP5 and how we got there. *Geophys. Res. Lett., 40*:1194-1199.

Kruger, A.C. and Shongwe, S. 2004. Temperature trends in South Africa: 1960–2003. *Int. J. Climatol, 24*:1929-1945.

Kruger, A.C. 2006. Observed trends in daily precipitation indices in South Africa: 1910–2004*. Int J Climatol*, 26:2275–2285

Kruger, A.C. and Nxumalo, M.P., 2017. Historical rainfall trends in South Africa: 1921–2015. *Water SA*, 43:285-297.

Jubb, I., Canadell, P. and Dix, M., 2013. Representative concentration pathways (RCPs). Australian Government, Department of the Environment.

Lamberty, B., Wise, M.A., Clarke, L.E and Edmonds, J.A. 2011. RCP4. 5: a pathway for stabilization of radiative forcing by 2100. *Climatic change*, *109:*.77.

Lazenby, M.J., Todd, M.C., Chadwick, R. and Wang, Y., 2018. Future precipitation projections over central and southern Africa and the adjacent Indian Ocean: What causes the changes and the uncertainty? *J. Clim. 31*:4807-4826.

Leighly, J. 1937. A note on evaporation. *Ecology*, *18*:180-198.

Lennard, C., and Kalognoumou, L. 2013. Analysis of the CORDEX evaluation runs (ERA_Interim) over Southern Africa. In: EGU General Assembly Conference Abstracts. p. 200.

Lindesay, J.A.1988. South African rainfall, the southern oscillation and a Southern Hemisphere semi-annual cycle. *J Climatol,* 8:17–30.

Llasat, M.C., Martín, F. and Barrera, A. 2007. From the concept of “Kaltlufttropfen” (cold air pool) to the cut-off low. The case of September 1971 in Spain as an example of their role in heavy rainfalls. *Meteorol Atmos Phys*, 96:.43-60.

LTAS, 2013a. Climate trends and scenarios for South Africa. Long-term Adaptation Scenarios Flagship Research Programme (LTAS). Phase 1, Technical Report no 1:69

Longobardi, A and Villani, P. 2010. Trend analysis of annual and seasonal rainfall time series in the Mediterranean area. *Int. J. Climatol*, 30:1538-1546.

Lucarini V, Ragone F. 2011. Energetics of PCMDI/CMIP3 climate models: energy budget and meridional enthalpy transport. *Rev Geophys,* 49: RG1001. Doi: 10.1029/2009RG000323

Luhunga, P.M. 2016. Evaluation of climate change impacts on rain-fed crop production in the Wami-Ruvu basin of Tanzania. Doctoral dissertation, University of Pretoria.

Lumsden, TG, Schulze RE and Hewitson BC (2009). Evaluation of potential changes in hydrologically relevant statistics of rainfall in Southern Africa under conditions of climate change. *Water SA* 35:649-656.

MacKellar, N., New, M. and Jack, C. 2014. Observed and modelled trends in rainfall and temperature for South Africa: 1960-2010. *S. Afr. J. Sci,* 110:1-13.

Majisola O.R. 2010. Trends in precipitation features as an index of climate change in the Guinea Savana Ecological Zone of Nigeria its implications of crop production, Global Journal of Science Frontier Research, 10:13-23

Martin G. M., Bellouin, N., Collins, W.J, et al., 2011. The HadGEM2 family of Met Office Unified Model Climate configurations. *Geosci. Model Dev*. Discuss. 4, 765–841.

Malherbe J, Engelbrecht FA, Landman WA, Engelbrecht CJ. 2011. Tropical systems from the southwest Indian Ocean making landfall over the Limpopo River Basin, southern Africa: a historical perspective. *Int J Climatol*. doi: 10.1002/joc.2320.

Malherbe, J, Engelbrecht, F,A and Landman, W. 2013 Projected changes in 8 tropical cyclone climatology and landfall in the Southwest Indian Ocean 9 region under enhanced anthropogenic forcing. *Clim Dyn* 40: 2867- 10 2886'

Manatsa, D, Siziba, E and Chinyanganya, T. 2010. Analysis of multidimensional aspects of agricultural droughts in Zimbabwe using the standardized precipitation index (SPI). *Theor. Appl. Climatol*., 102, 287–305, doi: 10.1007/ s00704-010-0262-2

Mason, S.J., Waylen, P.R., Mimmack, G.M., Rajaratnam, B and Harrison, J.M. 1999. Changes in extreme rainfall events in South Africa. *Climatic Change*, *41*:249-257.

McInnes, K. L and Hess G. D. 1992: Modifications to the Australian region limited area model and their impact on an east coast low event. *Aust. Meteor*. Mag., 40, 21–31.

Molekwa, S. 2013. Cut-off lows over South Africa and their contribution to the total rainfall of the Eastern Cape Province. Doctoral dissertation, University of Pretoria.

Moss, R.H., Edmonds, J.A., Hibbard, K.A., Manning, M.R., Rose, S.K., Van Vuuren, D.P., Carter, T.R., Emori, S., Kainuma, M., Kram, T. and Meehl, G.A. 2010. The next generation of scenarios for climate change research and assessment. *Nature*, 463:747.

Moncrieff, M. W, Waliser, D. E., Miller M. J, Shapiro, M. E., Asrar, G., and Caughey J. 2012. Multiscale convective organization and the YOTC Virtual Global Field Campaign. *Bull. Amer. Meteor. Soc*, 93:1171–1187.

Monteith, J.L. 1981. Evaporation and surface temperature. *Q. J. Royal Meteorol Soc*, *107:*1-27.

Mulenga, H.M. 1998. Southern African Anomalies, Summer Rainfall and the Angola Low. *PhD thesis*, *University of Cape Town*, 231pp.

Monyela, B.M. 2017. A two-year long drought in summer 2014/2015 and. 2015/2016 over South Africa. Masters dissertation, University of Cape Town.

Mulenga, H.A. 1998. Southern African climatic anomalies, summer rainfall and the Angola low. PhD thesis, University of Cape Town.

Muthige, M.S., Malherbe, J., Englebrecht, F.A., Grab, S., Beraki, A., Maisha, T.R. and Van Der Merwe, J. 2018. Projected changes in tropical cyclones over the South West Indian Ocean under different extents of global warming. *Environ. Res. Lett.,* 13:065019.

Mwafulirwa, N.D. 1999. Climate variability and predictability in tropical southern Africa with a focus on dry spells over Malawi. MSc Thesis, University of Zululand.

Myra, N. 2015. Modeling the potential impacts of vegetation change on the future climate of Southern Africa (Doctoral dissertation, University of Cape Town

Nikulin, G., Jones, C., Giorgi, F., Asrar, G., Büchner, M., Cerezo-Mota, R., Christensen, O.B., Déqué, M., Fernandez, J., Hänsler, A. 2012. Precipitation climatology in an ensemble of CORDEX-Africa regional climate simulations. *J. Climate.* 25:6057–6078.

Palmer, T.N., Doblas-Reyes, F.J., Hagedorn, R. and Weisheimer, A. 2005. Probabilistic prediction of climate using multi-model ensembles: from basics to applications. *Philosophical Transactions of the Royal Society of London B: Biological Sciences*, *360*:1991-1998.

Phakula, S. 2018. Modelling intra-seasonal rainfall characteristics over South Africa. Doctoral dissertation, University of Pretoria.

Pinto, I., Lennard, C., Hewitson, B. 2013. Intercomparison of precipitation extremes over southern Africa in CORDEX simulations. In: EGU General Assembly Conference Abstracts. p. 8872.

Pohl, B., and Camberlin, P. 2006a. Influence of the Madden–Julian Oscillation on East African rainfall. Part I: Intraseasonal variability and regional dependency. *Quart. J. Roy. Meteor. Soc.*, 132:2521–2539.

Pomposi, C., Funk, C., Shukla, S., Harrison, L. and Magadzire, T. 2018. Distinguishing southern Africa precipitation response by strength of El Nino events and implications for decision-making. Environmental Research Letters, 13:074015.

Potgieter, C. 2009. Cut-Off Low Characteristics over South Africa in the Future Climate. ARC Technical Report No. GW/A/2009/26. Project GW/050/054. Agricultural Research Council, Pretoria, South Africa.

Porcu, F., Carassi A., Medaglia C. M., Prodi F., Mugnai, A. 2007. A study on cut-off low vertical Structure and precipitation in the Mediterranean region. *Meteorol Atmos Phys*. Nr. 96, 121-140.

Preston Whyte, R. A and Tyson, P. D. 1988: The Atmosphere and Weather of Southern Africa. Oxford University Press, 347

Qwabe, S.T. 2014. Daily rainfall variability in Southern Africa. Doctoral dissertation, University of Witwatersrand.

Reason, C.J.C., 2001. Subtropical Indian Ocean SST dipole events and southern African rainfall. *Geophys. Res. Lett*., *28*:2225-2227.

Reason, C.J.C and Rouault, M. 2005. Links between the Antarctic Oscillation and winter rainfall over western South Africa. *Geophys Res Lett,* 32:L07705. doi:10.1029/2005GL022419.

Reason, C.J.C., Hachigonta, S. and Phaladi, R.F. 2005. Interannual variability in rainy season characteristics over the Limpopo region of southern Africa. *Int. J. Climatol*., 25:1835-1853.

Reason, C.J. and Smart, S., 2015. Tropical south east Atlantic warm events and associated rainfall anomalies over southern Africa. *Frontiers in Environmental Science*, *3*:24.

Rockel, B., and B. Geyer. 2008. The performance of the regional climate model CLM in different Climate regions, based on the example of precipitation, Meteorologische Zeitschrift, 17(4), 487– 498

Riahi, K., Grübler, A., Nakicenovic, N. 2007. Scenarios of long-term socio-economic and environmental development under climate stabilization. *Technol Forecast Soc* Chang 74:887–935.

Roeckner, E., Baeuml, G., Bonaventura, L., et al., 2003. The atmospheric general circulation model ECHAM 5. PART I: Model description, Max-Planck-Institute for Meteorology, Report No. 349 *(PDF) Interactive coupling of regional atmosphere with biosphere in the new generation regional*

*REMOiMOVE.Availablefrom:*https://www.researchgate.net/publication/307846857_Interactive_coupling_of_regional_atmosphere_with_biosphere_in_the_new_generation_regional_climate_system_model_REMO-iMOVE#pf15 [accessed Sep 06 2018].

Rouault, M., Florenchie, P., Fauchereau, N. and Reason, C.J. 2003. South East tropical Atlantic warm events and southern African rainfall. *Geophys. Res. Lett*. pp*30*.

Rouault, M., White, S.A., Reason. C.J.C., Lutjeharms, J.R.E., Jobard, I. 2002. Ocean–atmosphere interaction in the Agulhas current region and a South African extreme weather event. Weather Forecast 17:655–669.

Rouault, M., Richard, Y. 2003. Intensity and spatial extension of drought in South Africa at different time scales. *Water SA,* 29:489–500.

Rudolf, B., Becker, A., Schneider, U., Meyer-Christoffer, A and Ziese, M. 2011. New Full Data Reanalysis Version 5 provides high-quality gridded monthly precipitation data. GEWEX News, Vol. 21, No. 2, 4-5, May 2011.

Rummukainen, M. 2010. State-of-the-art with Regional Climate Models. Wiley *Interdiscip. Rev. Clim. Chang*. 82–96.

Salas y Me´lia D. 2002. A global coupled sea ice-ocean mod el. *Ocean Model,* 4:137–172

Salas y Me´lia, D., Chevallier, M.2012. The impact of the inclusion of new sea ice processes on the simulation of sea ice by CNRMCM5 global coupled model. *Clim Dyn*.

Schneider, U., Fuchs, T., Meyer-Christoffer, A. and Rudolf, B. 2011. Global precipitation analysis products of the GPCC. *Global Precipitation Climatology Centre (GPCC), DWD, Internet Publikation*, *112*.

Schneider U, P. Finger, A. Meyer-Christoffer, M. Ziese, A. Becker. 2018. Global Precipitation Climatology Centre (GPCC) Deutscher Wetterdienst, Offenbach a. M., Germany,

Shaffrey, L. C., and Coauthors. 2009. U.K. HiGEM: The new U.K. high-resolution global environmental model—Model description and basic evaluation. *J. Climate*, 22:1861–1896.

Shalaby, A., Zakey, A. S., Tawfik, A. B., Solmon, F., Giorgi, F., Stordal, F., Sillman, S., Zaveri, R. A., and Steiner, A. L. 2012. Implementation and evaluation of online gas-phase chemistry within a

regional climate model (RegCM-CHEM4), *Geosci. Model Dev*., 5:741–760, https://doi.org/10.5194/gmd-5-741-2012,

Sheinbaum, J. 2003. Current theories on El Nino-southern oscillation: a review. Geofísica internacional, 42:.291-305.

Shongwe, M.E., Lennard, C., Liebmann, B., Kalognomou, E., Ntsangwane, L., Pinto, I., 2014. An evaluation of CORDEX regional climate models in simulating precipitation over Southern Africa. Atmos. Sci. Lett, 16:199-207.

Siderius, C., Gannon, K.E., Ndiyoi, M., Opere, A., Batisani, N., Olago, D., Pardoe, J. and Conway, D., 2018. Hydrological response and complex impact pathways of the 2015/2016 El Niño in eastern and southern Africa. Earth's Future, 6:2-22.

Singleton, A.T and Reason, C.J.C. 2007. A numerical model study of an intense cutoff low -pressure system over South Africa. *Mon. Weather Rev.,* 135:1128-1150.

Smith, R.N.B., Gregory, D., Wilson, C., Bushell, A.C and Cusack, S. 1999. Calculation of saturated specific humidity and large-scale cloud. *UM Documentation Paper*, *29*, p.27.

Smith, R.K., 2006. Lectures on tropical cyclones.

Solomon, S., D. Qin, M. Manning, M. Marquis, K. Averyt, M. M. B. Tignor, H. L. Miller Jr., and Z. Chen, Eds. 2007. Climate Change 2007: The Physical Science Basis. Cambridge University Press, 996 pp.

South African Weather Service. 2017. *Climate Change* reference *Atlas* for South Africa.

Stevens, B. 2013. Atmospheric component of the MPI-M Earth system model: ECHAM6, *J. Adv. Model. Earth Syst*., 5, 146–172, doi:10.1002/jame.20015

Tadross, M., Jack. C., Hewitson, B. 2005. On RCM-based projections of change in southern African summer climate. *Geophys Res Lett*. 32: L23713, DOI: 10.1029/2005GL024460.

Tadross, M., Gutowski Jr A., Hewitson, W .J, Jack C and New M. 2006. MM5 simulations of interannual change and the diurnal cycle of southern African regional climate. *Theor. Appl. Climatol.*, 86:63–68.

Tadross, M., Davis, C., Engelbrecht, F., Joubert, A. & Archer van Garderen, E. 2011. Regional scenarios of future climate change over southern Africa. In: C. Davis, Climate risk and

vulnerability: A handbook for southern Africa, 1st Edition. Pretoria, South Africa: Council for Scientific and Industrial Research.

Tadross, M. and Johnston, P. 2012. Climate systems regional report: Southern Africa. Local governments for sustainability—Africa climate systems regional report: Southern Africa, ISBN, pp.978-0.

Taljaard, J.J. 1996. Atmospheric circulation systems, synoptic climatology and weather phenomena of South Africa: Synoptic climatology and weather phenomena of South Africa, rainfall in South Africa. South African Weather Bureau Technical paper no. 32, Pretoria, South Africa, 98 pp

Taylor, K.E. 2001. Summarizing multiple aspects of model performance in a single diagram. *J. Geophys. Res*., 106:7183-7192

Taylor, K.E. 2005. Taylor diagram primer. *Work. Pap*, pp.1-4.

Thompson, D. W. J., S. Solomon, P. J. Kushner, M. H. England, Grise, K. M and D. J. Karoly. 2011. Signatures of the Antarctic ozone hole in Southern Hemisphere surface climate change, *Nat Geosci*., 4, 741–749, doi: 10.1038/ngeo1296.

Trenberth, K.E. 1992. Climate System Modeling. Cambridge University Press.

Trenberth, K.E. 1996. El Nino Southern Oscillation (ENSO) Sea. Cambridge University Press.

Tyson, P and Preston-Whyte, R .2000. The Weather and Climate of Southern Africa. Cape Town: Oxford.

UK Met Office. 2011. Climate: Observations, projections and impacts – South Africa. Report commissioned by the Department for Energy and Climate Change.

Usman, M.T and Reason C.J.C, 2004. Dry spell frequencies and theirr variability over southern Africa, Climate Research, 26:199-211.

Van Vuuren, D.P., Den Elzen, M.G., Lucas, P.L. et al., 2007. Stabilizing greenhouse gas concentrations at low levels: an assessment of reduction strategies and costs. Climate Change, 81: 119. https://doi.org/10.1007/s10584-006-9172-9

Van Vuuren, D.P, Edmonds, J., Kainuma T. 2011. Climatic Change109: 5. https://doi.org/10.1007/s10584-011-0148-z

Van Vuuren, D.P. 2011a. The representative concentration pathways: an overview. Climatic Change.

Vitart, F, Anderson, D, Stockdale, T. 2003. Seasonal forecasting of tropical cyclone landfall over Mozambique. *J Climatol*. 16: 3932–3945.

Voldoire, A, E. Sanchez-Gomez, D. Salas y Mélia, B, et al., 2012. The CNRM-CM5.1 global climate model: description and basic evaluation.

Wachs, S., 2009. What is a standard deviation and how do I compute it? *Integral Concepts, Inc*.

Wang, C., Deser, C., Yu, J.Y., DiNezio, P and Clement, A. 2017. El Niño and southern oscillation (ENSO): a review. In Coral Reefs of the Eastern Tropical Pacific (pp. 85-106). Springer, Dordrecht

Watanabe, M., Suzuki, T., O'ishi, R., Komuro, Y., Watanabe, S., Emori, S., Takemura, T., Chikira, M., Ogura, T., Sekiguchi, M and Takata, K. 2010. Improved climate simulation by MIROC5: Mean states, variability, and climate sensitivity. *J. Clim*, *23*:6312-6335.

Wayne, G. 2013. The Beginner's Guide to Representative Concentration Pathways. (Accessed online 10-02-2019).

WCRP CORDEX. Available online: http://wcrp.ipsl.jussieu.fr/SF_RCD_CORDEX.html (accessed on 04 September 2018).

Wise, M., Calvin, K., Thomson, A., Clarke, L., Sands, R., Smith, S.J., Janetos, A., Edmonds, J. 2009a. The implications of limiting CO2 concentrations for agriculture, land-use change emissions, and bioenergy. Technical report. [PNNL-17943].

Wright, C.Y., Norval, M. and Albers, P.N. 2015. Climate change, public health and COP21-a South African perspective. *S Afr Med J.,* 105:997-998.

Yang, T., Hao, X., Shao, et al., 2012. Multi-model ensemble projections in temperature and precipitation extremes of the Tibetan Plateau in the 21st century. *Global and Planetary Change*, *80*:1-13.

Yamazaki, D., T. Oki, and S. Kanae. 2009. Deriving a global river network map and its sub-grid topographic characteristics from a fine-resolution flow direction map. *Hydrol. Earth Syst. Sci*., 13:2241–2251.

Zainal, Z. 2007. Case study as a research method. *J. Kemanusiaan*, 9:1-6.

Ziervogel, G., New, M., Archer van Garderen, E., Midgley, G., Taylor, A., Hamann, R., Stuart-Hill S., Myers, J and Warburton, M. 2014. Climate change impacts and adaptation in South Africa. Wiley Interdisciplinary Reviews: Climate Change, 5: 605-620.

Zhang, C., 2013. Madden–Julian oscillation: Bridging weather and climate. *Bull. Amer. Meteor. Soc*, *94*:1849-1870.

Zhao, M. and Dirmeyer, P.A., 2004. Pattern and trend analysis of temperature in a set of seasonal ensemble simulations. *Geophys. Res. Lett*., *31*.

Zhou L, B. Neale R, Jochum M, Murtugudde R. 2012. Improved Madden–Julian oscillations with improved physics: The impact of modified convection parameterizations. *J. Climate,* 25:1116-36.